PERFORMANCE-BASED SEISMIC DESIGN OF REINFORCED CONCRETE FRAME BUILDINGS: A DIRECT DISPLACEMENT-BASED APPROACH

A Thesis submitted to
Graduate School of Engineering and Sciences of
İzmir Institute of Technology
in Partial Fulfillment of the Requirements for the Degree of

MASTER OF SCIENCE

in Civil Engineering

by
Nisar Ahmad KARIMZADA

July 2015
İZMİR

We approve the thesis of **Nisar Ahmad KARIMZADA**

Examining Committee Members:

_____

Assoc. Prof. Dr. Engin AKTAŞ
Department of Civil Engineering, İzmir Institute of Technology

_____

Assist. Prof. Dr. Gürsoy TURAN
Department of Civil Engineering, İzmir Institute of Technology

_____

Assoc. Prof. Dr. Kasım Armağan KORKMAZ
Department of Civil Engineering, İstanbul Technical University

03 July 2015

_____

Assoc. Prof. Dr. Engin AKTAŞ
Supervisor, Department of Civil Engineering
İzmir Institute of Technology

_____

Prof. Dr. Gökmen TAYFUR
Head of the Department of Civil Engineering

_____

Prof. Dr. Bilge KARAÇALI
Dean of the Graduate School of Engineering and Sciences

AKNOWLEDGEMENT

I would like to express my deepest gratitude and respect to my supervisor Assoc. Prof. Dr. Engin. AKTAŞ, department of civil engineering, İzmir Institute of Technology (İYTE) for his keen, interest and valuable guidance, strong motivation and constant encouragement through this work. Without his help and support it would be very difficult to complete this task.

I would like to express my gratitude to the ministry of higher education of Afghanistan to grant me this wonderful opportunity and for their supports to complete my master degree.

I would like to express my gratefulness to İzmir Institute of Technology (İYTE), without its infrastructure this work would have been a distant reality. And it is an honor for me to be one of the master students of this university.

I would also like to convey my sincere gratitude to the members of the thesis defense committee Assist. Prof. Dr. Gürsoy TURAN, department of civil engineering, İzmir Institute of Technology (İYTE) and Assoc. Prof. Dr. Kasım Armağan KORKMAZ, department of civil engineering, İstanbul Technical University (İTÜ) for their help and advices for reviewing my thesis.

Finally, I would like to express my special thanks to my family for their endless love and patience and their support for completing my master degree, especially to my respected parents, and the meaning of my life and work is incomplete without paying my regards to them whose blessings and continuous encouragement have shown me the path to achieve my goals. This thesis is dedicated to them.

ABSTRACT

PERFORMANCE-BASED SEISMIC DESIGN OF REINFORCED CONCRETE FRAME BUILDINGS: A DIRCET DISPLACEMENT-BASED APPROACH

Structures are designed using current seismic design codes which are mostly based on Force-Based Design approach. The initial aim of the current codes is the public safety. However, no clear information are provided regarding economic losses and business interruptions or downtime. Some information about damage states of structural components are provided, but very limited information is given for the damage states of non-structural members and content systems. Performance-Based Seismic Design (PBSD), which is a new concept in seismic design of structures, is a reliable approach capable of providing more detailed information on the performance levels of both structural and non-structural elements.

Direct Displacement-Based Design (DDBD) approach, which is one of the available PBSD procedures, is implemented in this study. This approach has been utilized on four reinforced concrete irregular frames which are different in terms of number of stories. Story drift ratios were chosen as deformation limits to define the performance levels for specific earthquake hazard levels.

DDBD approach in this study has been utilized in compliance with Turkish Seismic Design Code 2007. Furthermore, capacity design principles were adopted to make sure that plastic hinges occur in beams rather than in columns. After obtaining design internal forces (design moments, shear forces and axial forces), TS500 2003, is utilized to design members. Damage states for each member was determined, and non-linear pushover and time history analysis were carried out using SAP2000 v17.10 to check if story drift ratios meet the ones chosen. The base shear forces and the top displacements, in addition, for each frame were also checked with the ones obtained through DDBD approach.

ÖZET

BETONARME ÇERÇEVE TİPİ YAPILARIN PERFORMANS ESASLI SİSMİK TASARIMI: DİREKT DEPLASMAN ESASLI YAKLAŞIM

Yapılar çoğunlukla Kuvvet Tabanlı Tasarım yaklaşımına dayalı mevcut sismik tasarım kodları kullanılarak tasarlanmaktadir. Mevcut sismik tasarım kodlarının ana amacı, kamu güvenliğinin sağlanmasıdır. Ancak, ekonomik kayıplara ve oluşan iş kayıplarına veya yapının kullanım dışı kalma süresine dair net bir bilgi sunmamaktadırlar. Bu kodlar, yapı elemanlarının zarar durumları hakkında bazı bilgiler verilmiş olsalar da, yapısal olmayan elemanlarin ve sistemlerin hasar durumları için ancak çok sınırlı bilgi vermektedirler. Yapıların sismik tasarımında yeni bir kavram olan Performans Esaslı Sismik Tasarım (PEST), hem yapısal ve hem de yapısal olmayan elemanların performans düzeyleri hakkında daha fazla detaylı bilgi sağlayabilecek, güvenilir bir yaklaşımdır.

Bu çalışmada, PEST prosedürlerden biri olan Direkt Deplasman Tabanlı Tasarım (DDTT) yaklaşımının uygulanması gösterilmiştir. Bu yaklaşım, kat adetleri farklı, dört düzensiz betonarme çerçevenin tasarımında kullanılmıştır. Belirli deprem düzeylerinde performans seviyelerini tanımlamak için göreli kat ötelenme oranları kullanılmıştır.

Bu çalışmada DDTT metodu uygulanmasında, 2007 yılında yayınlanan Deprem Bölgelerinde Yapılacak Binalar Hakkında Yönetmelik göz önüne alınmıştır. Ayrıca sünek bir davranış elde etmek amacıyla, plastik mafsalların kolonlardan ziyade kirişlerde oluşmasını temin etmek için kapasite tasarım prensipleri izlenmiştir. Tasarım kesit talepleri (tasarım momentleri, kesme kuvvetleri ve eksenel kuvvetler) hesaplanıp, TS 500 2003 izlenerek, eleman kesitleri tasarlanmıştır. Her bir betonarme çerçeve için hasar durumları tespit edilerek, SAP2000 v.17.10 ticari yazılımı ile yapılan doğrusal olmayan itme ve zaman tanım alanında analizler sayesinde göreli kat ötelenmelerinin, hedeflenmiş oranlari aşmadığının kontrolü gerçekleştirilmiştir. Bu analizler sonucunda elde edilen taban kesme kuvveti ve çatı deplasmanları, DDTT yaklaşımı ile elde edilen sonuçlar ile karşılaştırılmıştır.

TABLE OF CONTENTS

LIST OF FIGURES

Figure **Page**

LIST OF TABLES

Table **Page**

LIST OF ABBREVIATIONS

ARS	Acceleration Response Spectrum
ASCE	American Society of Civil Engineers
ATC	Applied Technology Council
BSE	Basic Safety Earthquake
BSO	Basic Safety Objectives
BSSC	Building Seismic Safety Council
CQC	Complete Quadratic Combination
DM	Damage Measures
DV	Decision Variables
DDBD	Direct Displacement-Based Design
DRS	Displacement Response Spectrum
DBD	Displacement-Based Design
EERC	Earthquake Engineering Research Center
EERI	Earthquake Engineering Research Institute
EDP	Engineering Demand Parameters
EC8	Eurocode8
FEMA	Federal Emergency Management Agency
FBD	Force-Based Design
HAZUS	Hazards United States
IM	Intensity Measure
MCE	Maximum Considered Earthquake
MAF	Mean Annual Frequency
MDOF	Multi Degree of Freedom
NEHRP	National Earthquake Hazards Reduction Program
PGA	Peak Ground Acceleration
PGV	Peak Ground Velocity
PBEE	Performance-Based Earthquake Engineering
PBSD	Performance-Based Seismic Design
SDOF	Single Degree of Freedom
SRSS	Square Root of Sum of Squares
SEAOC	Structural Engineers Association of California
ICC	The International Code Council

CHAPTER 1

INTRODUCTION

The aim of structural engineering is to design structures to sustain various types of loads imposed by their service requirements and natural hazards. Currently, design of structures are guided through codes and standards. Structures designed with current seismic design codes and standards, should be able to satisfy specific performance level, defined as life safety performance level, for a specific intensity of ground motion (design earthquake with mean return period of 475 years). However, economic losses and occupancy interruptions are not provided (i.e. human lives are protected, but the damages are not limited which may not be economic to repair, the period for re-occupancy is not given). In addition, although life safety performance level is obtained for different structures, the concept of uniform risk is not satisfied (i.e. the response of various structures are different in terms of damages for the same earthquake hazard levels) [1].

Performance-Based Seismic Design (PBSD), continuously under development, is a new approach for the design of new structures and evaluation and retrofitting of existing structures, which attracts many professionals and researchers, recently. Structures can be designed with PBSD approach with more realistic understanding of the risk of casualties, occupancy interruption and economic losses. Furthermore, structures designed through PBSD approach, would be able to show different performance levels for different earthquake ground motions [1].

The procedure of PBSD is an iterative procedure, which will be discussed in details in Section 2.4. In the 3rd step of PBSD (Develop Preliminary Building Design, Section 2.4.2) direct and indirect displacement approaches can be used to gain the performance objectives [2]. Performance objectives are the combination of performance levels and hazard levels, and performance levels can be determined by damage states of the structural and nonstructural components and content systems [3]. Since the damages are related directly to displacements, therefore, in this study Direct Displacement-Based Design (DDBD) approach in the content of PBSD is implemented.

DDBD approach, proposed by Priestley and Kowalsky [4] for RC structures, is one of the simplest design approaches, widely accepted by researchers and it is based on

PBSD approach [5]. In DDBD approach maximum displacement in inelastic deformation of the structure is considered, and in contrast with Force-Based Design (FBD) approach displacement response spectrum is used for obtaining base shear force. Figure 1.1, adopted from Priestly et al. 2000 [4], gives fundamentals of DDBD approach. From Figure 1.1a, it is clear that Multi-Degree of Freedom (MDOF) system is substituted by an equivalent Single-Degree of Freedom (SDOF) system. Equivalent SDOF system is presented by effective height (H_e) and effective mass (m_e, Figure 1.1a), at the maximum displacement by a secant stiffness (i.e. effective stiffness, K_{eff}, Figure 1.1b), and an equivalent viscous damping (Figure 1.1c).

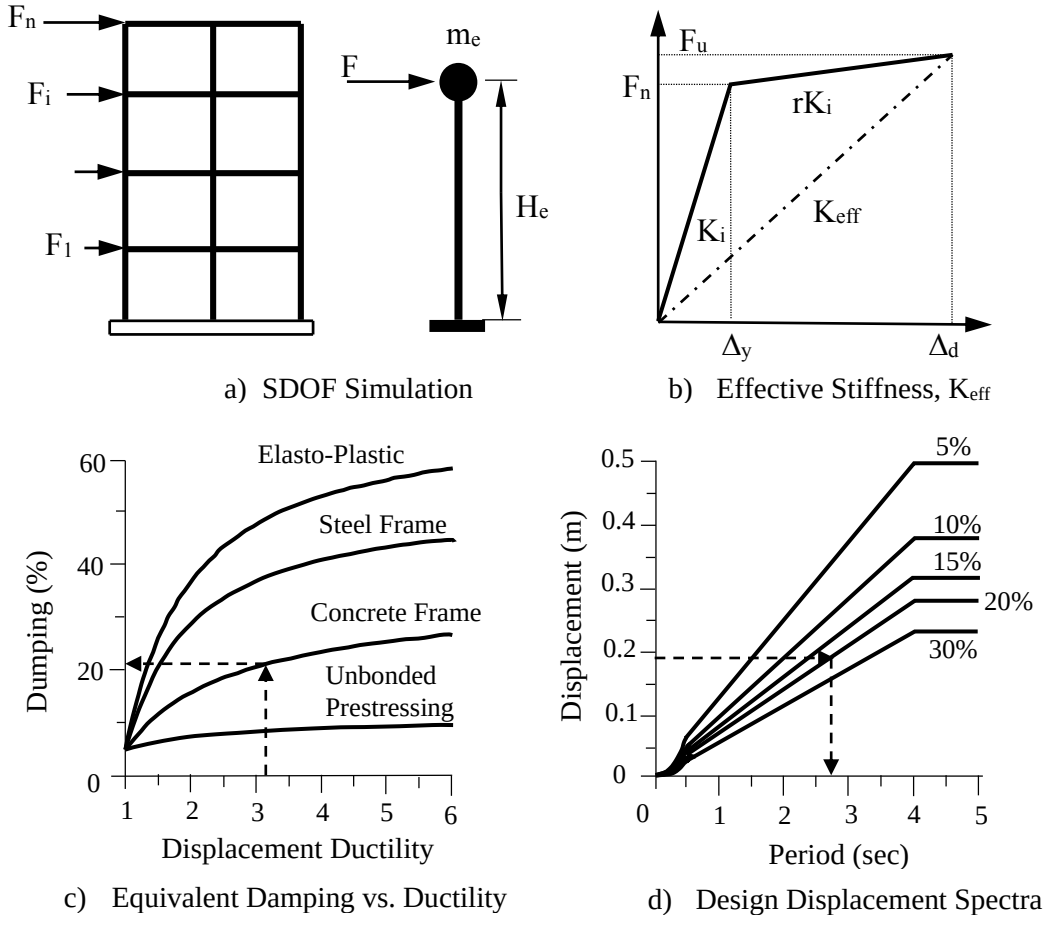

a) SDOF Simulation

b) Effective Stiffness, K_{eff}

c) Equivalent Damping vs. Ductility

d) Design Displacement Spectra

Figure 1.1. Fundamentals of DDBD Approach
(Adopted from Priestley et al., 2000 [4])

1.1 Objective and Scope

Current seismic design codes are based on FBD approach. Extensive damages to the civil infrastructures, designed with current code provisions, due to earthquakes in past 2 or 3 decades, implies that FBD approach has some deficiencies. Therefore, it became necessary to establish a reliable approach for seismic design of structures. PBSD approach is one of the most reliable seismic design approaches that attracted the attention of researchers, recently. Thus, DDBD approach which is a relatively new PBSD procedure is conducted in this study for seismic design of irregular reinforced concrete frame buildings. If the length of the spans in a reinforced concrete frame building are not equal in the direction of the earthquake, and/or if the height of the stories are not equal, then according to DDBD it is counted as irregular reinforced concrete frame building [6].

For this study, four irregular reinforced concrete frames, different in terms of number of stories, are chosen. It is assumed that these frames are related to an office type building. Two different performance objectives are chosen. The performance objectives are immediate occupancy and life safety performance levels under frequent (with mean return period of 72 years) and rare (with mean return period of 475 years) earthquake hazard levels, respectively. The immediate occupancy and life safety performance levels are presented in terms of story drift ratios, 1% and 2%, respectively [7].

The frames were then analyzed using DDBD approach. In the content of DDBD approach, rules and regulations given in Turkish Seismic Design Code [8] is used. The base shear forces obtained through DDBD approach for 2% drift ratio are much larger than the base shear forces found for 1% drift ratio. Consequently, for further calculations the base shear forces obtained for 2% drift ratio have been used.

In addition, capacity design principles were used for reinforced concrete frames to get the desired beam sway mechanism (Figure 4.9a). Using requirements of TS500 [9], and the procedures given by Ersoy et al. 2013 [10], flexural and shear design of members of the frames (beams and columns) are carried out. For the design of columns second order moments are also considered.

For assessing the behavior of frames, nonlinear static pushover and nonlinear time history analysis were carried out, using Sap2000 v17.10. Before modelling frames in Sap2000 v17.10, each member was analyzed, moment curvature diagrams were obtained, and the damage states, limited by strain limits given in Turkish Seismic Design Code [8],

are found. After analyzing the frames, story drift ratios were obtained, and they were compared with the chosen design drift ratio. Meanwhile, top displacement with base shear corresponding to the performance level chosen were compared with the ones obtained through DDBD approach.

1.2 Thesis Organization

Chapter 1: Introduction

In first chapter of this study, a brief introduction about PBSD and DDBD approach, which is included in the contents of PBSD is provided. Further, objective and scope of this study is summarized.

Chapter 2: General Information

In chapter two of this study, general information about PBSD approach has been provided. The historical background, why PBSD is needed, and its procedure has been provided.

Chapter 3: Literature Review

This chapter starts with brief information about Force-Based Design (FBD) approach, next problems with FBD have been summarized, and later its procedure has been given. Consequently, in connection with PBSD, brief information has been provided for N2 and Capacity spectrum methods. In addition, in connection with PBSD, DDBD approach has been discussed, and finally some background studies about DDBD approach have been summarized.

Chapter 4: Direct Displacement-Based Seismic Design

The procedure of DDBD approach, for seismic design of irregular reinforced concrete frame buildings, has been discussed in details. At the end of the chapter brief information about the capacity design principles for DDBD approach has been provided.

Chapter 5: Application of DDBD for the Case Study

In this chapter, DDBD approach has been applied to the case study. Descriptions of frames have been provided. Four identical frames of office type building, different in number of stories which are 3, 5, 8, and 12 story frames, are conducted. As an example for application of the procedure 8 story frame has been chosen, and the results for others are provided in appendices.

Chapter 6: Performance Assessment

In this chapter, performance evaluation of the designed frames are carried out, for this purpose nonlinear pushover and nonlinear time history analysis are conducted. And the results are discussed.

Chapter 7: Conclusions

Summary of the study with conclusions have been provided, and at the end recommendations for the future studies are given.

CHAPTER 2

GENERAL INFORMATION

Earthquake is a natural hazard which may cause extensive damages especially to the built environment. Earthquakes are random in nature and unpredictable, therefore, for analysis of the structures under the action of earthquakes require better engineering approaches and tools to economically design structures. Besides, changes are made in earthquake engineering methods for the past few decades. Performance-Based Earthquake Engineering (PBEE) is one of the improved approaches to achieve a better prediction of the behavior of the structure under seismic activities.

Performance-Based Seismic Design (PBSD), which is under continuous development, takes into account the probable performance of a building for the given hazard which probably the building may experience, considering the uncertainties inherent in the quantification of these hazards and uncertainties in assessment of actual building's response. The most important part of the design process is to identify and assess the performance capability of the building, and guide the design decision which must be made. In addition, PBSD can design buildings with more realistic understanding of the risk casualties, occupancy interruption and economic losses that can be the result of future earthquakes [1].

2.1 Performance-Based Seismic Design (PBSD)

PBSD provides a new pattern for structural design, and it is able to design a structure with an acceptable performance expected by the owner, stakeholders and society [11]. Gibson stated that "*first and foremost, the performance approach is [...] the practice of thinking and working in terms of ends rather than means. [...] It is concerned with what a building or building product is required to do, and not with prescribing how it is to be constructed"* [12]. It means that it is a design approach for the achievement of specified results rather than adherence to particular technologies or prescribed means. It is a consequence based approach and it deals with the outcome.

Performance-based seismic design (PBSD) is based on the promise that prediction and evaluation of the structure's performance can be made with quantifiable confidence (i.e. it vows the structure the performance of which can be quantified and confirmed to the owner's desires). A building can be designed with such an approach which will be able to satisfy different performance levels at different earthquake ground motions. Further, existing buildings can be evaluated and vulnerable buildings can be retrofitted using PBSD approach such that to show better performance under different earthquake hazard levels [1, 13].

2.2 Historical Background

Earthquake is one of the damaging natural disasters for structures. For the first time in 18th century buildings were designed to resist such phenomena. Such design was carried out for the first time, in Portugal and Italy to prevent the overall collapse of the buildings [14]. At the beginning of the 20th century after earthquakes in Messina, Italy in 1911 and Kanto, Japan in 1923, the modern codes developed which involved different level of engineering calculations. In addition, after an earthquake in 1925 in Santa Barbara, California, which caused lots of damages (life loss and many loss), for the first time design requirements for buildings were added in code formats. The aim of these requirements were to prevent the collapse of some large members of a building or overall collapse of the building [14].

In traditional seismic design codes, the aforementioned requirements were set well for the initial goal of these codes which is life safety performance level. And it is still the essential aim of the current code provisions (life safety performance level). After studies for several years and improvements in traditional code provisions, it has been noticed that important or critical buildings (e.g. hospitals, emergency facilities, etc.) should be able to perform better compared to the normal buildings. The better performance means that beside life safety of occupants, they should be operable after severe earthquakes, but still it is of doubtful to fulfil these requirements [14].

Retrofitting of the old buildings for the requirements of traditional seismic design codes, were started in1960s when it was realized by engineers and professionals that old buildings are very risky especially in high seismic regions and that they do not match the requirements of the codes [11, 14]. For the first time, while retrofitting existing buildings,

in 1980s in the United States engineers were getting interested in PBSD. The reason behind this was the requirements of the owners of the buildings. Since they wanted to know what would be the probable performance of a building after retrofitting in future earthquake that it may experience. It was realized that current codes do not give information on how an existing building will probably behave in an earthquake, explicitly. In addition, implementation of the traditional building code requirements, which are mainly for the seismic design of new buildings, were difficult and economically not reasonable to retrofit the existing buildings. Thus, to find out the probable performance of an existing building, some primary assessment procedures were developed by engineers, which depended on their own judgments [15].

Furthermore, for probable repair cost, statistical data were presented in ATC-13 report, *Earthquake Damage Evaluation Data for California*, published in 1985 by Applied Technology Council (ATC). In 1987, ATC-14 report, *Evaluating the Seismic Resistance of Existing Buildings*, was published. This report contains a standard methodology for life safety assessment in an earthquake. These reports, however, did not include information on how to retrofit an existing building to obtain a better performance [15]. Thus, Federal Emergency Management Agency (FEMA) funded a series of studies in 1989 [14]. The aim of these studies were the development of the PBSD guidelines for existing buildings. The first report was published in 1992, FEMA-237 report, *Seismic Rehabilitation of Buildings, Phase I: Issues Identification and Resolution* (ATC-1992). It was a good starting point to move toward PBSD when the concept of performance goals were introduced efficiently at the beginning of these studies [16].

ATC with the cooperation of the Building Seismic Safety Council (BSSC) and American Society of Civil Engineers (ASCE) implemented a FEMA-funded project following the previous studies. These works resulted in three documents. FEMA-273, *NEHRP Guidelines for the Seismic Rehabilitation of Buildings* (ATC/BSSC, 1997a) [15, 16]. FEMA-274, *NEHRP Commentary for the Guidelines for the Seismic Rehabilitation of Buildings* (ATC/BSSC, 1997b). And FEMA-276, *Example Applications of the NEHRP Guidelines for the Seismic Rehabilitation of Buildings*. In these documents, detailed information is provided about the concept of PBSD for rehabilitation of the existing buildings for achieving better performance in future earthquakes. Different performance levels for different ground shakings are covered in these documents [16].

In 1995, Structural Engineers Association of California (SEAOC) developed *Performance-Based Seismic Engineering of Buildings*, known as Vision 2000. A frame

work for Performance-Based Seismic Design of new buildings is given in Vision 2000 [14, 16]. Further, Applied Technology Council provided ATC-40 report, *Seismic Evaluation and Rehabilitation of Concrete Buildings*, in 1996. Performance-Based Seismic Design concepts were adopted and detailed procedures were presented for evaluation and rehabilitation of the existing buildings in this manual (ATC-40) [16].

Later some documents of the FEMA discussed earlier (FEMA-273, FEMA-274, and FEMA-276) were converted to a single document funded by FEMA, FEMA-356, *Pre-Standard and Commentary for the Seismic Rehabilitation of Buildings*, by American Society of Civil Engineers (ASCE, 2000). The concept and performance levels of the FEMA-273 and its other information were maintained as they were without any changes while conversion was made [16]. In addition, ASCE-41, American Society of Civil Engineers national standard-*Seismic Rehabilitation of Existing Buildings*, was published in 2006. This document is the result of revision and refinement of the FEMA-273 procedures. It is mainly about rehabilitation of existing buildings, however its performance objectives and technical data have been used for the design of new buildings, therefore, it can be said that ASCE-41 presents the first generation PBSD procedures [13, 14].

FEMA-445, *Next-Generation Performance-Based Seismic Design Guidelines, A Program Plan for New and Existing Buildings*, is published in 2006. The preparation for this program plan and the developments were carried out under ATC-58 project, by Applied Technology Council (ATC). ATC-58 project, *Development of Next-Generation Performance-Based Seismic Design Guidelines for New and Existing Buildings,* was a contract between ATC and FEMA signed in 2001 [1]. FEMA-445 has emerged from two other FEMA program plans by making some modifications and refinements. They are, FEMA-283, *Performance-Based Seismic Design of Buildings-an Action Plan*, prepared by the Earthquake Engineering Research Center in 1996 (EERC, 1996), and FEMA-349, *Action Plan for Performance-Based Seismic Design*, prepared by the Earthquake Engineering Research Institute in 2000, (EERI, 2000) [1].

Furthermore, this program plan has two phases. The first phase is *Developing a Methodology for Assessing the Seismic Performance of Buildings* in earthquake, and the second phase is *Developing Performance-Based Seismic Design Procedures and Guidelines*. This program plan, in addition, will make the following issues more detailed and advanced to be implemented in practice, to have better performance from buildings in future earthquakes [1].

- Performance Based Assessment
- Performance-Based Design
- Performance-Based Upgrades of Existing Buildings.

Furthermore, it is worth mentioning that some countries have performance based codes. For example, in the United States, The International Code Council (ICC) has had a performance code available since 2001 (ICC 2001). England, New Zealand and Australia have had also Performance-Based Building Codes for decades [14].

2.3 Need for Performance-Based Seismic Design

Generally, owners, occupants and society believe that the structures designed with current codes' prescriptive criteria are safe, and they never consider extent of the damages to the structures. Since 1980s, experiencing severe damages to the buildings due to earthquakes in urban areas, such as Northridge and Kobe earthquakes in 1994 and 1995 respectively [1], made owners and society to worry about the performance of their structures, and made them to consider that structures are prone to damages even built by current codes. These significant damages are far from socio-economic levels [13]. Thus, it concludes that there are some urgent need of revising the current seismic codes. This can be done in many ways, such as providing more reliable seismic codes, or providing precise implementation of current codes using improved engineering facilities.

In current code provisions a structure can be designed which will be capable of providing a certain level of performance (i.e. life safety performance level), but the actual performance of a structure is not assessed. Thus, structures designed with current codes will have different performance levels. For instance, the performance of most structures, designed with current codes' prescriptive criteria, will be much better than the minimum described in current codes (e.g. structure may be experiencing limited damages and disruption in use under large ground shaking intensities), while the performance of some other structures will be worse (e.g. structure may have extensive damages under even moderate level of earthquake ground motions). This implies that the structures cannot be designed with uniform risk in same seismic zones with the same criteria. PBSD may serve effectively to overcome this problem, therefore, it attracts many researchers recently [1].

PBSD indeed is an approach capable of creating various types of structures (e.g. various types of buildings) with uniform risk. Its aim is to control the structural and non-structural damages which are based on the evaluation of proper response parameters. Besides, it provides information to the owners, and stakeholders which are necessary to make rational business or safety related decisions. On the other hand, since the strength and ductility demands in current codes are only applicable for the design of new buildings, and they are not suitable for seismic evaluation of existing buildings, thus it caused the practice toward a predictive method, the development of PBSD for designing of new buildings and evaluation of existing buildings.

2.4 Performance-Based Seismic Design Procedure

PBSD is an iterative procedure, it starts with the selection of design criteria which is stated in the form of one or more performance objectives, following the development

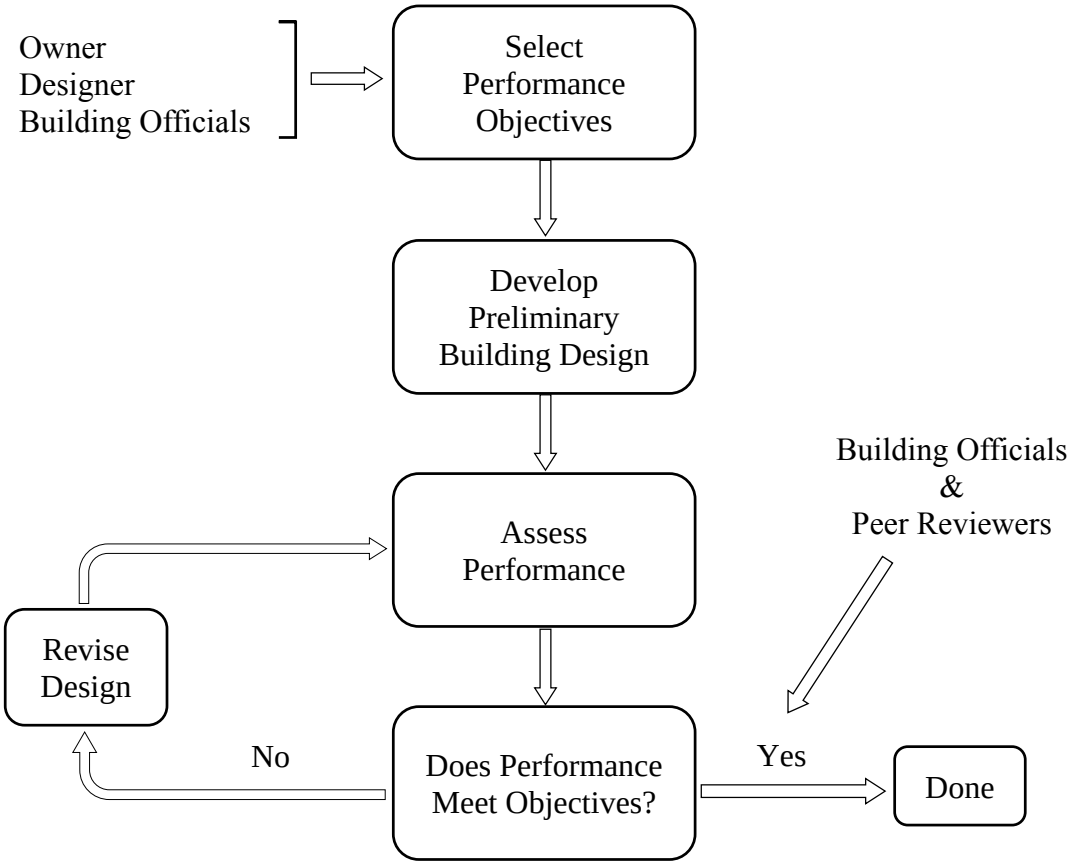

Figure 2.1. Performance-Based Flow Diagram
(Adopted from FEMA-445, 2006 [1])

of preliminary design. After the preliminary design process is done, the next step is to assess the performance of the building. It will be checked if the performance objective meets the one chosen in the first step, if the performance object is not met, the design is revised else the design is done. A simple flow chart for PBSD procedure, which contains the key steps, has been shown in Figure 2.1 (Adopted from FEMA-445 [1]).

2.4.1 Select Performance Objectives

Performance objectives clearly describe the desired seismic performances of the structures, they reflect the acceptable risks. In the selection of performance objectives a group of decision makers such as stakeholders, owners, design professionals etc., are involved. It is the responsibility of the stakeholders to evaluate the hazard and to obtain the agreement of all parties of the group for acceptable performance. Three different risk formats can be stated for these performance objectives [1, 13].

The first risk format which can be stated for performance objectives is intensity-based performance objective. In this risk format the acceptable level of loss is quantified assuming that a specific intensity of ground shaking is experienced. For instance, assuming if 475 years mean return period intensity of ground shaking has occurred, there should be no life loss and injury should not be significant, the repair cost must not be larger than 20% of the building's replacement cost, and the re-occupancy period should not exceed 30 days [1].

The second one is a scenario-based performance objective. In this risk format the acceptable level of loss is quantified assuming a specific earthquake event occurs. For example, if an earthquake of magnitude 7 occurs on a site such as the San Andreas Fault, there should be no life loss and injury should not be significant, and the cost of repair should not exceed 5% of the total building replacement cost. Further, the period for re-occupancy of the building should not exceed one week [1]..

The third risk format is called a time-based performance objective. In this risk format an acceptable probability is quantified over a period of time that a certain level of loss will be experienced or exceeded, by taking into account all other earthquakes which may affect the building in that period and their probability of occurrence. As an example of this risk format, due to earthquake damages the chance of life loss occurrence in a building is 2% in 50 years. Mean reparation costs (i.e. the cost for losses in each year due

to earthquakes) should be at most 1% of the total cost of the replacement of the building, and "*the mean return period for occupancy interruption exceeding one day should be 100 years*" [1].

Each performance objective is the relationship of the seismic performance level of a structure with a specific earthquake hazard level. In this case, it means that a structure can tolerate different levels of damages and some losses caused by these damages at a specific level of earthquake intensity i.e. at a specific earthquake hazard level. Figure 2.2 recommended in SEAOC vision 2000 [17, 18], shows a concept for performance objectives of buildings. The horizontal axis shows the performance level, and vertical axis is the representation of the earthquake hazard levels. In addition, each square shows a performance objective, and the inclined lines show the design criteria [3, 13].

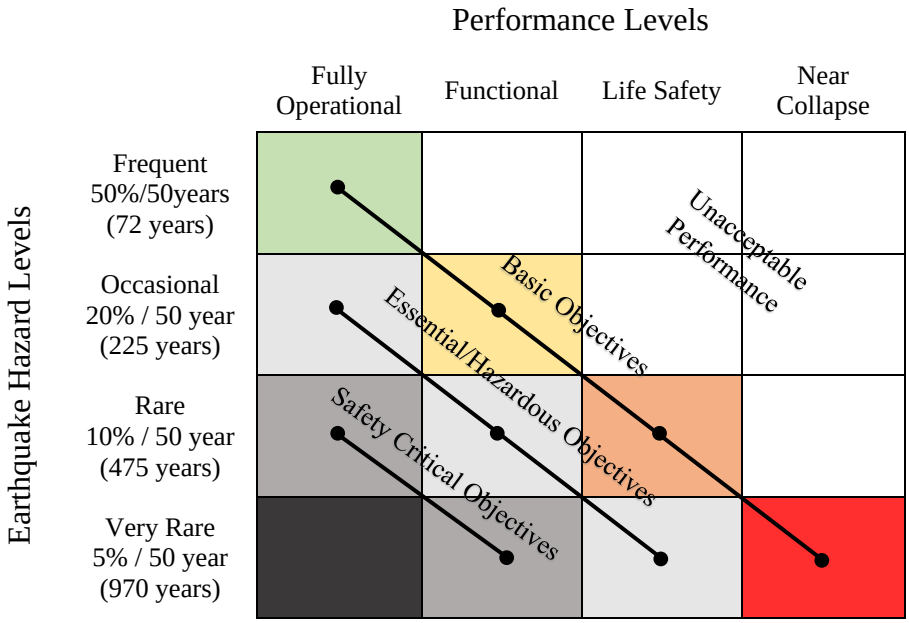

Figure 2.2. Performance Objectives for Buildings
(Adopted from National Research Council, 2003 [17])

Table 2.1 is recommended in several other guidelines and provisions, such as FEMA-389 [16], FEMA-356 [19], FEMA-273 [20], etc. Table 2.1, which presents performance objectives for existing buildings, is adopted from FEMA-389 [16]. Although this concept is recommended for rehabilitation of the existing buildings, it can be applied in the design of new buildings [16]. Different performance levels of Table 2.1 are similar with the one recommended in SEAOC vision 2000 (Figure 2.2), i.e. operational, immediate occupancy, life safety and collapse prevention performance levels of Table 2.1

are similar with fully operational, functional, life safety and near collapse performance levels of Figure 2.2 respectively.

Table 2.1. Performance Objectives [16]

		Target Building Performance Levels			
		Operational (1-A)	Immediate Occupancy (1-B)	Life Safety (3-C)	Collapse Prevention (5-E)
Earthquake Hazard Levels	50% / 50 years	a	b	c	d
	20% / 50 years	e	f	g	h
	BSE-1 10% / 50 years	I	j	k	L
	BSE-2 2% / 50 years	m	n	o	p

*Alpha-numeric identifiers in parentheses are defined in Table 2.2

Note:

1. Each cell in the above table represents a discrete rehabilitation objectives
2. Three specific rehabilitation objectives are defined in FEMA-356.
   Basic Safety Objective = cells kip
   Enhanced Objectives = cells k+p+any of a, e, i, b, f, j, or n
   Limited objectives = cell k alone or cell p alone.
   Limited objectives = cells c, g, d, h, l.

2.4.1.1 Performance Levels

Limited level of damages to structural and non-structural members of a structure designate the expected behavior of this structure in a design earthquake, this behavior of the structure is called performance level [20], i.e. performance level describes a damage condition of the building which is limited and may be considered as allowable damage for the given structure [7].

Performance levels for a building are the combination of performance levels of structural and non-structural members. Performance levels for structural and non-structural components are independent of each other. Table 2.2 (Adopted from FEMA-356 [19]) shows the combination of performance levels of the structural and non-

structural members to create the target performance levels of the building. The target performance levels of the building are indicated in Table 2.2 by numbers and letters. The numbers are the representation of the structural performance levels (S-1 to S-6) and the letters are of the nonstructural performance level (N-A to N-E). For example, at the target building performance level designated as life safety 3-C, 3 stands for the life safety S-3 performance level of the structural elements and C stands for the life safety N-C performance level of the non-structural components.

Table 2.2. Target Building Performance Levels and Ranges [19]

Nonstructural Performance Levels	**Structural Performance Levels and Ranges**					
	S-1 Immediate Occupancy	**S-2 Damage Control Range**	**S-3 Life Safety**	**S-4 Limited Safety Range**	**S-5 Collapse Prevention**	**S-6 Not Considered**
N-A Operational	Operational 1-A	2-A	NR*	NR*	NR*	NR*
N-B Immediate Occupancy	Immediate Occupancy 1-B	2-B	3-B	NR*	NR*	NR*
N-C Life Safety	1-C	2-C	Life Safety 3-C	4-C	5-C	6-C
N-D Hazard Reduced	NR*	2-D	3-D	4-D	5-D	6-D
N-E Not Considered	NR*	NR*	NR*	4-E	Collapse Prevention 5-E	NR*

* NR= Not Recommended

Four common building performance levels (Figure 2.2, Table 2.1) are recommended in several guidelines [16, 18] for the design of new buildings and evaluation of the existing buildings. They are summarized as follows:

1. Operational Building Performance Level (1-A)

The overall damage for a building, designed for such a performance level, is negligible. The building will maintain almost its original stiffness and strength after the earthquake as prior to the earthquake. In addition, necessary facilities will be functional, and there will be some disruption for the normal use of some unnecessary facilities, such

as water, electric power etc. The risk for life safety during earthquake is ignorable. The building's structural and non-structural members are expected to have minimal or no damage.

Furthermore, as it can be seen from Table 2.2, that this performance level is the combination of the immediate occupancy performance level of structural components and operational performance level of non-structural components. Thus, there will be some minor cracks (expected damages at this level of performance) in structural and non-structural elements of the building. Minor cracks of the facades, partitions and ceilings of the building can be good examples for the minor damages of the non-structural components of a building.

Most buildings should meet or exceed this performance level under low level of earthquake ground motion, i.e. under low intensity of earthquake. Designing buildings for this performance level under rare earthquake hazard level (e.g. 10% probability of exceedance in 50 years) will not be economically practical. However, for buildings with safety critical facilities (e.g. buildings with large quantities of hazardous materials such as toxins, radioactive materials, or explosives with significant external effects of damage to building) it will be mandatory.

2. Immediate Occupancy Performance Level (1-B)

The overall damage of the building at this performance level of the building is light. The building will maintain almost its original stiffness and strength after earthquake. Structural components will experience similar damages as the operational performance level of the building, while there are some more damages to the non-structural components of the building as is expected at this level of performance. The risk to life safety is very low.

This performance level of the building is the combination of the immediate occupancy performance level of the structural and non-structural elements of the building. The important utility services will be operational, if they are necessary for normal function of the building. However, there will be some disruption for unnecessary services. Although, the building will be safe to reoccupy, some cleanup, repair and restoration will be required.

Most owners want their buildings to have such performance under moderate level of earthquake ground shaking, on the other hand, some owners want to have this performance level for critical facilities under severe level of earthquake ground motion.

3. Life Safety Performance Level (3-C)

The overall damage of the building, designed for this performance level, is moderate. There will be significant loss from the initial (original) stiffness of the building, but it will have some lateral strength and margins against collapse, in addition, the structural gravity load carrying elements will be functional. Structural and non-structural components will experience significant damages. Contents, systems and falling hazards, selected for the building, are secured, however, they are not operable. Life safety is protected, which mean the risk to life safety is low.

This performance level of the building can be achieved by the combination of the life safety performance levels of the structural and non-structural components of the buildings. The building can be reoccupied after repair and restoration. Repair is possible, but economically it will not be practical.

This performance level of the building is the base for the design of new structures in current codes and provisions. Many owners wish to achieve this performance level for their buildings under severe level of earthquake ground shaking.

4. Collapse Prevention Performance Level (5-E)

The overall damage of the building at this performance level is severe. Building lateral load resisting system will lose its significant amount of original stiffness and strength. However, gravity load carrying elements, columns and walls, are functional and the building is near collapse. The risk to life safety is severe.

At this level of performance of the building, the structural components are in collapse prevention performance level, while for non-structural components no performance level is considered. Further, the damages for the structural members are severe, and non-structural elements, such as infill walls, may fall and probably the exits of the building may be blocked as a consequence of this fall.

Note: Detailed information about performance levels of structural and non-structural components is not covered here. For detailed information about them, it can be referred to the references from which the summary about building performance levels are provided here [7, 16, 19, 20].

Graphical interpretation of aforementioned performance levels is shown in Figure 2.3 (Adopted from FEMA-389 [16]).

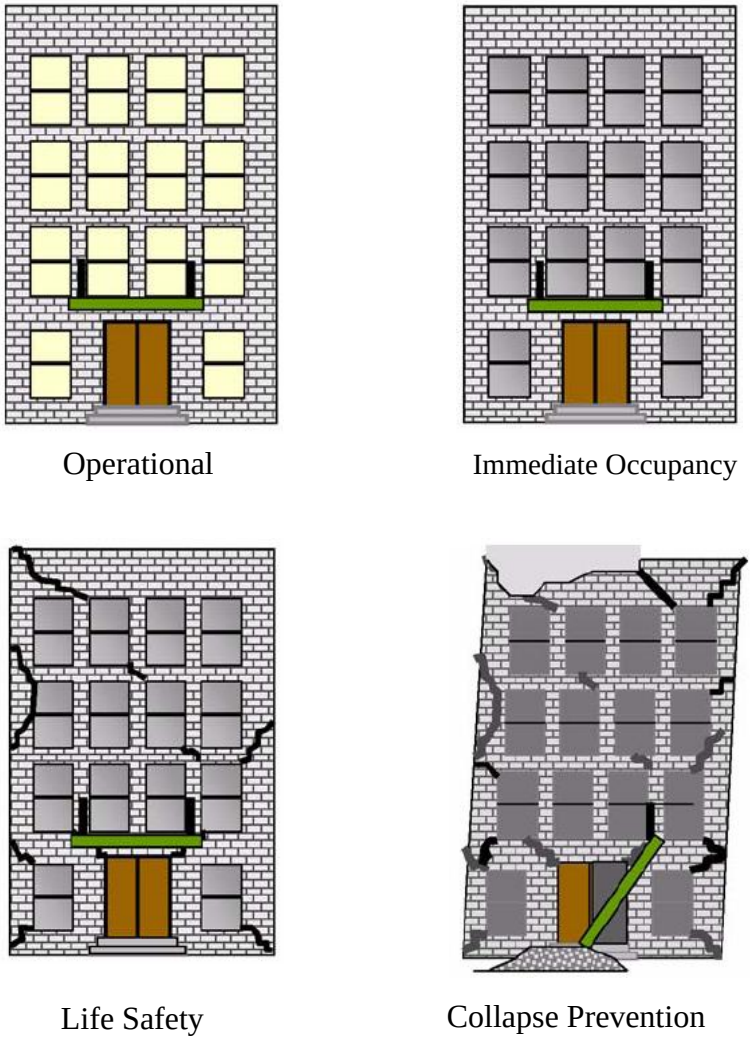

Figure 2.3. Graphical Representation of the Performance Levels
(Adopted from FEMA-389, 2004 [16])

2.4.1.2 Earthquake Hazard Levels

Earthquake hazard levels together with performance levels create performance objectives. Design ground shaking and other hazards; for example, landsliding,

liquefaction, and settlements are determined by earthquake hazard (i.e. seismic hazard). These hazards are defined as acceleration response spectra or acceleration time histories on the basis of deterministic or probabilistic analysis.

A specific magnitude of ground motion on a specific fault can create an event which can cause a maximum ground shaking, this approach is defined as a deterministic approach of earthquake ground motion. On the other hand, if a ground shaking is defined in terms of a level of shaking together with the probability of occurrence, it would present a probabilistic approach of earthquake ground motion [7]. The first three earthquake hazard levels, shown in Figure 2.1 and Table 2.1 are defined probabilistically, and the last one is defined deterministically. The set of earthquake ground shaking, i.e. earthquake hazard levels shown in Figure 2.1 and Table 2.1 strongly depends on the site in a specific seismic region [21]. This is, because site conditions vary from site to site in a specific seismic region, such as soil profile, topography of the site, etc.

Three earthquake hazard levels are given in the guidelines (e.g. ATC-40 [7]). They can be specified by the corresponding site intensity scale, their mean return period and the probability of exceedance. Brief information is given on these hazard levels as follows.

1. The Serviceability Earthquake Hazard Level

This category of earthquake hazard level, in some guidelines, is only given as a single earthquake hazard level, 50% probability of exceedance in 50 years (72 years mean return period) for frequent earthquake hazard level. However, in some others in addition to this hazard level another earthquake hazard level, 20% probability of exceedance in 50 years (225 year mean return period) for occasional seismic hazard levels, is also given as serviceability earthquake hazard level (see Figure 2.1 and Table 2.1).

2. The Design Earthquake Hazard Level

For rehabilitation purposes, this earthquake hazard level is also called Basic Safety Earthquake 1 (BSE-1). The design level of earthquake hazard is expressed as 10% probability of exceedance in 50 years (475 years mean return period). This hazard level is used in rehabilitation purposes to satisfy the basic safety objectives (BSO) [7, 20]. In

addition, this level of ground shaking is used as the design earthquake in seismic codes such as Eurocode8 (EC8) [22], Turkish Seismic Design Code [8], etc.

3. The Maximum Earthquake Hazard Level

This earthquake hazard level is also called, Basic Safety Earthquake 2 (BSE-2), and in some guidelines as Maximum Considered Earthquake (MCE). This hazard level is also used in rehabilitation of the buildings to satisfy the Basic Safety Objectives (BSO). And it is defined as 2% probability of exceedance in 50 years (2475 years mean return period). It should be noted that in some standards and guidance it is defined as 5% probability of exceedance in 50 years (970 years mean return period, as can be seen in Figure 2.2).

2.4.2 Develop Preliminary Building Design

The next step in performance-based seismic design, recommended in FEMA-445 [1], is the development of the preliminary building design. Qiang Xue et al. 2008 [2], and Li Wei et al. 2012 [23], presented a step called conceptual design, between developing preliminary design and selecting performance objectives.

According to Qiang Xue et al. 2008 and Li Wei et al. 2012, "*in conceptual design step, some basic conceptual design rules are given with an emphasis on the redundancy and uniform continuity of the strength, stiffness and ductility, respectively*". For dissipating energy after the system is reached to its yield capacity i.e. after yielding of the system, the ductile capacity of the system is given as ultimate ductility according to its relative capacity. Furthermore, to design a special structural system based on reliable technology, flexibility is given to the system. In addition, the limits for the building height are specified, and energy dissipation and yield mechanisms with vertical and horizontal irregularities of the building are determined.

Descriptions of a number of important characteristics of a structure are included in the preliminary building design. These features can considerably influence the performance capability of the structures in a future earthquake hazard which it may experience [1, 23].

The most important characteristic is the feature of the site of the structure and location of the structure on that site. The other parameter is the configuration of the structure or arrangement of elements of the structures. For example, in building configuration, number of stories, height of each story, the presence of vertical or horizontal (or both) irregularities, floor plate arrangement in each story, foundation type, etc., are included. Besides, the types of the basic structural system are also included in the definition of building attribute. In a building; for example, steel or reinforced concrete moment frame, only shear wall building, or dual wall-frame system are different types of basic structural systems. In addition, stiffness and strength of the structure, energy dissipation and seismic isolation systems, which are good examples for protective or response modification technologies, also play important role to influence the performance capability of the structure [1].

In most cases of earthquake in the past, except if there were no gross failure and collapse of the structural elements of a building, showed that most losses and injuries happened because of the failure of the non-structural members. This implies that, not only the size and location of the structural components and systems, but also the approximate size and location of the non-structural components and systems also influence greatly the performance capability of the building [24].

As it has been mentioned in Section 2.4 that the procedure of performance-based seismic design is an iterative procedure, to implement this method effectively and efficiently, it is very important to select a suitable preliminary design concept. Improper selection of a preliminary design concept may result in large iterations, before reaching an acceptable solution, or may give a solution which may not meet the performance objectives well enough [23]. Furthermore, since performance objectives guide the design process in performance-based seismic design, thus to obtain these objectives, in preliminary design step, direct or indirect displacement based design procedure is used [2]. Finally, in preliminary design step, fundamental period of the structure, its ductility ratio, stiffness and base shear force are found. Then, using structural analysis methods, member forces are attained, and at last according to these forces the members are designed.

2.4.3 Assess Performance

In this step of the performance-based seismic design procedure, the detailed seismic performance assessment of the building is required to obtain the probable performance of the building and to compare it with the performance objectives selected in the first step. The acceptance of the performance of the building with respect to the

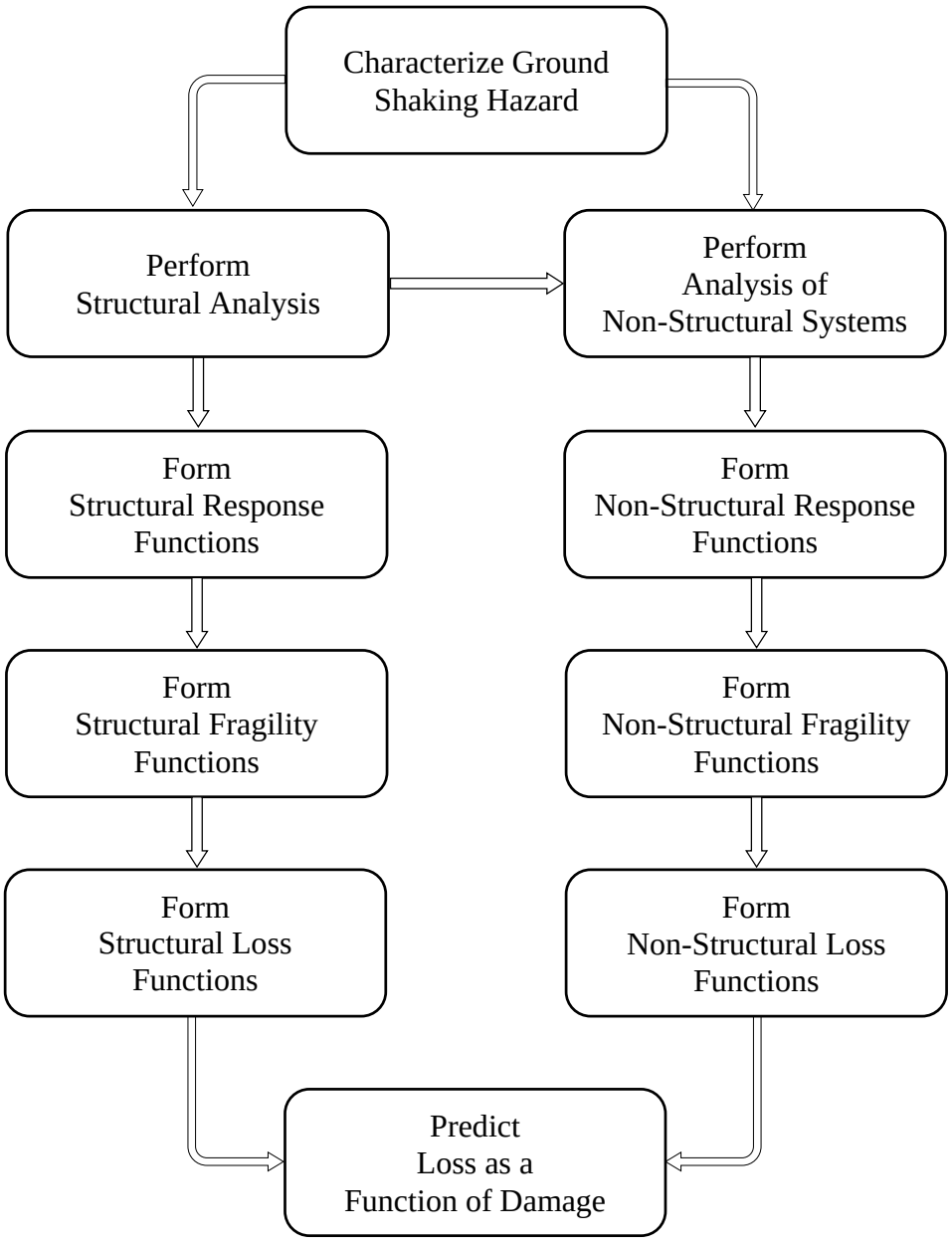

Figure 2.4. Performance Assessment Process
(Adopted from FEMA-445, 2006 and Hamburger 2004 [1, 25])

performance objectives selected in the first step, requires a combination of checks [24]. These checks are done for the structural, non-structural and content systems, and for the overall system. If these checks satisfy the acceptance criteria, i.e. selected performance objectives the design is over and other details are provided, otherwise revision of the design must be done till the performance of the building meets the mentioned performance objectives.

The probable performance of the building is assessed by utilizing a series of simulations, i.e. response analysis of the building due to loadings. The process of the detailed performance assessment of the building is shown in Figure 2.4 (Adopted from FEMA-445 (2006) and Hamburger (2004), [1, 25]), it starts with the characterization of the ground shaking hazard and ends with the prediction of the losses as a function of the damage. Moreover, it is essential to gain statistical relationship between, earthquake hazard, building response, damage and then loss to accomplish the performance assessment process [1]. Four types of generalized random variables, denoted as Intensity Measure (IM), Engineering Demand Parameters (EDP), Damage Measures (DM), and Decision Variables (DV), are the outcomes of the performance assessment process [26, 27]. The steps of the performance assessment process are briefly discussed in the following sections.

2.4.3.1 Characterization of Ground Shaking Hazard

Characterization of ground shaking depends on the type of performance objective (i.e. intensity-based, scenario-based or time-based performance objectives). Amongst performance objectives, if intensity-based performance objective is used, then characterization of ground shaking hazard takes the simple form [1]. In this case, intensity of ground motion is presented by IM. For example, acceleration response spectrum, or displacement response spectrum at first mode period of the building, Peak Ground Acceleration (PGA), Peak Ground Velocity (PGV), etc.

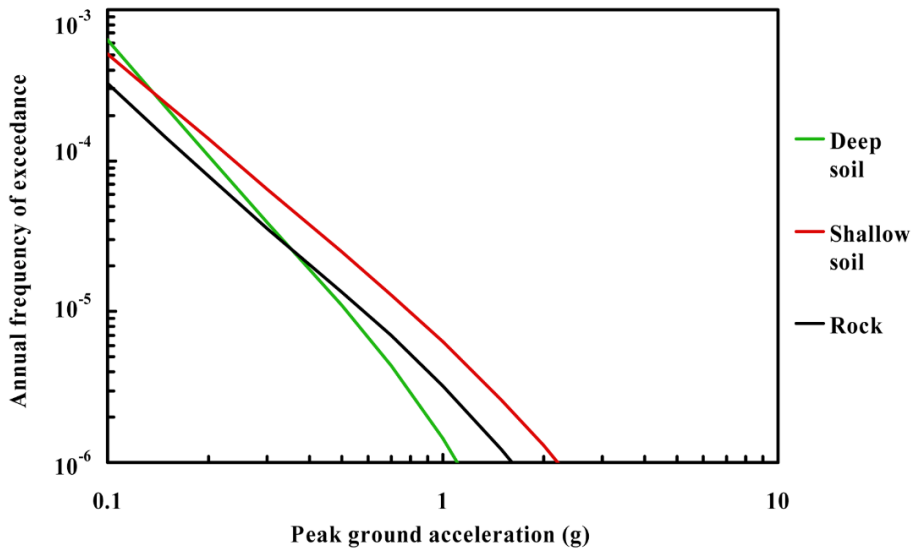

Figure 2.5. Hazard Curves for Different Type of Site Condition at Central Illinois, USA. (Adopted from CEIS-SSC)

Hazard curves are obtained on a probabilistic basis of the seismic hazard analysis, i.e. characterization of ground shaking hazard procedure. The hazard curve itself is the relationship between IM and its Mean (expected) Annual Frequency (MAF) of exceedance. Figure 2.5 (Adopted from official website of the Central Eastern United States-Seismic Source Characterization for Nuclear Facilities (CEUS-SSC), by using following link, http://www.ceus-ssc.com/Report/Chapter8.html) represents an intensity based hazard curve in logarithmic scale. It can be clearly seen from the hazard curves of Figure 2.5 that with increasing PGA, the probability of exceedance is decreasing.

2.4.3.2 Structural Analysis and Structural Response Function

In this step of the performance assessment process (Note that structural analysis and its response functions are shown separately in Figure 2.4), non-linear static or dynamic analysis (e.g. non-linear static pushover analysis and non-linear time history analysis) are implemented given that intensity measure is already known. Structural analysis is being carried out to obtain structural response parameters, i.e. structural response quantities (Engineering Demand Parameters), non-structural demand parameters and their response functions for a given building at a given earthquake hazard level i.e. at a given intensity of ground motion [1, 28].

The examples for EDPs, are interstory drift ratio, maximum roof drift, floor accelerations, member forces and their deformations, story displacements, etc. Non-structural demand parameters, such as interstory drift ratio, floor acceleration, etc. are presenting intensity demand on non-structural elements and content systems [1]. Moreover, after obtaining these parameters for structural and non-structural components and content systems, the damages for these elements are predicted in the next step of the performance assessment process. This implies that to make a relation between IMs and components DMs, EDPs are used [28]. This relation can be obtained through structural analysis methods mentioned above.

The example for structural response in term of the interstory drift ratio is given in Figure 2.6 (Adopted from FEMA-445, 2006 [1]).

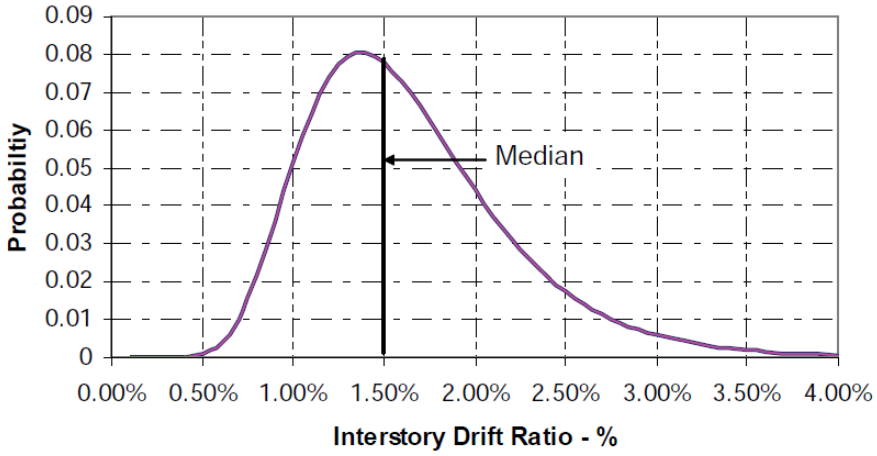

Figure 2.6. Probability Distribution for Structural Response, Expressed as Interstory Drift Ratio for a Particular Structure and Ground Shaking Intensity (Adopted from FEMA-445, 2006 [1])

The structural response of Figure 2.6 for a specific building at a specific intensity of ground motion is obtained by choosing different ground motions records and keeping the other parameters (e.g. stiffness, mass, damping, etc.) unchanged. Different ground motion records which may be experienced at the site are selected and scaled to the specific intensity of ground motion (e.g. elastic spectral response acceleration for 5% damping), and different values of EDPs (e.g. interstory drift ratios) are obtained [1, 25]. Not only structural response, but also structural response function is obtained in the same manner, if instead of only one parameter for intensity of ground motion, a range of intensity of

ground motions are selected. An example of structural response function is shown in Figure 2.7 (Adopted from Hamburger, 2004 [25]).

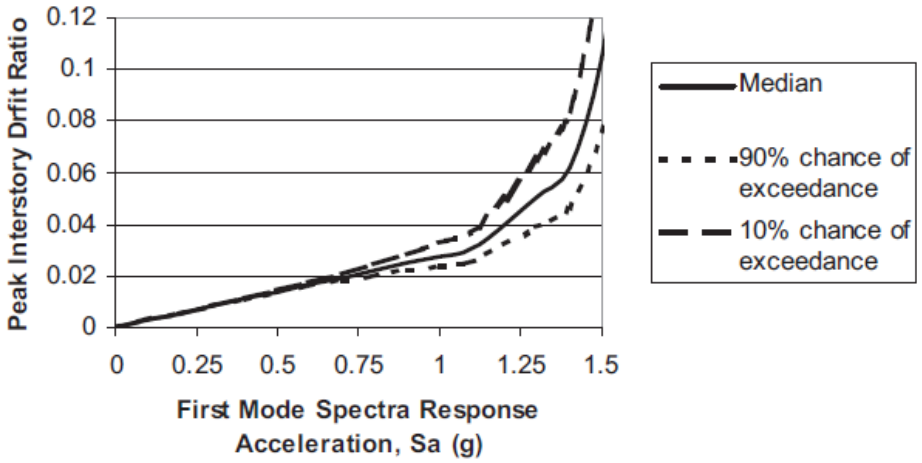

Figure 2.7. Representative Structural Response Function
(Adopted from Hamburger R.O, 2004 [25])

In Figure 2.7, a range of spectral response acceleration from 0 to 1.5g for the first mode period is shown in horizontal axis, and peak interstory drift ratio is shown on vertical axis. From this figure, it can be seen that up to approximately 0.6g of ground motion, the drift ratio can be 2% for a structure. Further, there will be 10% chance for a structure to have 6% or larger drift ratio under approximately 1.25g of intensity of ground motion, while 90% chance to have approximately 3.8% and lower drift ratio.

2.4.3.3 Non-Structural Response Function

Response function of the non-structural component or its behavior depends on its rigidity. The shaking, given by the structure to its non-structural components (e.g. in the form of floor acceleration, peak interstory displacement), can be used directly to obtain the response of infinitely rigid non-structural components. On the contrary, if a non-structural element has a finite rigidity, its behavior or response can be acquired through structural analysis of the non-structural component itself, for a shaking which is given to the mentioned component as a non-structural demand parameters (e.g. component's acceleration, or its displacement) [1].

2.4.3.4 Formation of Structural Fragility Function

Fragility function shows a relationship between damage and response. As mentioned in earlier sections that structures as complete systems or their components (i.e. structural elements) show certain responses to ground motions, which are quantified by EDPs. Taking into account such responses, structural system or components may experience damages greater or less than a certain level. This type of probability is presented by fragility function. While predicting the structural damages, there are variability and uncertainty inherent in the process of structural damage prediction. To account for variability and uncertainty, instead of a deterministic representation of the relationship, fragility functions are presented as probability distribution [1, 25].

There are some factors correlated to the aforementioned uncertainty, such as random nature of the response of the structure to the different ground motions, and the weakness of the EDPs to obtain the difference between this variation of the response of the structure and the damage due to this response to the structure. For instance, if two different ground motions are considered, which yields same peak interstory drift ratio demand of 4% for the structure, one of these two ground motions may cycle the structure to this level of drift ratio only once, while the other ground motion may cycle the structure to this drift level many times. In addition, in the first ground motion, the structure will be returned back to its initial position with small oscillation within its initial position, on the contrary the other ground motion may leave the structure to a displaced position close to the drift ratio. Thus, it is obvious that, although, the EDP (drift ratio of 4%) is the same for both of the aforementioned ground motions, the later ground motion will cause more damage to the structure with compare to the first ground motion. If ground motion and corresponding structural response can be obtained precisely then there is possibility to predict these effects [1, 25].

First and important, it is mandatory to create damage measures for forming fragility functions. One of the methods, used to create such measures for forming fragility functions is the concept of damage indices. This concept was used widely in early researches. Damage indices present the measure of damage to structural elements and systems [1]. They are dimensionless parameters, having values between 0 and 1. If there is no damage or negligible damage, the value of damage index will be equal to 0, conversely if total damage exist, then the value of damage index will be equal to 1.

Furthermore, most of these parameters are developed on element basis, few of them have been found on the basis of the global structural level. It is worth mentioning that there are specific damage indices for specific type of structural components or structural systems [1, 25].

Assigning a series of discrete damage states or ranges is another method for measuring damage parameters. More severe states of damages are presented by these discrete damage states progressively. FEMA 356 and Hazards United States (HAZUS) adopted this approach. Operational, Immediate Occupancy, Life Safety and Collapse Prevention performance levels are being used in FEMA 356 as damage states. As discussed in earlier sections that in operational performance level damages can be neglected (i.e. negligible damage state), while collapse prevention performance level shows severe damage (i.e. near complete damage state). On the other hand, slight, moderate, severe and complete damage states are used in HAZUS [1].

In addition to the aforementioned methods there is another method for measuring damages proposed by ATC-58 [25]. In this method the condition of each element is being tracked directly and then damages are measured on local basis, later on they are combined with the damages measured on overall condition of the structure. In a moment resisting frame, for instance, checking and measuring the damages of columns and beams, their joints, beam plastic hinges, column buckling etc. For a global system (e.g. building) measuring residual interstory drifts (e.g. 1%, 2% etc.) in each story. The combination of the results obtained from the above measures on the system basis must be done for the entire structure [1, 25].

For the purpose of explanation of the fragility functions, Figure 2.8 and Figure 2.9 are adopted from FEMA-445 (2006) [1]. They are the illustrations for the fragility functions which show the probability that damage will be equal or greater than a certain level of damage (this implies that fragility curves do not show the probability that damage will be in any of these state) which corresponds to each of several damage states. Figure 2.8 presents fragility functions of a beam-column connection behavior for a steel moment resisting frame, and Figure 2.9 represents fragility functions for the building-wide structural behavior.

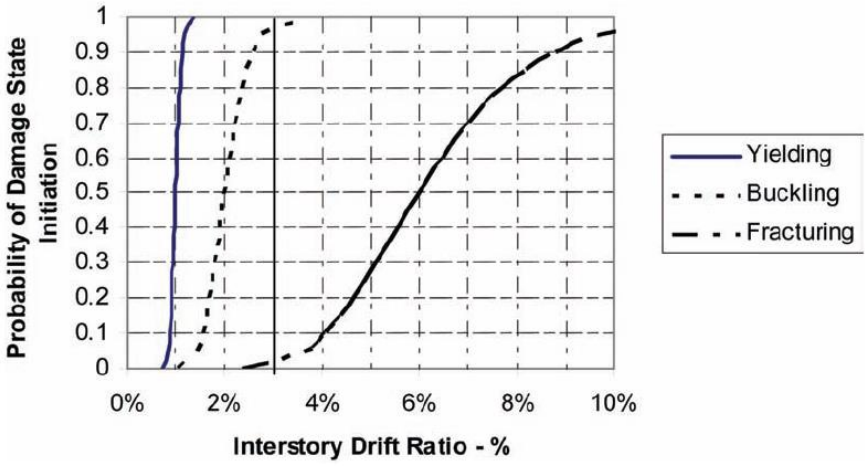

Figure 2.8. Fragility Function for Beam-Column Connection Behavior
(Adopted from FEMA-445, 2006 [1])

In Figure 2.8, three different lines are shown, which correspond to different initial damage states (i.e. yielding, buckling and fracturing of beam flanges). For example, 3% interstory drift demand is considered in Figure 2.8, for this demand there is a 100 % chance of probability that beam flange will yield in beam-column connection. Almost 95% of chance is that buckling of beam flange initiates in beam column connection. And finally about 5% chance of fracturing of beam flange initiates in beam-column connection. 100%-95%=5% is a range which shows the probability of a damage state of a structure which it may experience for a given response. In this range the beam flange has yielded but it does not buckle yet. Other damage state (95% - 5%=90%), in this example, that structure may experience is the probability that the beam flange has buckled but no fracturing has happened.

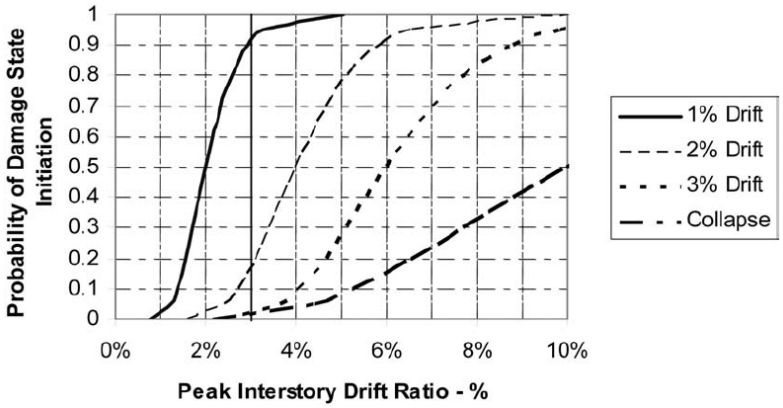

Figure 2.9. Fragility Function for Building-Wide Structural Behavior
(Adopted from FEMA-445, 2006 [1])

The same peak drift ratio (3%) has been considered in Figure 2.9 for the building-wide structural behavior. Three lines which correspond to different residual drift ratios (1%, 2%, 3%), and the fourth line presenting the collapse state of the structure, are shown in this figure. From Figure 2.9 it can be clearly seen that for this drift demand the probability that structure will have 1% of interstory residual drift is 96%, while there is almost 18% chance of having 2% of interstory residual drift, 5% chance to have 3% residual drift and maximum 3% chance to have collapse state.

2.4.3.5 Formation of Non-Structural Fragility Function

Non-structural fragility functions also represent the probability that a non-structural element or system may experience a damages equal to or greater than a certain level of damage. As stated in Section 2.4.3.3 that some non-structural components will have infinite rigidity while some others will have finite rigidity, thus their response functions can be obtained in different ways. Since fragility functions shows the relationship between damage and response, thus similar logic can be implemented for forming fragility functions. If a non-structural component has infinite rigidity, then structural demand (e.g. interstory drift, peak floor acceleration) can be directly used to form fragility function of such components. On the other hand, if a nonstructural component has finite rigidity (i.e. if a non-structural component is flexible), then non-structural demand obtained through analysis of non-structural component, is used to form fragility function for such component.

Moreover, fragility functions should be developed for non-structural systems as well, such as for building lighting system, for HVAC system, etc. The relationship between components of such systems should be considered while forming fragility functions for such systems. Besides, understanding the failure state of each element of such systems and their effects, individually and as a combination on performance of non-structural systems, are very necessary for developing fragility functions of such systems.

Aforementioned discussion implies that, non-structural components and systems have different fragility functions. Figure 2.10 (adopted from Hamburger, 204 [25]) is a representative fragility function for exterior curtain walls (it does not belong to real data). The probability of four different damage states is shown. These damage states are panel

cracking, glass breaking, glass fallout, and connection failure, and they are given as a function of structural interstory drift ratio.

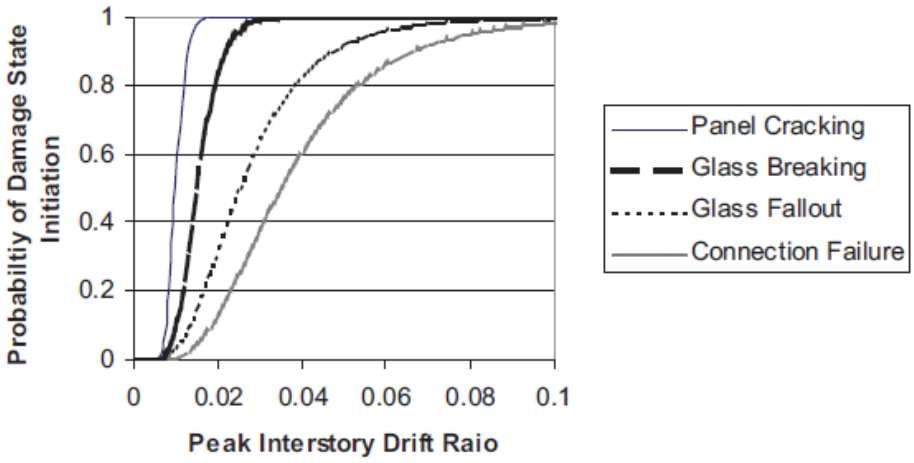

Figure 2.10. Fragility Function for Exterior Curtain Wall
(Adopted from Hamburger R.O., 2004 [25])

2.4.3.6 Evaluation of Structural and Non-Structural Loss Functions

Loss function shows the probability of losses equal to or less than a certain value for a given damage state of the building (or damages of the structural and non-structural elements and systems). Losses can be expressed in terms of repair cost, downtime or out of service and casualties, which can be injury or death. Uncertainty in loss function is significant with compare to other functions, such as hazard function, response function and fragility function [1, 25]. This is because of some factors related to the human called human factors. For example, how quickly owner can take the action regarding repair of the damage? How much effective will be the solution for repairing these damages, presented by the professionals? Finally, how much time it will take to approve such solution by a building department?

For illustration purposes, Figure 2.11 is adopted from FEMA-445 [1]. This figure present hypothetical loss curve, and it is created knowing that there are some structural and non-structural damages, and the fragility function which presents these damages is available, and losses are calculated.

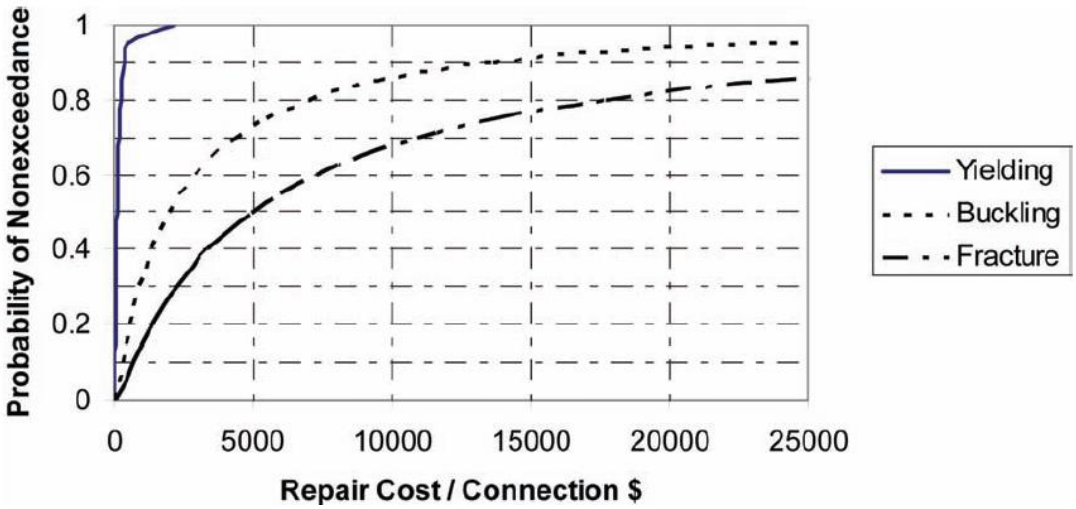

Figure 2.11. Loss Curve for Repair Cost for Damaged Beam-Column Connection (Adopted from FEMA-445, 2006 [1])

Figure 2.11 is created for a beam-column connection in steel moment resisting frame for different damages states of the connection. For example, if the beam flange or column flange has buckled or both of them might buckle in this connection, then there is almost 75% chance that repair cost will be equal or less than 5000$, and around 85% chance that repair cost will be equal or less than 10000$.

2.4.3.7 Predicting Loss as a Function of Damage

For selecting desired building performance by decision makers, it is necessary to calculate the risk of different losses which are meaningful to decision makers and stakeholders. Most stakeholders and decision makers prefer to have scenario based performance objective and risk information. For example, they may want to know the expected loss for a given intensity of ground motion. Some of them, in this group, may want to know this information on probable maximum basis. While some others may want to know the estimated probable losses, and some of them may wish to know that probability of occurrence of such losses in a year or years which a building may experience. These losses can be obtained by knowing the hazard function, response function, fragility function and loss function. This will make possible to determine the performance of the building, and hence performance objective [1].

Once the assessment process is finished, it will be checked if the performance of the building, obtained through performance assessment process, meets the performance

objective selected at the beginning of the performance based design procedure or not, if it meets that performance objective, the design is over and this will be the end of the performance-based design procedure, and after that more detailed drawings must be provided for the implementation. On the other hand if the performance of the structure does not meet the performance objectives, then iterations are needed till the performance objectives are met.

CHAPTER 3

LITERATURE REVIEW

Before getting into Direct Displacement Based Design (DDBD) approach, it has been found necessary to discuss the Force-Based Design (FBD) approach on which most current codes are based. Subsequently, some of the problems inherent in the FBD approach will be discussed. Further, the procedure for FBD approach will be discussed as well. Further, at the end DDBD approach has been discussed with some background studies.

3.1 Force-Based Design (FBD) Methods

Present seismic codes for designing earthquake resistance structures are based on Force-Based Design (FBD) approaches [29, 30]. Although they have some problems, which will be discussed later (Section 3.1.4), they are still used because of their traditional aspect and satisfying the current codes' minimum requirements. The initial aim of the current code provisions is to protect life safety in the rare earthquakes (design earthquake, 10% probability of exceedance in 50 years, with mean return period of 475 years). FBD approach is used to obtain the minimum strength of a structure (to obtain the minimum requirements of life safety), with assuming initial stiffness of the members of the structure, design earthquake intensity level and a force reduction factor. Force reduction factor is used to account for ductile capacity of the structure [31] or non-linear hysteresis effects of the structure.

The first elastic natural vibration period is obtained (it is true for equivalent static lateral load method which is one of the FBD methods), and consequently base shear force is calculated. Then base shear force is distributed up the height of the building to obtain the lateral loads at the top of each floor [31]. Later these forces are applied at the top of each floor, and using any structural analysis method, forces in each members are obtained. Following the design of the structure for these loads, displacement of the structure in terms of interstory drift ratios, for example, for building structures, are checked if they satisfy the minimum requirements of the codes.

In the content of FBD approach, according to Turkish Seismic Design Code [8] different analysis methods are used for buildings and other structures similar to buildings. They are Equivalent Static Lateral Force Method (i.e. Equivalent Seismic Load Method), Mode Superposition Method, and Analysis Methods in the Time Domain.

3.1.1 Equivalent Seismic Load Method

In Equivalent Seismic Load Method, it is assumed that first mode shape is a dominant mode shape of the structural response of a building, and higher modes are not accounted directly. The elastic period of this mode shape is used for obtaining base shear force. And as mentioned earlier, that base shear force is then distributed linearly, up the height of the Building. This distribution of the force (i.e. profile of the force) will have an inverted triangle shape which matches the first mode shape of the structural response. There are some restrictions in this method, for instance, the height of the building, horizontal and vertical irregularities. And the first natural vibration period should not be larger than the one specified by the code (i.e. Equation 2.11 of Turkish Seismic Design Code [8]).

3.1.2 Mode Superposition Method

In this method from the responses of a structure different mode shapes are taken into account, and the maximum forces and displacements are obtained by considering sufficient number of mode shapes. According to Turkish Seismic Design Code [8] the number of sufficient modes is determined, the total of effective participating masses for the modes included is at least equal to 90% of the total mass of the structure. In order to obtain the response for each mode considered, design acceleration response spectrum for 5% damping is considered. They are combined statistically by two different approaches according to Turkish Seismic Design Code, namely, Square Root of Sum of Squares (SRSS) and Complete Quadratic Combination (CQC). If the natural vibration period of two modes satisfies the condition of $T_i/T_j<0.80$ (where $T_i<T_j$), SRSS method will be applicable, otherwise, CQC method should be used [8].

3.1.3 Analysis Method in Time Domain

Here, different ground motions are used for elastic linear and nonlinear analysis of the structures. The number of the ground motions used for such analysis should be at least 3 according to Turkish Seismic Design Code [8]. These ground motions can be artificially created or they can be real earthquake ground motions recorded previously, or they can be numerically generated ground motions from existing ground motions using simulation techniques. Note that for linear and nonlinear analysis, if only 3 ground motions are used, the maximum result, amongst the results of these ground motions be used, on the other hand, if at least 7 ground motions are used, the average of these ground motions shall be used for the design purposes [8].

3.1.4 Problems with FBD Approach

There are some problems with FBD reported in the literature (e.g. assuming initial stiffness for elements, choosing a ductile factor which implies that a ductile capacity has been given to the structure, etc.), some of them are discussed here.

The first problem is the assumption of initial stiffness for the elements of a structure, and assuming that initial stiffness can determine displacement response of that structure. Utilizing initial stiffnesses of the elements of a structure to obtain the first natural vibration period of the structure, and determination of the distribution of the story shear forces to the elements of that story [6, 30, 32]. Assigning initial stiffness for pre-defined members, sometimes as gross stiffness of the members and sometimes as reduced stiffness of the members (to reflect cracking of concrete in members) means that stiffness is constant and does not depend on the strength, and yield curvature or displacement depends on the strength of the structure [30, 33] (refer to Figure 3.1a).

This assumption has been shown to be an invalid assumption in many researches, such as Priestley, 1998 [34] and Priestley and Kowalsky, 1998 [35]. It has been proven, that yield curvature or displacement is free of strength and they are only related to the geometry (set of Equation 3.1, and stiffness is directly proportional to the strength (refer to Figure 3.1b). Set of Equation 3.1, which represents yield curvature for different types of member sections and Equation 3.2 which represents story yield drift of a reinforced

concrete frame, are proposed in aforementioned references [34, 35]. From these equations it can be clearly seen that yield curvature, and story drift is only dependent on geometry.

$$\emptyset_y h_b = 1.70\varepsilon_y \ \pm 10\% \quad \text{Rectangular or Flanged Beam} \tag{3.1a}$$
$$\emptyset_y D = 2.35\varepsilon_y \ \pm 15\% \quad \text{Circular Column} \tag{3.1b}$$
$$\emptyset_y h_c = 2.12\varepsilon_y \ \pm 10\% \quad \text{Rectangular Column} \tag{3.1c}$$
$$\emptyset_y l_w = 1.70\varepsilon_y \ \pm 10\% \quad \text{Shear Wall} \tag{3.1d}$$

$$\theta_y = 0.5\varepsilon_y l_b / h_b \tag{3.2}$$

Where:

h_b is the depth of the beam.

l_b is the length of the beam.

D is the diameter of the column.

h_c is the depth of the column.

l_w is the length of the wall.

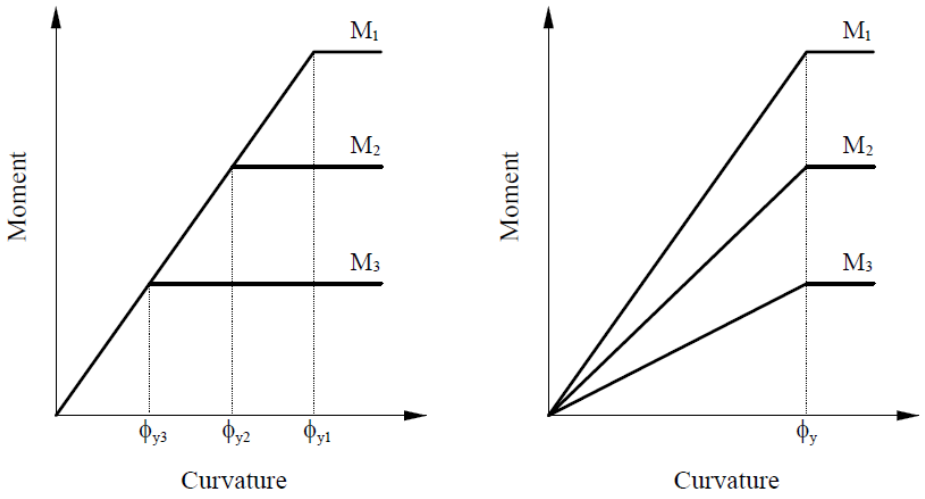

a) Design Assumption (Constant Stiffness)

b) Realistic Conditions (Constant Yield Curvature)

Figure 3.1. Influence of Strength on Moment Curvature Relationship (Adopted from Priestley et al., 1998 [35])

Equation 3.3 which shows the flexural rigidity of a beam from moment curvature relationship, implies that stiffness is dependent on strength.

$$E_c I_{eff} = \frac{M_n}{\emptyset_y} \quad (3.3)$$

Where:

M_n is nominal moment capacity.

$\emptyset_y$ is yield curvature.

E_c is the modulus of elasticity of the concrete.

I_{eff} is the effective moment of inertia.

The second problem is the assumption of giving ductile capacity to a structure without considering its geometry, strength of members, and foundation conditions [4]. As stated above, in FBD to take into account ductile behavior for a structure, the force reduction or ductility factor is applied to reduce the total base shear force. This factor, according to FBD, for a given type of a structure and material used in the structure, depends on the ductile capacity of the structure [30, 36]. This implies that structural type and material type (e.g. in Turkish Seismic Design Code) are the two important parameters for determining the force reduction factor (i.e. in Turkish Seismic Design Code, they can define the behavior factor (R) which in terms is directly proportional to force reduction factor). In addition, according to Turkish Seismic Design Code [8] natural vibration period (T) and spectrum characteristic period (T_A) have also influence on the aforementioned factor to some extent. However, it has been shown that there are various other factors influencing the force reduction factor, such as reinforcement ratio for a section, axial load ratio, and more important, geometry of the structure, etc., which have to be considered while defining force reduction factor [30], whereas in FBD approaches they are not being considered.

Moreover, if different structures (e.g. two different buildings), are designed for the same seismic code, given that same force reduction or ductility factors are used, they may experience different damage levels for the same earthquake hazard. This shows that the concept of uniform risk for these structures with the same force reduction factors is not satisfied, and this is because that ductility presents damage potentials of the structure poorly [36]. Further, it is also known that the relationship between strength and damages is not clear, and it is widely accepted that damages are related to strain and drift [30].

Another problem with FBD approach is the implementation of extensive iterations and complex design procedure. To be more comprehensible, in FBD approach, check for

displacement of the structure is being carried out to find out that what will be the performance level of the structure, and it has been seen that most of the time, the drift limits defined in codes control the design. The force reduction or ductility factors, while using the realistic values for stiffness, will be much smaller with compare to the ones given in codes [36] (i.e. in many frame buildings, the calculated stiffnesses are excessive, thus these frame buildings are not being able to get the design ductility level given in codes, unless the code drift limits are exceeded [34]). Therefore, it causes iterations for redesign and meanwhile it makes the design procedure more complex and time consuming.

Furthermore, in FBD approach, equal displacement approximation of seismic response of the structure has been adopted to find the inelastic deformation capacity of the structure. For this purpose, the base shear force, obtained from the elastic response of the structure, has been reduced using force reduction factor (i.e. in seismic response, design displacement of the inelastic structure is related to the design displacement of the elastic structure through equal displacement approximation rules) [33, 36]. This approach, after long time, was discovered that it would not be proper for structures with very long and very short natural vibration periods. And even, it would be questionable for structures with medium natural vibration periods [36].

3.1.5 Force-Based Design Procedure

For the purpose of comparison between FBD approach and Direct Displacement-Based Seismic Design (DDBD) approach, FBD procedure has been discussed here and in later chapter the procedure of DDBD, for irregular reinforced concrete frames, has been discussed. A simple procedure for FBD approach, commonly used in most codes, is given in Figure 3.2 and explained briefly.

1. Estimate Structural Dimensions

As starting point, structural geometry is chosen and some preliminary calculation, usually based on vertical load combinations, are carried out for member sizes [6].

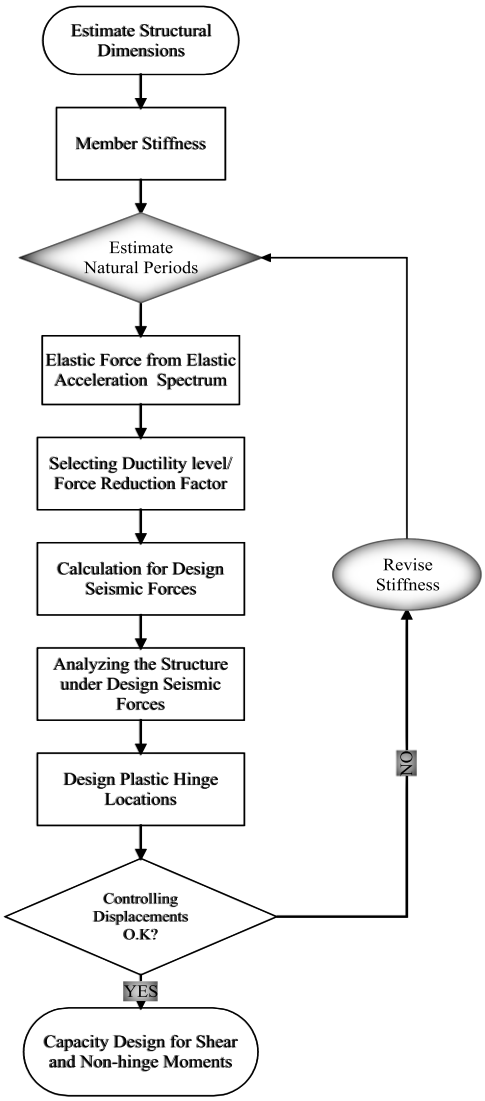

Figure 3.2. Force-Based Design Procedure
(Adopted from Priestley et al., 2007 [6])

2. Member Stiffness

Based on the initial member sizes, elastic stiffness of the members are calculated. In different codes, different assumptions are made for stiffness of the members. Sometimes as gross stiffness and sometimes as reduced stiffness to reflect the cracking of the section, especially in inelastic response region [6]. For example, in Turkish Seismic Design Code [8], to take into account the cracked section stiffness, gross section stiffness is reduced to 40% for beams, and for columns and shear walls it is reduced to between 80% and 40% , which depends on the axial load ratio.

3. Estimate Natural Periods

The next step in FBD procedure is to obtain the first natural vibration period. This can be found in most codes using Equation 3.4. From Equation 3.4 it is clear that fundamental vibration period of a structure is related to two parameters. Stiffness (K) and effective seismic mass (m_e) of an equivalent SDOF system which represent the MDOF system. The effective seismic mass is usually taken as total mass of the structure. For equivalent lateral force approach, only a single period is estimated, while in mode superposition method, multi periods are required [6].

$$T = 2\pi\sqrt{\frac{m_e}{K}} \tag{3.4}$$

In some codes some other formulas exist for calculating fundamental period, which implies that, fundamental period does not have any relation with the member stiffness and geometry. An example is given in Equation 3.5 [33].

$$T = C_1(H_n)^{0.75} \tag{3.5}$$

Where:

H_n is the building height.

C_1 is a constant which depends on the structural system.

According to Turkish Seismic Design Code, the first natural vibration period, for example, for a building type structure shall not be larger than the value given in Equation 3.6.

$$T_1 = 2\pi\left[\frac{\sum_{i=1}^{N} m_i d_{fi}^2}{\sum_{i=1}^{N} F_{fi} d_{fi}}\right]^{1/2} \tag{3.6}$$

Where:

m_i is the mass of the ith story.

F_{fi} is the fictitious force at the top of the ith story.

d_{fi} displacement at the top of the ith story due to F_{fi}.

N is the number of stories.

The fictitious forces can be obtained using Equation 2.9 of Turkish Seismic Design Code [8], assuming any value for $(V_t - \Delta_{FN})$.

4. Elastic Force from Elastic Acceleration Spectrum

In this step, the base shear force is found without considering any force reduction factor from elastic acceleration response spectrum. For example in Turkish Seismic Design Code, this force can be calculated by using following relation:

$$V_{tE} = WA(T_1) \tag{3.7}$$

Where:

W is the total seismic weight of the building structure, considering live load participation factor.

$A(T_1)$ is the spectral acceleration coefficient. And how to obtain this, will be discussed in Section 4.1.1, step 8.

T_1 is the first natural vibration period.

5. Selecting Ductility level/Force Reduction Factor

In Turkish Seismic Design Code, force reduction factor (R_a) is directly proportional to behavior factor (R), and to some extent to natural vibration period (T) and spectrum characteristic period (T_A). Force reduction factor (R_a), can be calculated using Equation 3.8. Behavior factor, in addition, is related to the type of structure, and materials used in that structure, this factor can be taken from Table 2.5 of Turkish Seismic Design Code [8].

$$R_a(T) = 1.5 + (R - 1.5)\frac{T}{T_A} \qquad (0 \leq T \leq T_A) \tag{3.8a}$$

$$R_a(T) = R \qquad (T_A < T) \tag{3.8b}$$

6. Calculation for Design Seismic Base shear

Once the force reduction factor has been obtained, to evaluate design seismic base shear, the elastic force obtained from elastic acceleration response spectrum, is divided by force reduction factor. This has been given in following equation.

$$V_t = \frac{V_{tE}}{R_a(T_1)} \tag{3.9}$$

Then this force is distributed up the height of the building, to obtain a set of lateral forces acting at the top of each floor. In Turkish Seismic Design Code, calculation for lateral force vector is directly proportional to the height of each story and the weight of that story. This has been shown in Section 4.1.2 of this study by Equation 4.24.

7. Analyzing the Structure under Calculated Design Seismic Forces

In this step, structure is analyzed under calculated lateral force vector, and internal forces in each member, especially moments at plastic hinge locations are obtained.

8. Design Plastic Hinge Locations

Here, the plastic hinge locations are designed, and then under seismic load (lateral load vector) displacements are determined.

9. Controlling Displacements

The displacements are obtained through analysis under given intensity of ground motions. The displacements are then checked with pre-defined limits of the codes. It means that it will be confirmed whether the displacements are smaller than the ones defined in the codes or not. If the calculated displacements are larger than the ones defined in codes, then redesign have to be implemented by revising the stiffness, and the calculations are repeated from step 3. If the condition is satisfied, then move to step 10 [6].

10. Capacity Design for Shear and Non-hinge Moments

Once the condition of the code limits for displacements are satisfied, the shear design of the members and the flexural design for the parts of the members which are not supposed to be in plastic hinge regions, and those members which must be protected against plastic hinge formation, are designed [6]. For this, purpose capacity design principles are recommended. Capacity design principles, are discussed in Section 4.3.

3.2 Performance-Based Seismic Design

As mentioned in previous chapters that PBSD is one of the developed approaches for performance evaluation and retrofitting of existing structures, and seismic design of new structures. Through PBSD it is possible to achieve better prediction of the behavior of the structures under seismic activities. It has attracted the attention of many researchers, recently. Different methods, such as N2 method, Capacity Spectrum method, and DDBD method were developed in connection with PBSD approach [5].

The N2 method is an approximate simple nonlinear analysis method for the seismic analysis of the structures. N stands for nonlinear and 2 stands for 2 mathematical models. Furthermore, two different mathematical models and three steps of analysis are used. Besides, in this method, pushover analysis of MDOF system is combined with response spectrum analysis of an equivalent SDOF system [37]. This method is based on the assumption that structure oscillates predominantly in first mode. In addition, in this method instead of elastic spectra, inelastic spectra with equivalent damping and period is utilized [37, 38].

Three steps of analysis are briefly explained as follows:

1. In the first step, under monotonically increasing lateral load, nonlinear analysis of MDOF system is being carried out, and stiffness, strength and ductility of the MDOF system is determined.
2. In second step, an equivalent SDOF system is defined. The nonlinear characteristics of such system are based on the relationship between base shear and top displacement of the MDOF system obtained in the first step. It should be noted that in this step one of the assumption which must be made is that the deflected shape does not change during an earthquake.

3. In the third step, nonlinear dynamic analysis of the SDOF system is performed and from this analysis maximum displacements and the corresponding ductility demands are obtained.

The capacity spectrum method is a well-known nonlinear static analysis method, which become popular rapidly. It is a graphical representation which compares the capacity of a structure with the corresponding demand due to earthquake ground motion on the structure. In this method the capacity of the structure is determined in terms of base shear force vs top displacement (i.e. force-displacement curve). Force-displacement curve is obtained through nonlinear static analysis such as nonlinear static pushover analysis. Once this curve is obtained, then it is transformed from base shear force vs roof displacement coordinates to spectral acceleration vs spectral displacement coordinates, which is then called capacity spectrum [39].

The demands of earthquake are defined in terms of acceleration-displacement response spectrums. In this format, acceleration response spectrum is plotted against displacement response spectrum, and the periods are defined as radial lines. The intersection of the capacity spectrum curve and demand spectrum curve will give the approximate performance of the structure. The corresponding displacement at this point will present the estimated displacement demand on the structure under specific earthquake ground motion [7].

A simple procedure for capacity spectrum method is briefly given as follows:

1. Obtaining capacity curve in terms of base shear force vs roof displacement by using nonlinear static analysis method, such as nonlinear static pushover analysis.
2. Calculating dynamic characteristics of the structure, for example, periods of vibration, mode shapes, modal participating factors, and effective modal mass ratios.
3. Determining capacity spectrum curve by transforming force vs displacement capacity curve to spectral acceleration vs spectral displacement spectrum format.
4. Obtaining demand curve, in acceleration-displacement response spectrum format for various damping (5% damping and upper).
5. Plotting capacity spectrum and demand curves in acceleration-displacement response spectrum format.

6. Determining the demand displacement on the structure under the given earthquake ground motion from the intersection point.

The other method is DDBD approach, which is discussed in details as follows and the detailed procedure is presented in Chapter 4.

3.2.1 Direct Displacement-Based Design

In the past for many years strength and performance of structure were considered to have same meaning, but later it was recognized that they are totally different [36]. Current codes for design of earthquake resistance structures are based on FBD approach. The strength of a structural system designed with such a method have to be larger than the design seismic force obtained by using force reduction factors. This method has several problems which are covered in earlier sections. The main problem with FBD is that it cannot design a structure for a target design objective for a given intensity of ground motion (i.e. Hazard level) with confident [29], and it cannot produce different structures with uniform risk [36].

Damages due to earthquakes for the last few decades have shown that there are still some problems exist in current seismic design codes, and that are because of the deficiencies inherent in the FBD approach (as discussed in Section 3.1.4). Therefore, a more reliable approach is needed to improve resistance of the structures to withstand such earthquakes. PBSD, initially utilized for evaluation and retrofitting of existing structures, is believed to be more reliable approach for the design of new structures and evaluation of existing structures.

Since performance levels (Section 2.4.1.1) are determined by damage states of structural and non-structural members and contents systems, and damages are directly related to displacement. Besides, displacement is a key parameter in DDBD approach, therefore, DDBD approach, among other PBSD procedures, has been developed significantly. It is widely accepted between researchers and professionals and its procedure for different types of structures is progressively under development [40].

Performance level of a structure can be determined by Displacement limits (e.g. strain limits, interstory drift, etc.). The aim of DDBD approach, proposed by Priestley and Kowalsky (2000) [4], is to obtain such performance level for a given earthquake hazard level. DDBD procedure, which is a simple procedure, is illustrated in details in

Chapter 4. The following figure (Figure 3.3, repeated here for more convenience) only shows the fundamentals of DDBD principles.

In DDBD approach maximum displacement in inelastic deformation of the structure is considered. From Figure 3.3a, it is evident that a MDOF system is presented by an equivalent SDOF system. Equivalent SDOF system is presented by effective height (H_e) and effective mass (m_e, Figure 3.3a), at the maximum displacement by a secant stiffness (i.e. effective stiffness, K_{eff}, Figure 3.3b), and an equivalent viscous damping (ξ_{eq}, Figure 3.3c). The effective stiffness of SDOF systems is significantly lower than initial stiffness of the structure [4]. The reason is that, the SDOF system presents the MDOF system at maximum inelastic response [40] (refer to Figure 3.3). Lower stiffness, consequently gives lower base shear force.

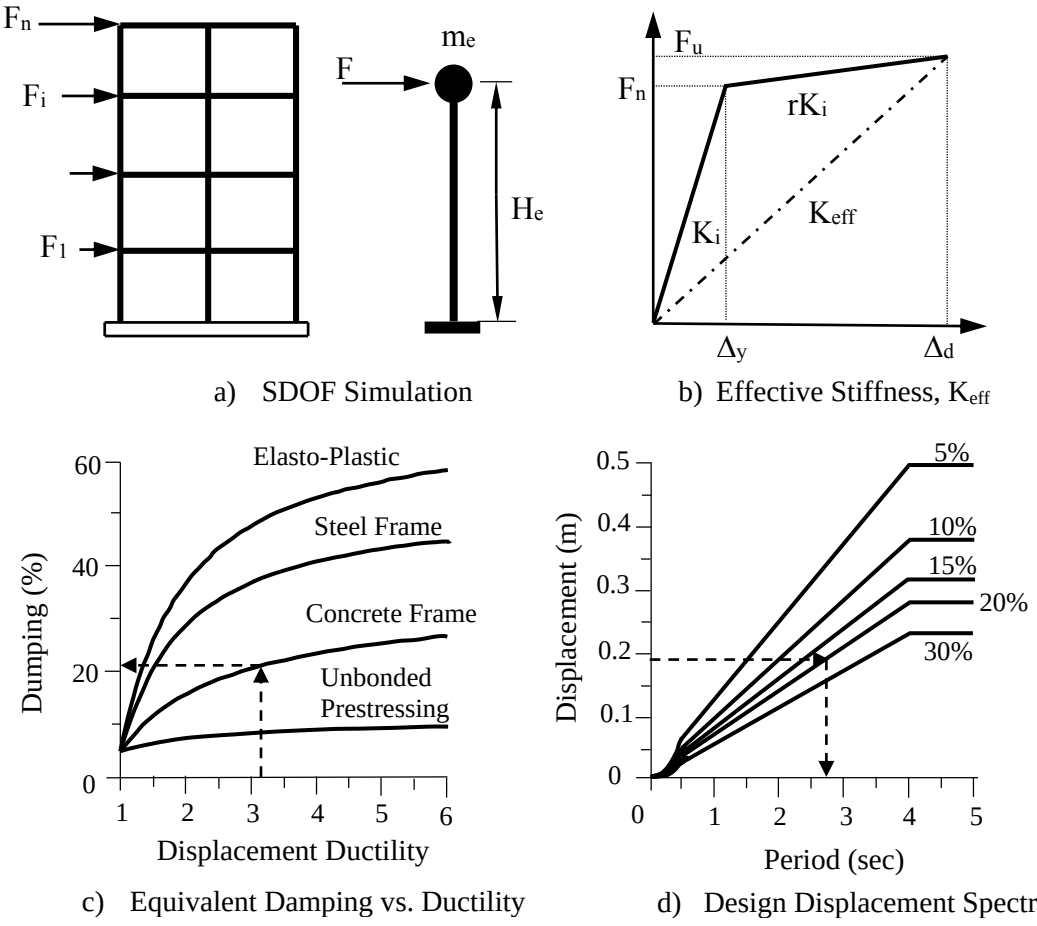

a) SDOF Simulation b) Effective Stiffness, K_{eff}

c) Equivalent Damping vs. Ductility d) Design Displacement Spectra

Figure 3.3. Fundamentals of DDBD Approach
(Adopted from Priestley et al., 2000 [4])

Once the performance level has been selected, then it is easy to find target design displacement and ductility demand. The equivalent damping, which is the combination

of 5% elastic damping and hysteretic damping due to inelastic deformation, for SDOF system can be read from Figure 3.3c for estimated displacement ductility (i.e. corresponding to ductility demand). Once the equivalent damping is determined, design displacement response spectrum for this damping is obtained, and from the design displacement response spectrum effective period corresponding to maximum design displacement is read [40].

3.3 Differences Between FBD and DDBD Approaches

The main differences between FBD and DDBD approaches are given briefly as follows:

1. First of all, FBD approach characterizes a structure with initial stiffness and elastic damping, while, DDBD approach characterizes a structures by secant stiffness and an equivalent damping.
2. Elastic natural vibration period is considered in FBD approach, in contrast, DDBD approach uses effective period.
3. In FBD approach design acceleration response spectrum is used to find the elastic base shear force. Then the obtained base shear force is reduced by using force reduction factor. On the other hand, in DDBD approach design displacement response spectrum is used to find the base shear, and there is no reduction of the obtained base shear force.
4. In FBD approach initial stiffness is assumed and the check for displacement is carried out at the end of the procedure, in order to control if the displacement is within limit. In contrary, in DDBD approach displacement limit (target displacement) is chosen, and the analysis are carried out for that displacement.
5. Ductility or force reduction factor is assumed on the bases of material type and the type of structure, in FBD approach, to reduce the base shear force (i.e. Ductility factor is used to give ductile behavior to a structure). Conversely, in DDBD approach displacement ductility demands (ductility ratio), which implies ductile behavior of a structure in inelastic region, are calculated. Ductility ratio, in DDBD procedure, is directly proportional to design

displacement and indirectly proportional to yield displacement (refer to Equation 4.9).

3.4 Background Studies

Recently, DDBD approach has been widely addressed in literature for the seismic design of different types of structures. Gulkan and Sozen (1974) [41], provided equivalent damping equations for an SDOF system, as a result of study of the non-linear behavior of RC structures for dynamic loadings. A substitute structure methodology has been developed by Shibata and Sozen (1976) [42] for RC structures, which is aimed to devise the Displacement-Based Design (DBD) method. A seismic resistance design and evaluation approach is suggested by Mohele (1992) [43]. In initial steps of this approach the calculation of stiffness, elastic period, and different strengths are included, however, it is different with compare to traditional methods for seismic design of the structure, since control of displacements are included directly in this method instead of indirect control using ductility factors. Furthermore, displacement response spectrum is used in the design process.

The initial step for the aforementioned approach, suggested by Kowalsky et al. 1995 [44], is to determine the maximum target displacement for the SDOF structure. To obtain the maximum target displacement for SDOF structure, ductile capacity of the structure is used. In this approach, an acceptable value for yield displacement is assumed, and dividing maximum target displacement of an SDOF system by the assumed yield value gives, demand displacement ductility [5]. Using this demand displacement ductility, as mentioned earlier, equivalent viscous damping is obtained, and following the same procedure, mentioned briefly in Section 3.2.1, obtaining effective period, effective or secant stiffness, and base shear force. This approach is generalized for MDOF structures by Calvi and Kingsley (1995) [45], and Calvi and Paves (1995) [46].

In addition, in DDBD approach, inelastic design spectra is applied by Chopra and Goel (2001) [47]. For the seismic design of reinforced concrete structures, the general procedure of DDBD approach, assuming initial displacement profile, has been proposed by Priestly and Kowalsky (2000) [4]. Later a DDBD procedure for RC dual wall-frame structures has been developed by Sullivan et al. 2006 [48]. In 2009, Displacement-Based Design (DBD) approach has been suggested by Belleri [49], for RC precast buildings.

DDBD code has been investigated by Sullivan et al in 2009 [50]. Pennuci et al. 2009 [51] investigated DBD approach for precast walls with additional dampers. DDBD approach for steel frame-RC wall has been proposed by Garcia et al in 2009 [52].

Furthermore, a simplified DDBD approach for the seismic design of moment resisting frames with viscous dampers is proposed in a study by Sullivan and Lago in 2012 [53]. Draft of a model code for the Displacement-Based Seismic Design of structures (DBD12), which is in "code + commentary" format, has been presented. This draft has been edited by Sullivan et al. 2012 [54]. In 2013, a DDBD approach for steel-braced reinforced concrete frames has been investigated by Malekpour et al. 2013 [55].

Some papers, related to past studies are summarized here.

M.J.N Priestley and M.J. Kowalsky (2000) [4]

In this paper the general procedure of DDBD approach is proposed for seismic design of concrete buildings. It is shown that application of this procedures is a very simple, and the results obtained are significantly different than FBD approach. The Buildings, designed with this approach should be able to satisfy the acceptable damage levels. These levels are given in terms of drift limits or material strain. Further, the acceptable limits are presented with displacement profile. Different multi-story frame and wall buildings are designed. Inelastic time history analysis are carried out and the results are compared with the target displacements.

The multi-story frame buildings presented in this study are 4, 8, 12, and 20 story frame buildings, and wall buildings are 4, 8 and 16 stories. Displacement profile (response) of the buildings designed with DDBD approach, which are obtained using time history analysis, showed good agreement with the target displacement profile, for both frame and wall buildings. Further, it was noticed that ductility level of the wall structures, decreases with increasing height of the wall.

Furthermore, it was demonstrated that the impact of foundation flexibility can merged in DDBD approach easily and accurately. Besides, it was also shown that required base shear strength from DDBD is proportional to the square of seismic intensity, while required base shear strength obtained through FBD approach is linearly proportional to the ground motion intensity.

Finally, it is concluded that DDBD approach can characterize a level of seismic design strength for the plastic hinge locations which will be better than that determined by FBD approach.

J. D. Pettinga and M. J. N Priestley (2005) [56]

In this study, regular type reinforced concrete tube-frame structures were designed, by using DDBD methodology, and their dynamic behavior were studied. Inelastic time history analysis were conducted for this propose. The results for story drift ratios, obtained from inelastic time history analysis, were little bit larger than the chosen drift limits. Therefore, some modifications were made for displacement profile and lateral force distribution. In addition, in order to reflect higher mode amplification of column shear forces, a revised form of the Modified Modal Superposition is proposed, and for bending moments of the columns an amplification factor is developed in capacity design procedure.

In this study, as mentioned earlier, six reinforced concrete tube-frame structures were designed by DDBD procedure which is proposed by Priestly and Kowalsky (2000) [4]. The frames are of 2, 4, 8, 12, 16 and 20 story height. They are of regular type in terms of story heights and span lengths. For the design displacement spectra, acceleration spectra of EC8 [22] was adopted.

Inelastic time history analysis were implemented, and the results were checked in terms of the maximum displacements with displacement profiles and the target design drift ratio, chosen 2% in this study. Initially, three different intensities of ground motion (i.e. earthquake intensities) were used in this study, which are 0.5x 1.0x and 1.5x of the design intensity. The results of the drift ratio from inelastic time history analysis exceeded the design drift ratio (2%), especially for taller frames. As a consequence some changes were made in DDBD approach proposed by Priestly and Kowalsky (2000) [4]. The first change was made in displacement profile, as given by Equation 3.10.

$$\delta_i = \frac{H_i}{H_n} \qquad \text{for } n \leq 4 \qquad (3.10a)$$

$$\delta_i = \frac{4}{3}\left(\frac{H_i}{H_n}\right)\left(1 - \frac{H_i}{4H_n}\right) \qquad \text{for } n > 4 \qquad (3.10b)$$

Where:

H_i is the height of the i^{th} story.

H_n is the total height of the frame from foundation level.

The following equation was proposed for lateral force distribution.

$$F_i = V_B \frac{\Delta_i m_i}{\sum_{i=1}^{n} \Delta_i m_i} \qquad \text{for } n \leq 10 \qquad (3.11a)$$

$$F_i = F_t + 0.9 V_B \frac{\Delta_i m_i}{\sum_{i=1}^{n} \Delta_i m_i} \qquad \text{for } n > 10 \qquad (3.11b)$$

Where:

V_B is the base shear force.

F_t is the additional force, acting at the top of roof level of the frame.

m_i is the mass of the i^{th} story.

Δ_i is the design displacement at the i^{th} story.

In addition, a drift reduction factor was also proposed to account for higher mode effects.

$$\omega_\theta = 1 - 0.01 \frac{H_n}{2} \qquad (3.12)$$

Further, a revised form of the Modified Modal Superposition approach was used. A factor in a capacity design procedure was proposed to amplify column bending moments to reflect higher mode effects. This factor, which depends on the ductility, is given in following equation.

$$\omega_m = \sqrt{\mu_\Delta} - 0.15 \frac{H_i}{H_n} \geq 1.3 \qquad (3.13)$$

Using these modification, designs for the frames were revised, and inelastic time history analysis was once again applied for the verification purpose. This time, the intensities for ground motions used in time history analysis were 0.5x, 1x, and 2x, the design intensity. The results for story drifts and displacement profile shown great agreement with respect to the results of modified DDBD approach.

T. J. Sullivan, M. J. N Priestley and G. M. Calvi (2006) [48]

In this study, DDBD procedure for dual wall-frame structures has been presented. Initially, strength proportions have been assigned to wall and frames. Displacement profiles has been developed by utilizing the strength proportions. Then the procedure of the DDBD was implemented on building type structures. And for verification, nonlinear time history analysis was carried out. The main aim of this study was to finalize the design procedure for such structures, proposed by Sullivan et al. 2005 [57].

The structures which were designed in this study are comprised of two sets of 4-, 8-, 12-, 16- and 20-story frame-wall structures. In the first set the walls are placed parallel to the frames, and no link beams were used to connect walls with frames, therefore the connection between wall and frames were maintained only by floor slabs. In second set of these structures the walls were connected with link beams to the frames. In this study, according to the procedure shown in Figure 3.4, the proportions of base shear were assigned to frames and walls as percentage. It has been mentioned that choosing of such proportions are arbitrary, and depends on the decision of designer.

However, it is noted that by choosing a larger proportions of base shear to frames (usually the proportion of base shear chosen for frames are lower than 50%) results in lower inflection height in the walls, causing maximum effective damping, and as a consequence giving possible lower base shear force. On the other hand, if lower proportion is assigned to the frames, causes walls to have heavy reinforcement and it causes to reduce story drift ratio, and as a consequence the design will not be as efficient as it must be.

In this study, the effects of beam-column joints were neglected and the strength of the beams were considered at the centerline of the columns. The strength of the beams were kept constant up the height of the frame except for roof level. The strength of the beams at roof levels were reduced 50% with compare to the beams of intermediate level. This results in a constant shear force up the height of the building for frames, satisfying the assumption made at the beginning.

Furthermore, the displacement profile was obtained as a function of the wall moment profile, by using strength proportions assigned for walls and frames. This can be

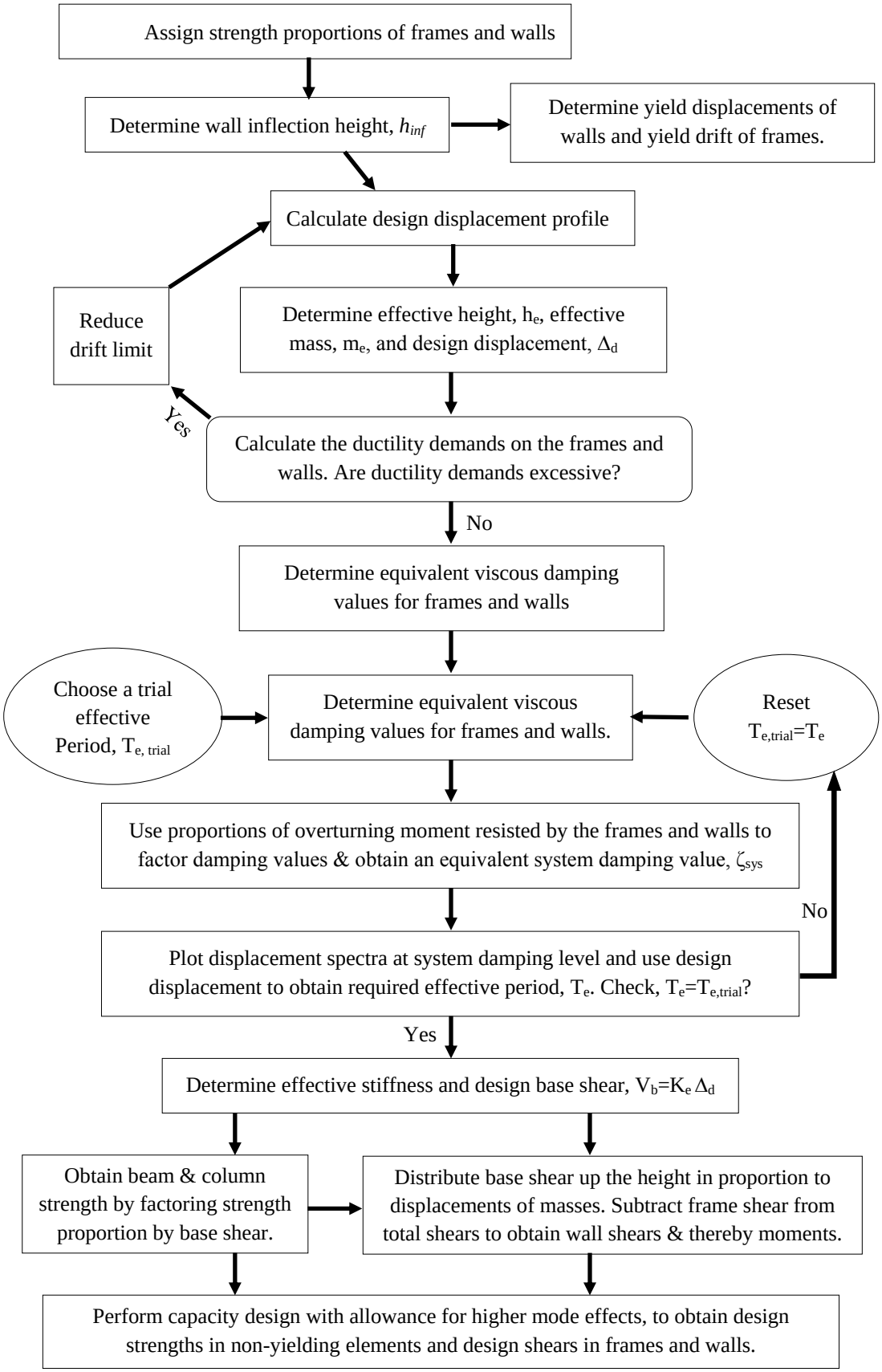

Figure 3.4. DDBD Flowchart for Frame-Wall Structures
(Adopted from Sullivan et al., 2006 [48])

seen clearly in Figure 3.4, adopted from Sullivan et al. 2006 [48], which presents DDBD procedure for frame-wall structures. Besides, equivalent viscous damping for SDOF system was obtained by combining the viscous damping of frames and walls factored by the overturning moment resisted by the frames and walls. It should be noted that the displacement profile and damping were obtained utilizing expressions suggested by Sullivan et al. 2005 [57].

Seismic weight at each story, depth of the beams at each story, and length of the walls for structures with different heights, were kept constant in this study. And it resulted in fairly constant effective damping of the system for structures with different heights. On the other hand, the results obtained for effective period and effective masses of structures with different height showed that these parameters are almost directly proportion to the height of the structures. This mean that, effective stiffness is proportion to the height of the structures inversely. As a consequence, design base shear obtained using DDBD procedure for all structures with heights from 4 to 20 stories, were close to each other.

Nonlinear time history analysis was conducted to verify the procedure, and the results of nonlinear time history analysis with the results from DDBD approach were compared in terms of displacement profile and interstory drift ratios. The results of comparison showed, excellent agreement, up to 20 story. Finally, through this study, it was shown that DDBD approach procedures for dual wall-frame structures works very good for both frame-wall structures with and without link beams.

R. Garcia, T. J. Sullivan, and G. D. Corte (2009) [52]

A DDBD procedure has been proposed for steel frame-RC wall structures, in this study. The methodology was then applied on a set of structures. To check lateral displacement of the structures and to investigate performance level of these structures, nonlinear time history analysis has been conducted. And it has been shown from the results of the analysis, that this methodology is capable of controlling lateral displacements of such system.

The procedure, proposed in this study is almost exactly similar to the procedure shown in Figure 3.4, with some differences in formulation. Which, indeed must be different for different type of materials (e.g. reinforced concrete, steel, etc.).

Five building structures comprises of steel frame and RC walls were designed using proposed methodology. The buildings are of regular type, with different number of stories (4, 8, 12, 16, and 20 story). The thickness of the walls, selected in this study, are identical, but their lengths increase as the height of the structures increase. Since walls behave as cantilever members, and it is clear that walls can take larger load in the lower levels while frames resist higher forces in upper levels. Therefore, in this study, proportions of strength assigned for walls were selected in such a way that with increase in the height of the structures, the proportions assigned for walls decrease.

It was also shown, that ductility decreases which causes the damping to decrease with increase in height of the structures. For example, for 4, 12 and 20 story steel frame-RC wall structures the ductility obtained are 3.22, 2.02, and 1.6 respectively. And meanwhile, the effective dumping of the systems are 13%, 10.6% and 9% for 4, 12 and 20 story structures, respectively.

In addition, in this study, for the verification of the responses of the structures designed with the proposed design procedure, time history analysis was conducted. The results of average displacement responses of the different structures, achieved from time history analysis, were compared with the design displacement profiles obtained through proposed DDBD methodology, for these structures. Agreement between results, were satisfactory. Meanwhile, interstory drift ratios, obtained from time history analysis, for each structure were in control of limiting drift ratio (i.e. drift ratios obtained from time history analysis for different structures, were lower than limit drift ratio). The conclusion from such results, indicate that the proposed DDBD methodology works well for the steel frame-RC wall building structures up to 20 story.

S. Malekpour, H. Ghafarzadeh, and F. Dashti (2013) [55]

DDBD procedure for structures composed of reinforced concrete frames and steel bracings is investigated in this study. Three identical structures with different heights were conducted. To verify the procedure for such type of structures, nonlinear time history analysis was implemented. The results obtained from nonlinear time history analysis, showed that the DDBD procedure for the seismic design of such structures are very effective.

The DDBD procedure for such types of structures is very similar to the one presented for dual wall-frame structures (shown in Figure 3.4).The procedure has been shown in Figure 3.5 for more convenience. As can be seen from this figure that initially, strength proportions must be assigned to RC frames and steel bracings. The important, step is to determine displacement profile for such structures. Once this has been done, then it would be easy to find ductility of the equivalent SDOF system, and consequently, equivalent damping, effective period, secant stiffness (effective stiffness) and finally base shear force.

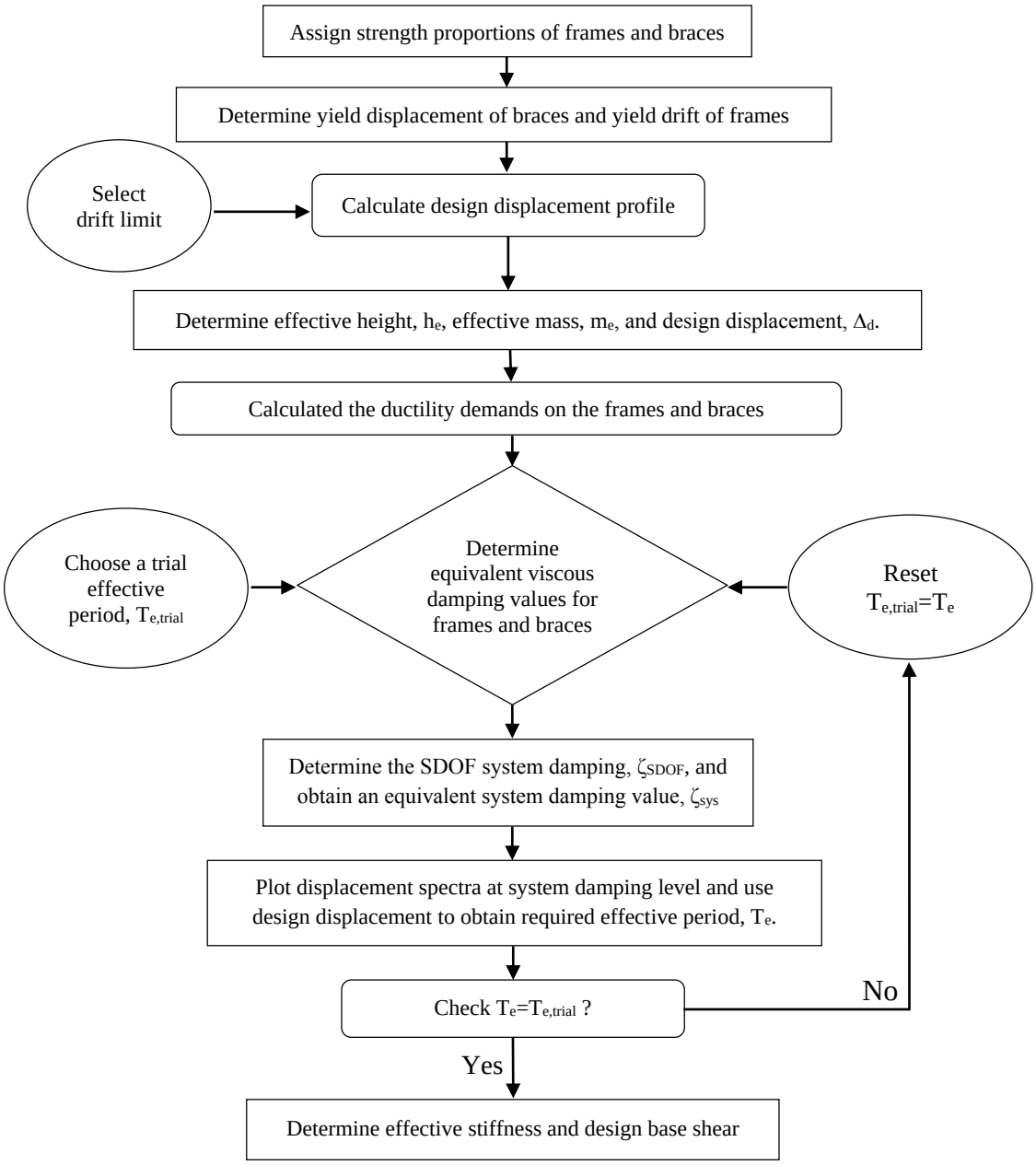

Figure 3.5. DDBD Flowchart for Steel Braced-RC Frames
(Adopted from Malekpour et al., 2013, [55])

The procedure has been implemented on three identical structures with different number of stories, in this study. The structures are composed of RC frames and steel bracings, and they have the height of 4, 8 and 12 story, besides, they are all regular in plans. The bracings and frames are connected directly. The portion of base shear assigned for 4, 8 and 12 story structures are 60%, 60% and 50% respectively. The equivalent viscous dampings obtained for these structures are almost constant values (i.e. equivalent viscous dampings are 13.62%, 13.64%, and 13.49% for 4, 8 and 12 story structures, respectively). The effective periods, obtained by this procedure, increase with increase in height of the structures.

For the evaluation purposes, nonlinear time history analysis was conducted and analysis were done using PERFORM 3D. Seven accelerograms were selected for the nonlinear time history analysis, they were scaled to design spectrum used in DDBD procedure.

The results from time history analysis, for 4 and 8 story structures showed good agreement. The interstory drift ratio were lower than the design interstory drift ratio, except for one case of acclerogram for 4 story, and three accelerograms for 8 story were higher than the design drift ratio. On the other hand, the results for 12 story showed, indeed this procedure is not suitable for 12 story structure. Because, the interstory drift ratios were significantly higher than design drift ratio for all acclerograms.

In addition, a check has been made on performance level of all three structures. For this purpose, plastic hinge rotations for each member were calculated. The demand capacity ratios were obtained, dividing calculated values by the limit values. The demand capacity ratios, showed that all three structures were satisfying the life safety performance level. On the contrary, only 4 and 8 story structures satisfied the immediate occupancy performance level.

CHAPTER 4

DIRECT DISPLACEMENT-BASED SEISMIC DESIGN

4.1 Direct Displacement-Based Seismic Design Procedure

The procedure is general, however, in some parts it is different for regular and irregular frame buildings. Regular frame buildings are those which has equal wide bays, there are no design torsional eccentricity and no vertical offset exists [6]. The irregularity discussed in this study, are not the ones provided in codes (e.g. Turkish Seismic Design Code). The frames used in this study, are all irregular type of frames in terms of height of the story heights and wide of the bays, according to Priestly et al. 2007 [6]. The Procedure has been described stepwise as follows.

4.1.1 Representation of MDOF System by an SDOF System

In this stage, a MDOF system is presented by an equivalent SDOF system. The equivalent SDOF system has equivalent mass and height (refer to Figure 4.1, adopted from B. Massena. 2010 [58]). The first mode of inelastic response of the structure is taken into account. The following steps are needed [6, 59].

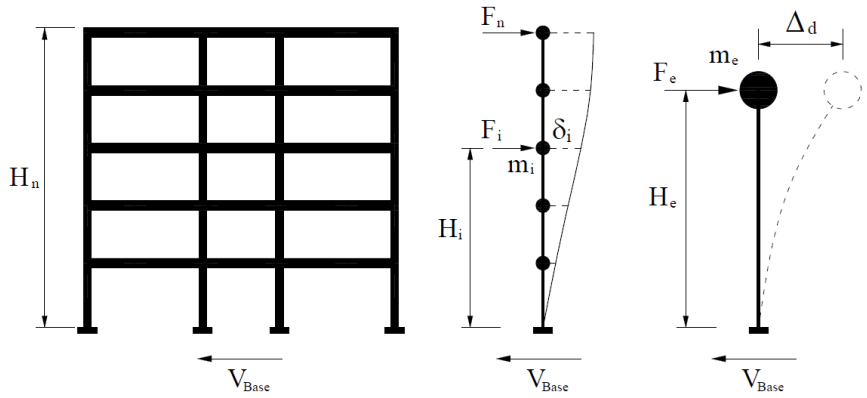

a) MDOF System b) SDOF System

Figure 4.1. Simplified Model of MDOF System Represented by SDOF System (Adopted from B. Massena, 2010 [58])

1. Choosing Deformation Level

In this step, it is needed to choose a deformation level. This can be strain, rotation, drift, curvature, or displacement. Usually an interstory drift limit is chosen, which can be a performance objective for a specific intensity of ground motion [6, 59].

2. Design Story Displacement

In order to find the design story displacements, it is required to find the normalized inelastic mode shape. For frame building structures, story height and total height of the frame are two parameters determining the normalized inelastic mode shape. The following formulas are used for this purpose [6, 29, 31].

$$\delta_i = \frac{H_i}{H_n} \qquad for \quad n \leq 4 \tag{4.1}$$

$$\delta_i = \frac{4}{3}\left(\frac{H_i}{H_n}\right)\left(1 - \frac{H_i}{4H_n}\right) \qquad for \quad n > 4 \tag{4.2}$$

Where:

H_i is the i^{th} story height from the ground/foundation level (Figure 4.1).

H_n is the total height of the structure.

n is the number of stories.

The design displacement is then equal to:

$$\Delta_i = \omega_\theta \, \delta_i \, \frac{\Delta_c}{\delta_c} \tag{4.3}$$

Where:

ω_θ is the drift reduction factor to take into account the higher mode effects.

δ_c is the inelastic mode shape of the critical story, and usually the first story will be critical story (the story which will have the largest drift ratio).

Δ_c is the design displacement of the critical story.

Drift reduction factor (ω_θ) will have negligible effects for the number of stories less or equal to 10 ($n \leq 10$), and it can be calculated using Equation 4.4 [58]:

$$\omega_\theta = 1.15 - 0.0034 H_n \leq 1.0 \tag{4.4}$$

Where:

H_n (in m) is the total height of the building.

Since the most critical displacement of a frame building structure in first mode shape corresponds to displacement of the first story, therefore, design displacement (Δ_c) can be calculated by using Equation 4.5 [6, 58]:

$$\Delta_c = \theta_d H_1 \tag{4.5}$$

Where:

H_1 is the height of the first story.

θ_d is the interstory drift ratio chosen at the beginning for a given intensity of ground motion.

3. Design Displacement of the Equivalent SDOF System

After obtaining the design displacement profile, it is then easy to find the design displacement of the equivalent SDOF system by using the following equation [6, 58].

$$\Delta_d = \sum_{i=1}^{n} (m_i \Delta_i^2) \Big/ \sum_{i=1}^{n} (m_i \Delta_i) \tag{4.6}$$

Where:

m_i is the mass of the i^{th} story

Δ_i is the displacement of the i^{th} story.

4. Effective Height of the Equivalent SDOF System

Effective height for the equivalent SDOF system can be easily obtained by using following equation [6, 58]:

$$H_e = \sum_{i=1}^{n} (m_i \Delta_i H_i) \Big/ \sum_{i=1}^{n} (m_i \Delta_i) \tag{4.7}$$

5. Effective Mass of the Equivalent SDOF System

Effective mass of the equivalent SDOF system can be obtained as follows [6, 58]:

$$m_e = \frac{\sum_{i=1}^{n} (m_i \Delta_i)}{\Delta_d} \tag{4.8}$$

6. Design Displacement Ductility Factor for Equivalent SDOF System

This factor is calculated as follows:

$$\mu = \frac{\Delta_d}{\Delta_y} \tag{4.9}$$

Where:

Δ_d is design displacement of the equivalent SDOF system, given by Equation 4.6.

Δ_y is yield displacement of the equivalent SDOF system.

Yield displacement (Δ_y) for irregular frames having three bays (refer to Figure 4.2), can be calculated through Equation 4.10 [6]:

$$\Delta_y = \frac{2M_1\theta_{y_1} + M_2\theta_{y_2}}{2M_1 + M_2} H_e \tag{4.10}$$

Where:

θ_{y_i} is the yield drift.

M_1 and M_2 are the moment contribution to the total overturning moment from outer and inner bays respectively.

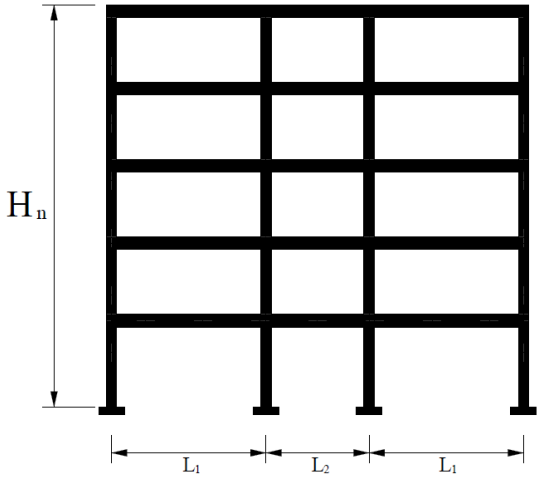

Figure 4.2. Irregular Reinforced Concrete Frame

Yield drift (θ_{y_i}) is given as follows:

$$\theta_{y_i} = 0.5\varepsilon_y \frac{L_{b_i}}{h_{b_i}} \tag{4.11}$$

Where:

L_{b_i} is the length of the beam of the i^{th} bay.

h_{b_i} is the depth of the beam of the i^{th} bay.

ε_y is the yield strain, it can be obtained using following equation [6, 58]:

$$\varepsilon_y = \frac{f_{ye}}{E_s} \tag{4.12}$$

Where:

E_s is the modulus of elasticity of the steel reinforcement.

f_{ye} is the expected yield strength of steel reinforcement.

The expected yield strength is taken 10% larger than characteristic yield strength of steel reinforcement as per recommended by Priestley et al. 2007 [6], and it is equal to:

$$f_{ye} = 1.1 f_y \tag{4.13}$$

For a three bay irregular frame the total overturning moment can be written in the following form (refer to Figure 4.5) [6, 58]:

$$M_{OTM} = 2M_1 + M_2 \tag{4.14}$$

The absolute values of M_1 and M_2 are not needed, here just the ratio of M_1/M_2 is required. And the selection of this ratio is arbitrary for designer. If the beam depth is being kept constant for all bays, and the moment capacities of the outer and inner frames are made equal [6], then:

$$\frac{M_1}{M_2} = 1 \quad \Rightarrow \quad M_1 = M_2$$

Therefore, Equation 4.10 can be simplified to the following form for a three bay irregular frame building [6, 58], (see Figure 4.5).

$$\Delta_y = \frac{2\theta_{y_1} + \theta_{y_2}}{3} H_e \tag{4.15}$$

7. Equivalent Viscous Damping for the Equivalent SDOF System

For reinforced concrete frames, the equivalent viscous damping of SDOF system is the combination of the elastic 5% viscous damping and hysteretic damping [6].

$$\xi_{eq} = 0.05 + 0.565\left(\frac{\mu - 1}{\mu\pi}\right) \tag{4.16}$$

In Equation 4.16, 0.05 is the elastic viscous damping and the remaining part is the hysteretic damping.

8. Effective Period at Peak Displacement Response

To find the effective period at peak displacement response, it is required to find the displacement response spectrum for effective or equivalent damping (i.e. the design displacement response spectrum). This can be obtained using following relation [6]:

$$\mathrm{S}_{D,\xi} = \mathrm{S}_{D_{e,5}} \left(\frac{0.10}{0.05 + \xi_{eq}} \right)^{0.5} \tag{4.17}$$

Where:

$\mathrm{S}_{D_{e,5}}$ is the elastic displacement response spectrum for 5% damping and it can be obtained through following equation [6].

$$\mathrm{S}_{D_{e,5}} = \mathrm{S}_{ae}(T) \frac{T^2}{4\pi^2} \tag{4.18}$$

Where:

$\mathrm{S}_{ae}(T)$ is elastic acceleration response spectrum for 5% damping, and according to Turkish Seismic Design Code [8], it is given as follows:

$$\mathrm{S}_{ae}(T) = \mathrm{A(T)}\ \mathrm{g} \tag{4.19}$$

Where:

g is gravity acceleration equal to $9.81\mathrm{m/sec^2}$

$\mathrm{A(T)}$ is spectral acceleration coefficient. It is given as follows:

$$\mathrm{A(T)} = A_0 I\ \mathrm{S(T)} \tag{4.20}$$

Where:

A_0 is the effective ground acceleration coefficient.

I is importance factor, and according to the importance of the building (e.g. office building, hospital, etc.), it can be taken from Table 2.3 of Turkish Seismic Design Code [8].

$\mathrm{S(T)}$ is spectrum coefficient.

Effective ground acceleration coefficient (A_0) is given in Table 2.2 of Turkish Seismic Design Code [8], for more convenience it has been presented as Table 4.1. From this table, it can be seen clearly that A_0 depends on the seismic zone.

Table 4.1. Effective Ground Acceleration Coefficient (A_0) [8]

Seismic Zone	A_0
1	0.40
2	0.30
3	0.20
4	0.10

Spectrum coefficient S(T) can be calculated using the set of Equation 4.21, adopted from Turkish Seismic Design Code [8].

$$\begin{aligned} &0 \le T \le T_A && S_e(T) = 1 + 1.5\,\frac{T}{T_A} \\ &T_A < T \le T_B && S_e(T) = 2.5 \\ &T_B < T && S_e(T) = 2.5\left[\frac{T_B}{T}\right]^{0.8} \end{aligned} \qquad (4.21)$$

Where:

T is the vibration period of linear single-degree-of-freedom system.

T_A and T_B are spectrum characteristic periods.

Spectrum characteristic periods, are given in Table 2.4 of Turkish Seismic Design Code [8], presented here for more convenience as Table 4.2. As can be seen that these periods have correlation with local site classes. In addition, each local site class (Table 6.2 of Turkish Seismic Design Code) depends on the soil group (Table 6.1 of Turkish Seismic Design Code) and the thickness of the soil layer (topmost layer) [8].

Table 4.2. Spectrum Characteristic Periods [8]

Local Site Class	T_A (sec)	T_B (sec)
Z_1	0.10	0.30
Z_2	0.15	0.40
Z_3	0.15	0.60
Z_4	0.20	0.90

Each Structure have a natural vibration period for a specific damping. Each of these structures shows a specific response to a particular component of ground motion. The behavior of such structural systems are similar to SDOF system. If peak values of the responses of these structures are plotted with respect to their natural vibration periods, given that damping is constant this will give a response spectrum, for a specific damping. Response spectrum can be presented in terms of acceleration, velocity or displacement [60]. In current seismic codes, for example, in Turkish Seismic Design Code, response spectrum is given in terms of acceleration.

In DDBD method, displacement response spectrum is used. There must be a corner period, which corresponds to the maximum value of the displacement response spectrum (i.e. the period in which displacement response spectrum reaches it is maximum value, and displacement becomes independent of period), and after reaching to the corner period the displacement will be constant. This value is denoted as T_D in EC8 (EUROCODE 8: *Design of structures for earthquake resistance -Part 1: General rules, seismic actions and rules for buildings* [22]), and according to EC8 this period is equal to 2sec. However, researches has shown that the assumption of constant displacement after 2sec is inappropriate for large magnitude earthquakes found in many regions. Facioli et al. 2004 [61], showed that the distance of structure from the epicenter and the magnitude of the earthquake affect the corner period (T_D), therefore it would be better to use larger values for corner period rather than 2sec. In addition, the lower effective stiffness of SDOF system will result in longer effective period, to adjust the design displacement spectrum to be useful for the longer value of effective periods of the SDOF system, it is required to use larger values for corner period [4].

In Turkish Seismic Design Code [8], nothing has been mentioned about such period, therefore, the displacement up to 5sec has been calculated, and after 5sec it has been assumed to be the maximum constant displacement [6]. In addition, since using Equation 4.17 to Equation 4.21, it is not possible to obtain a constant portion for displacement, therefore acceleration and displacement response spectrums are shown up to 5sec in Figure 4.3.

Finally, by entering design displacement (Δ_d) on the design displacement response spectrum for equivalent damping of the given figure, the corresponding effective period can be read as shown in Figure 4.3.

$$\Delta_d \quad \Longrightarrow \quad T_{eff}$$

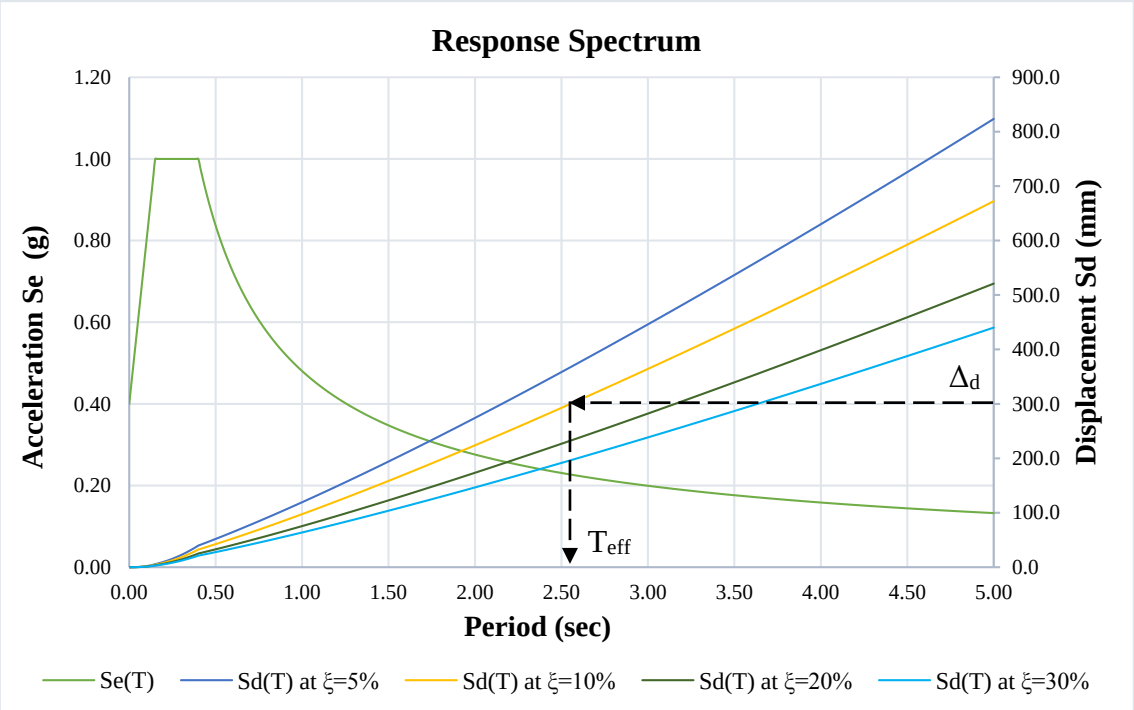

Figure 4.3. Elastic Acceleration (S_e) and Design Displacement (S_d) Response Spectrum for Different Damping Values.

9. Effective Stiffness of the Equivalent SDOF System

Effective stiffness of the SDOF system, shown in Figure 4.4, can be gained using Equation 4.22, given below [6].

$$K_{eff} = \frac{4\pi^2}{T_{eff}^2} m_e \tag{4.22}$$

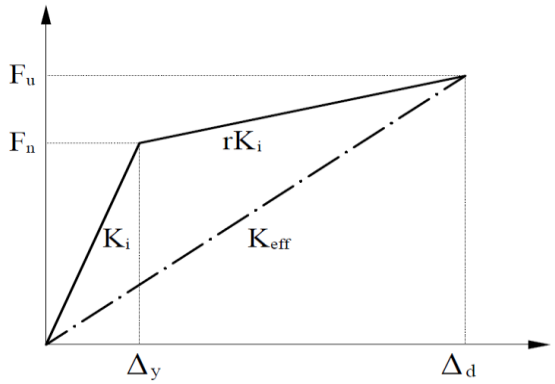

Figure 4.4. Effective Stiffness of the Equivalent SDOF System (Adopted from Priestley et al., 2007 [6])

10. Base Shear Force

The base shear force, finally is equal to:

$$V_{Base} = K_{eff}\, \Delta_d \tag{4.23}$$

4.1.2 Design Actions for MDOF System from SDOF Base Shear Force

1. Calculation of Lateral Forces at the Top of Each Story

In this section, the distribution of the base shear force found earlier (Equation 4.23) to each story of the MDOF system (i.e. MDOF frame) is summarized. For this purpose Equation 4.24, given in Turkish Seismic Design Code, is adopted (see Figure 4.5).

$$F_i = (\, V_{Base} - \, \Delta F_N) \frac{m_i H_i}{\sum_{i=1}^{n} m_i H_i} \tag{4.24}$$

ΔF_N is the additional equivalent seismic load, acting at the top of the Nth floor, and it is equal to:

$$\Delta F_N = 0.0075 N\, V_{Base} \tag{4.25}$$

N is the number of stories.

H_i is the height of the ith story of the building which is measured from the top foundation level (In buildings with rigid peripheral basement walls, height of ith story of the building measured from the top of ground floor level) [8].

2. Calculation of the Total Overturning Moment (M_{OTM})

Once the forces at the top of each story is obtained, then total overturning moment at the base of the building can be found from the following equation:

$$M_{OTM} = \sum_{i=1}^{n} F_i H_i \tag{4.26}$$

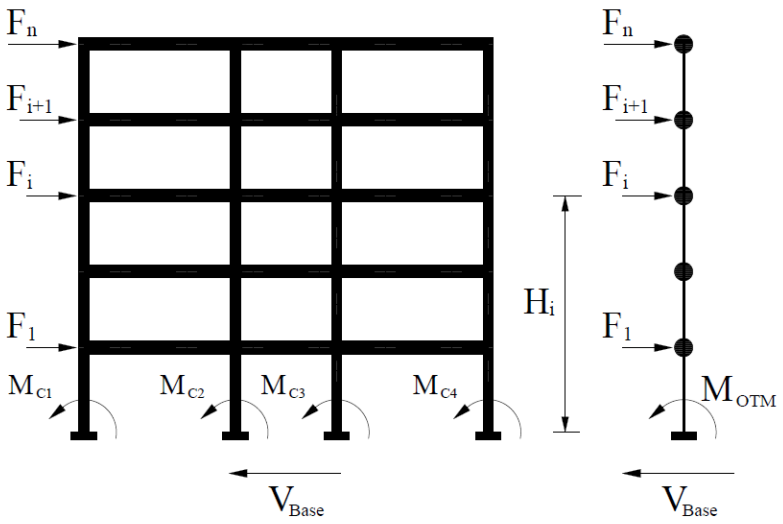

Figure 4.5. Story Forces and Total Overturning Moment (M_{OTM})
(Adopted from Priestley et al., 2007 [6])

3. P-Delta Effects

P-Delta effects should also be included if they are being required (the requirement has been provided in next paragraph). For this purpose, the stability index is calculated by following relation:

$$\theta_\Delta = \frac{P\Delta_{max}}{M_D} \tag{4.27}$$

Where

$M_D = M_{OTM}$ and $\Delta_{max} = \Delta_d$ [58].

P is the total seismic weight of the building considering 100% of live load.

If $0.1 \leq \theta_\Delta \leq 0.33$ P-Delta effects should be considered. If $\theta_\Delta > 0.33$, then the structure must be made stiffer [58], and the calculations should be revised. Further, if $\theta_\Delta < 0.1$, then there is no need to take into account the P-Delta effects. The base shear force is amplified (if $0.1 \leq \theta_\Delta \leq 0.33$) and will be found as follows [58]:

$$V_{Base} = K_{eff}\,\Delta_d + C\frac{P\Delta_d}{H_e} \tag{4.28}$$

C is a constant and for reinforced concrete structures, C=0.5 is used.

After calculating base shear considering P-delta effects, the base shear is distributed again using Equation 4.24.

4. Story Shear Forces

In next step the shear forces at each story level (i.e. story shears) are found using Equation 4.29. This has been shown in following figure:

$$V_{Si} = \sum_{k=i}^{n} F_k \tag{4.29}$$

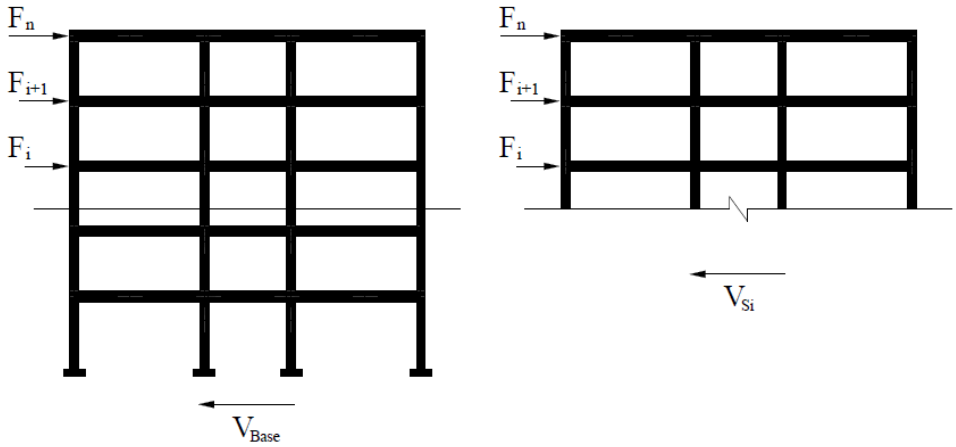

Figure 4.6. Story Shear Forces
(Adopted from B. Massena., 2010 [58])

4.2 Analysis of the Frame Based on Equilibrium Consideration

Two different methods of structural analysis under lateral forces vector are given by Priestley et al. 2007 [6], in DDBD approach, for determination of moment capacities at plastic hinge locations. The first one is analysis of the frame under lateral forces based on relative stiffness of the members. And the second one is based on equilibrium consideration of the nodes. Here only the latter is being considered.

4.2.1 Beam Internal Forces

4.2.1.1 Beam Shear Forces

Total beam shear forces up the height of the building, is equal to the tension (T) or compression (C) seismic axial force in the exterior columns. These forces are equal with each other in magnitude. For regular frames having three bays (i.e. frames with equal inner and outer bays) they can be obtained from the following relationship [6, 58].

$$\sum_{i=1}^{n} V_{Bij} = T = (\sum_{i=1}^{n} F_i H_i - \sum_{j=1}^{m} M_{Cj}) \Big/ L_{Base} \tag{4.30}$$

Where:

L_{Base} is the distance between columns under tension and compression (e.g. for regular three bays frame, this value can be taken as the distance between exterior columns).

$\sum_{i=1}^{n} V_{Bij}$ is the total beam shear forces up the height of the building for j^{th} bay.

$\sum_{j=1}^{m} M_{Cj}$ is the total moment at the base of the first floor columns (Figure 4.5).

To avoid soft story mechanism of the first story, the contraflexure height for columns of the first story is considered at the 0.6 of the height of that story ($0.6H_1$) [6] from the base of the column, therefor $\sum_{j=1}^{m} M_{Cj}$ will be equal to:

$$\sum_{j=1}^{m} M_{Cj} = 0.6 H_1 V_{Base} \tag{4.31}$$

For an irregular frame (e.g. a three bay irregular frame), Equation 4.30 can be arranged for different bays as follows (refer to Figure 4.7):

For outer bays:

$$\sum_{i=1}^{n} V_{Bi1} = \frac{M_1}{2M_1 + M_2} (\sum_{i=1}^{n} F_i H_i - \sum_{j=1}^{m} M_{Cj}) \Big/ L_1 \tag{4.32}$$

For inner bay:

$$\sum_{i=1}^{n} V_{Bi2} = \frac{M_2}{2M_1 + M_2}\left(\sum_{i=1}^{n} F_i H_i - \sum_{j=1}^{m} M_{Cj}\right) \Big/ L_2 \qquad (4.33)$$

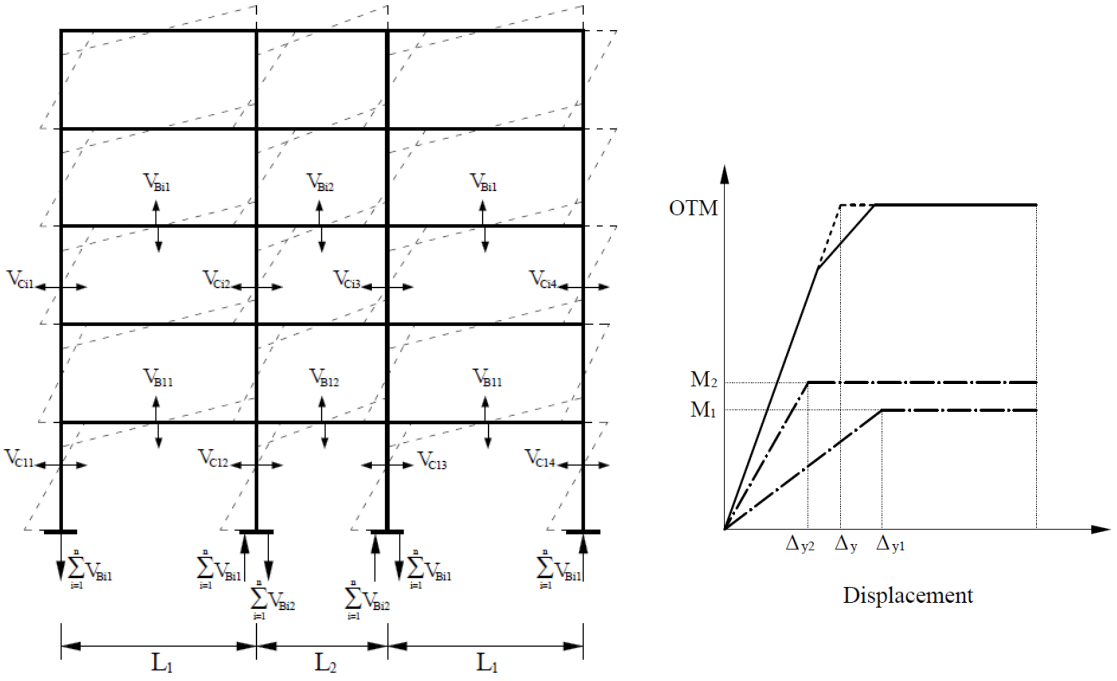

a) Beam and Column Moments and Shear forces b) Overturning Moment

Figure 4.7. Seismic Response of an Irregular Frame
(Adopted from Priestley et al., 2007 [6])

M_1 and M_2 are the moment contribution from the outer and inner bays, respectively, to the total overturning moment, and the ratio of M_1/M_2 is already known from Section 4.1.1, at 6th step while calculating design displacement ductility factor. L_1 and L_2 are the length of the outer and inner bays, respectively (see Figure 4.7).

Once the total beam shear forces up the building is attained for each bay. And to keep in mind that drift in each story shall not differ significantly than design drift, it is important to distribute total beam shear vertically according to seismic demand. Therefore, total beam shears are distributed to the beams vertically in a bay with proportion to the story shears below the beam under consideration. This can be done by following equation:

$$V_{Bij} = \sum_{i=1}^{n} V_{Bij} \ \frac{V_{Si}}{\sum_{i=1}^{n} V_{Si}} \tag{4.34}$$

Where:

V_{Si} is the i[th] story shear force, given by Equation 4.29.

4.2.1.2 Beam Moments

After obtaining shear forces in beams, then it becomes very easy to find the moments at centerlines of columns for each end of the beam, as follows:

$$M_{Bij,l} + M_{Bij,r} = V_{Bij}\, L_{Bij} \tag{4.35}$$

Where:

L_{Bij} is the length of the j[th] beam of the i[th] story from center to center of the columns.

$M_{Bij,l}$ and $M_{Bij,r}$ are the beam moments at the center of columns of the left and right side end of the j[th] beam in the i[th] story.

Normally $M_{Bij,l}$ and $M_{Bij,r}$ are not equal, but here assuming equal moments at the both end of the beams, Equation 4.35 can be simplified to the following form [6]

$$M_{Bij,l} = M_{Bij,r} = V_{Bij} \frac{L_{Bij}}{2} \tag{4.36}$$

Since for design purposes the design moments for beams should be taken at the face of the supports (e.g. at the face of columns), thus, the moments at the face of columns can be reduced which depends on the column size at the direction of the earthquake (h_c):

$$M_{Bij,des} = M_{Bij,l} - V_{Bij} \frac{h_c}{2} \tag{4.37}$$

4.2.2 Column Internal Forces

4.2.2.1 Column Shear Forces

Story shear forces are distributed to columns. This can be done by using a ratio of 1:2 outer and inner columns (i.e. shear forces in interior columns will be two times larger than shear forces in exterior columns) [6, 31, 58]. Shear forces, in this case, for each of exterior column at ith story is equal to:

$$V_{C,ext,i} = \frac{V_{Si}}{2(1 + \sum_{k=1}^{n} N_{int,k,i})} \tag{4.38}$$

Where:

V_{Si} is the ith story shear force.

$\sum_{k=1}^{n} N_{int,k,i}$ is the total number of k columns of the frame at the ith story.

As mentioned above, the shear force in each individual interior column will be doubled, thus:

$$V_{C,int,i} = \frac{V_{Si}}{(1 + \sum_{k=1}^{n} N_{int,k,i})} \tag{4.39}$$

4.2.2.2 Column Moments

As mentioned in Section 4.2.1, to avoid the soft story mechanism at the first story, the contraflexure height at the first story columns is considered at the height of 0.6 from the base of the column. Therefore, the column moments at the base of the first story is equal to (refer to Figure 4.8) [6].

$$M_{C1j,base} = 0.6 H_1 V_{C1j} \tag{4.40}$$

Where:

H_1 is the height of the first story (between level 0 and 1).

V_{C1j} is the shear force at jth column of the first story.

Moments at the top of first story columns at the center line of the beams are found using following equation:

$$M_{C1j,top} = 0.4H_1V_{C1j} \tag{4.41}$$

The moments at the base of the second story columns can be obtained from the equilibrium of the moments at the joints (Figure 4.8), this can be obtained from following relation:

$$M_{C2j,bot} = M_{B1,l} + M_{B1,r} - M_{C,1,top} \tag{4.42}$$

Where:

$M_{B1.l}$ is the left end beam moment at the centerline of the column.

$M_{B1.r}$ is the right end beam moment at the centerline of the column.

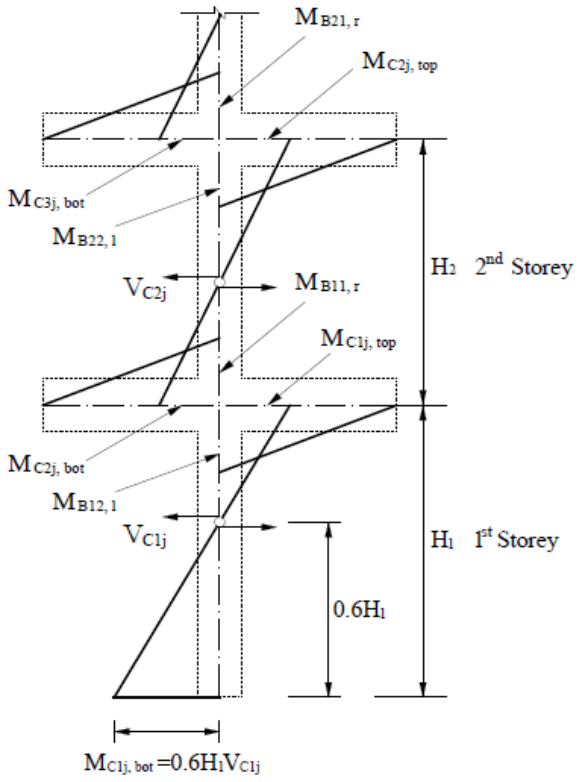

Figure 4.8. Column Moments from Joint Equilibrium
(Adopted from Priestley et al., 2007 [6])

The moment at the top of the same column is obtained using following relation:

$$M_{C2j,top} = V_{C2j}\, H_2 - M_{C,2,bot} \tag{4.43}$$

To obtain the moments at the top and bottom of the other columns up the building height vertically, the same procedure is implemented (Figure 4.8) [6].

4.3 Capacity Design Principles for DDBD

The main goal of DDBD is to make sure that a predefined performance objective of a structure for a given intensity of ground motion is obtained through determination of required strength of the structure. Usually, performance objectives are defined in terms of deformations (e.g. drift limits). Drift limit implies that a structure can go up to a maximum inelastic deformation and this requires the structure to be ductile. Hence, in members of the structure, it causes the occurrence of the inelastic rotations (plastic hinges). For ductile structures formation of plastic hinges in specific locations are important in order to dissipate energy, induced by earthquake ground motions [6].

Capacity design procedures are used for ductile structures in large earthquakes, to avoid plastic hinges in undesirable locations and to obtain the required moment capacity of the desired plastic hinge locations, and to make sure that inelastic shear failure in no case will occur even in plastic hinge locations. First of all, in capacity design process, different element of earthquake resistance system is chosen and plastic hinge locations are determined [62]. Next strength of the members at undesirable locations for plastic hinges are amplified in order that members remain elastic, by using overstrength factor ($\emptyset^0$), to take into account the applied maximum overcapacity moments at plastic hinge locations and dynamic amplification factor (ω) that higher mode effects are being considered [6, 54, 59].

The reason for using dynamic amplification factor is that, in DDBD approach, as mentioned, only first inelastic mode of vibration is considered. But the fact is that the higher modes of vibrations affect the actual response of the structure. However, for the flexural design of plastic hinge locations, the moments obtained from only first mode vibration is considered, because higher modes of vibrations do not affect plastic hinge

locations. And the remaining parts, for flexural and shear design, the moments and shears obtained from DDBD procedure are amplified.

Actual flexural strength of a member will be larger than the design strength in plastic hinge locations when inelastic behavior or response of the member is considered. The reason behind such exceedance is that, first of all, actual material strength will normally be larger than the nominal or characteristic values used in the design of the member. For example, in reinforced concrete members, compressive strength of concrete and yield strength of reinforcement. Secondly, ignoring strain hardening of reinforcement bars in such members while designing the members. The actual cross sectional size of the members or/and the area of reinforcement bars maybe larger than the exact required values. Therefore, for protecting other parts from inelastic failure (i.e. from occurring plastic hinges), overstrength factors are used [6, 59, 62].

General requirements for capacity design is given by following equation:

$$\emptyset_s S_D \geq S_R = \emptyset^0 \omega S_E \tag{4.44}$$

Where:

S_D is the design strength of the capacity protected action.

$\emptyset_s$ is strength reduction factor.

S_R is required strength.

S_E is the value of the design action being capacity protected, corresponding to the design lateral force distribution found from the DDBD procedure.

The focus of this study is on seismic performance of irregular reinforced concrete moment resisting frame buildings. Reinforced concrete frames are the combination of horizontal and vertical members (beams and columns). To have a desired mechanism for such frames, it is required to have strong columns and weak beams (i.e. to satisfy the concept of weak-beam strong-column, Figure 4.9), this implies that plastic hinges occur in beams rather than columns and in DDBD this concept can be satisfied by utilizing capacity design principles [6, 29].

4.3.1 Capacity Design for Frames

Since in previous paragraph it has been mentioned that the focus of this study is DDBD for irregular reinforced concrete frame buildings in the content of PBSD of structures. Therefore, here capacity design principles are limited for the design of columns and beams (individual elements of a frame) to obtain the desired mechanism. First of all it is necessary to choose a desired plastic mechanism, and once it has been chosen then it becomes necessary to determine plastic hinge locations.

In Figure 4.9, for example, two different mechanisms for a frame has been shown with the same maximum displacement. Figure 4.9a presents a beam sway mechanism, a desired mechanism, having smallest inelastic rotation (θ_1) demands in plastic hinges which are very close to the inelastic drift ratio in each story. On the other hand, Figure 4.9b represents column sway mechanism, an unwanted mechanism. As can be seen from Figure 4.9b that inelastic rotation at first story is very large to compare it with the inelastic rotation of the Figure 4.9a ($\theta_1 \ll \theta_2$) which causes the soft story to be form (a critical failure of the frames) [6, 62].

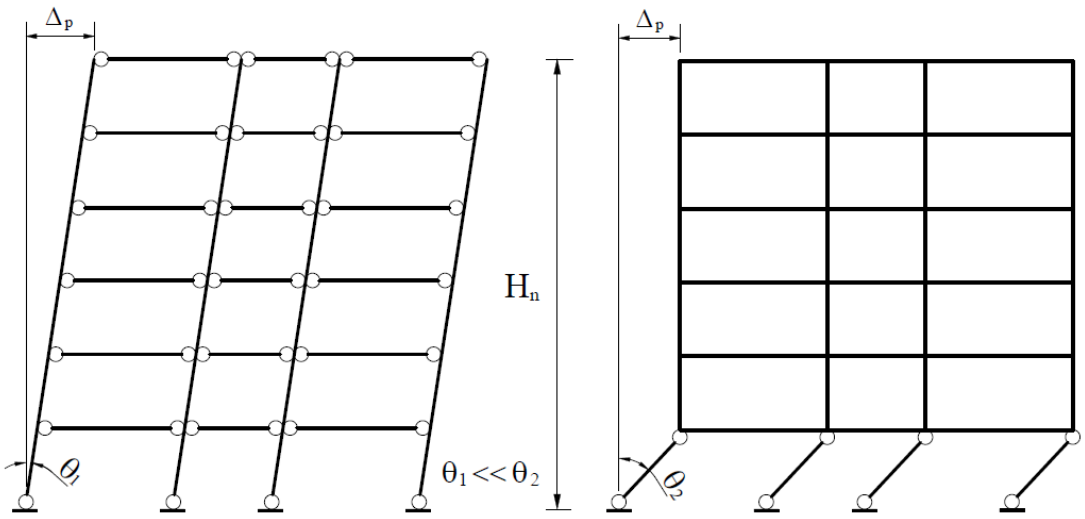

a) Beam Sway b) Column Sway

Figure 4.9. Mechanism for Frame with Inelastic Response
(Adopted from Priestley et al., 2007 [6])

From desired mechanism of Figure 4.9a it is apparent that plastic hinges should form at the end of the beams, and at the base of first story columns. Further, formation of

plastic hinges at the top of the columns of the roof level are also allowed. However, the remaining elements (columns in a frame) has to remain elastic, they have to be protected from inelastic deformations (i.e. formation of plastic hinges). Furthermore, the inelastic shear failure even in plastic hinges locations should be avoided [6, 62].

Flexural and shear strength of beams, flexural and shear strength of columns are the considered objectives of capacity design in this section. Thus, brief information is provided here for capacity design of flexural and shear strength of beams, and flexural and shear strength of columns.

4.3.1.1 Beam Flexural Design Forces

As mentioned above, that plastic hinges occur at the end of beams in a ductile moment resisting frames. For flexural design at plastic hinge regions of a beam, no strength reduction factor ($\emptyset_s$), no overstrength factor ($\emptyset^0$) and no dynamic amplification factor (ω) are used (i.e. $\emptyset_s = \emptyset^0 = \omega = 1$). In addition, material reduction factors (e.g. according to TS500, γ_{mc} is material factor for concrete and γ_{ms} is material factor for steel reinforcement [9]) used in the flexural design of plastic hinge location of the beams are taken as unity [6, 54]. Whereas, for flexural design of remaining regions of the beams, the aforementioned factors should be considered except dynamic amplification factor (ω). Recently using dynamic amplification factor (ω), due to vertical acceleration of the structure, has attracted little attention of researchers. Note that this factor, in this case is used to amplify the moments due to gravity loads [6, 54].

For a typical beam of a frame with 6m span, design moments and shears are shown in Figure 4.10 (Adopted from Priestley M.J.N. [6]), due to different loading cases and their combinations. It should be noted, that the gravitational load on the beam is triangular due to tributary area. In Figure 4.10a, F.G and G_E are moments for the factored gravity load and reduced gravity load from seismic load combination (e.g. seismic load combination given in TS500, here described by set of Equation 4.45, respectively. E is moment due to seismic lateral forces obtained through DDBD procedure and amplifying E by using overstrength factor ($\emptyset^0$) gives E^0. In Figure 4.10a, line E^0+G_E corresponds to the seismic load combination given by Equation 4.45 [6].

$$F_d = 1.4G + 1.6Q \quad (4.45a)$$

$$F_d = 1.0G + 1.0Q + 1.0E \quad (4.45b)$$

$$F_d = 0.9G + 1.0E \quad (4.45c)$$

Where:

G is the permanent or dead load effects.

Q is the live load effects.

E is the earthquake load effects.

For flexural design of plastic hinge regions, the larger of factor gravity load (F.G) or earthquake load (E) is used. However, for flexural design of beams in regions rather than plastic hinge regions (i.e. flexural design of midspan of beams), E^0+G_E combinations are used. Moment of the beam due to such combination is given by Equation 4.46. It should be noted that moments due to G_E in these combinations correspond to the moments as normally obtained for a simply supported beam (i.e. the beams are assumed to be simply supported, which gives zero moments at the supports and largest moment at the midspan) [6].

$$M_x = M^0_{E,l} + \left(M^0_{E,r} - M^0_{E,l}\right)\frac{x}{L_B} + \frac{w_G L_B}{2}x - \frac{w_G x^2}{2} \quad (4.46)$$

Where:

M_x is the moment at a distance x from the left centerline of the column.

$M^0_{E,l}$ and $M^0_{E,r}$ are the moments due to earthquake, amplified by using overstrength factor, at the left and right columns centerline.

L_B is the span wide of the beam (center to center of the columns).

w_G is the gravity load.

x is the distance of the section of interest from the left column centerline.

In Figure 4.10a, G_{E^0} is an amplified form of reduced gravitational load (G_E) in seismic combination. For amplification of this load, dynamic amplification factor (ω) is used, to account for vertical ground acceleration. In the example of Figure 4.10, $\omega = 1.3$ is considered as given in Priestley M.J.N et al. 2007 [6]. Furthermore, line F.G_E shown in Figure 4.10a is a factored gravity load, which is the result of redistribution of the moments due to softening of beam ends (i.e. formation of plastic hinges). Redistribution causes

reduction of the moments at the two ends of the beam and increase the moment at midspan of the beam [6].

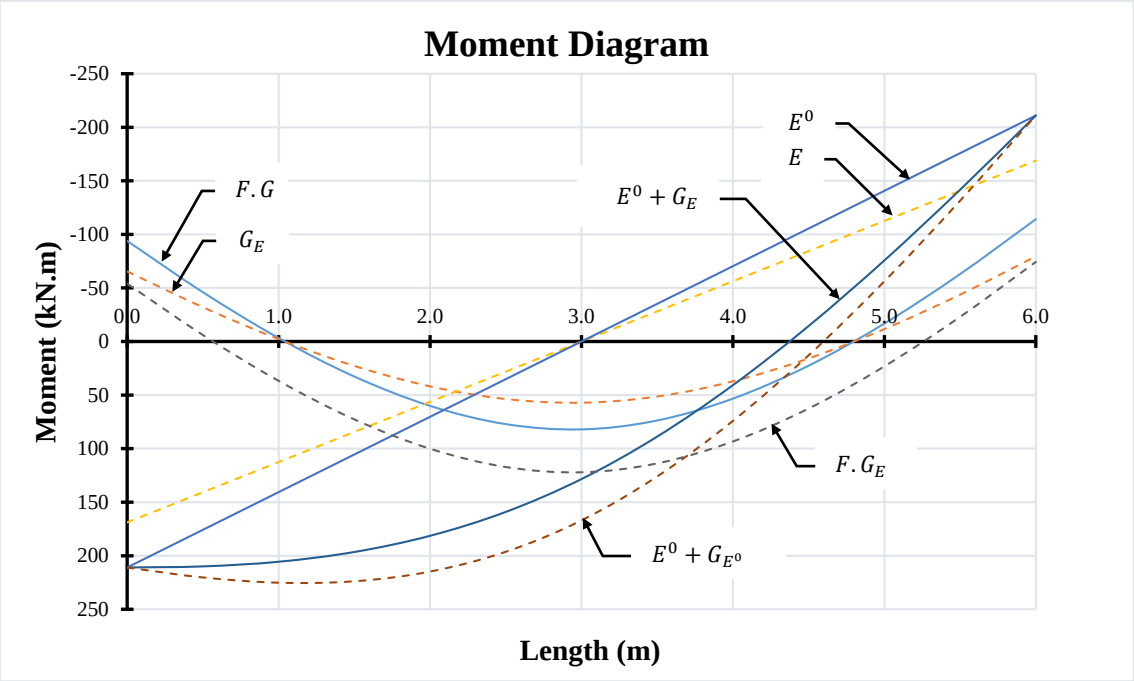

a) Moment Diagram

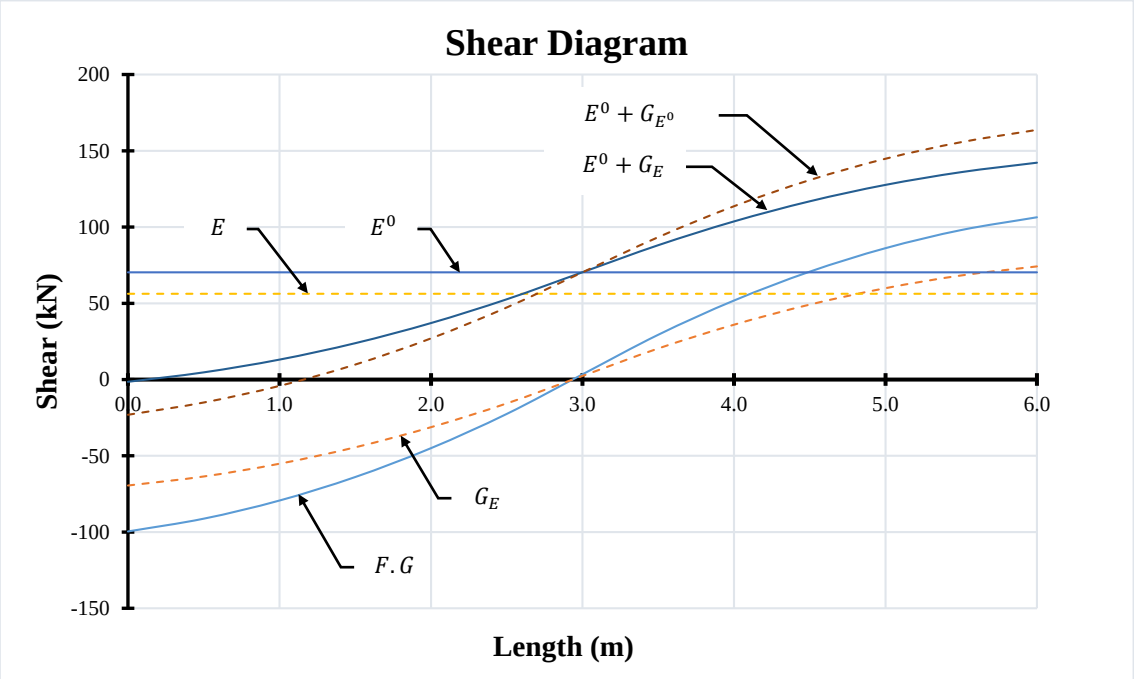

b) Shear Diagram

Figure 4.10. Moment and Shear Diagrams of a Beam with 6m Span, Due to Various Loads and Their Combinations
(Adopted from Priestley et al., 2007 [6])

4.3.1.2 Beam Shear Design Forces

Shear diagram for a beam with 6m span, due to gravitational and seismic loads and their combinations, has been shown in Figure 4.10b. Design shear forces of beams no matter whether at plastic hinge regions or at regions between plastic hinges, should be chosen for the largest design shear force obtained from different load combinations, given by Equation 4.45. Usually, load combination due to gravitational load and seismic load gives the largest value for design shear forces (i.e. E^0+G_E, if vertical acceleration is being considered then, $E^0 + G_{E^0}$). Equation 4.47 can be used to obtain the design shear forces for this combination at each section along the beam [6].

$$V_x = \frac{M^0_{E,r} - M^0_{E,l}}{L_B} + \frac{w_G L_B}{2} - w_G x \tag{4.47}$$

Where:

V_x is the design shear force at a distance x from the left column centerline.

4.3.1.3 Column Flexural Design Forces

Earlier, it has been mentioned that plastic hinges should not occur at the columns, except at the base of first story columns, and at the top of roof level columns. For this reason, columns should be designed such that, they should be protected against plastic hinges. Thus, the required moments in columns should be determined by using Equation 4.48.

$$\emptyset_f M_N \geq \emptyset^0 \omega_f M_E \tag{4.48}$$

Where:

M_N is nominal moment of the columns.

$\emptyset_f$ is moment reduction factor.

M_E is moment due to earthquake load obtained through DDBD procedure.

ω_f is dynamic amplification factor for flexural design of the columns.

$\emptyset^0$ is overstrength factor.

Overstrength factor, used for amplifying column moments due to earthquake loads, should be determined using detailed moment-curvature analysis. In this case, maximum strength for materials (determined by Equation 4.49) should be used, during implementation of moment-curvature analysis. In case, strain hardening is considered, the default value of $\emptyset^0 = 1.25$ shall be considered, if strain hardening is ignored then $\emptyset^0 = 1.6$ shall be used [6]. However, a conservative value for overstrength factor, given in DBD12 [54] is equal to 1.25.

$$f'_{ce} = 1.3\, f'_c \tag{4.49a}$$

$$f_{ye} = 1.1\, f_y \tag{4.49b}$$

Where:

f'_{ce} is expected compression strength of concrete.

f'_c is compressions strength of concrete.

f_{ye} is expected yield strength of steel reinforcement.

f_y is yield strength of steel reinforcement.

Dynamic amplification factor (ω_f) for flexural design of columns, are used to amplify the column moments due to earthquake loads. However, since dynamic amplification factor depends on the height and ductility of the frame, thus up to the 75% height of the frame, it should be calculated by using Equation 4.50, while at the top and bottom of the frame (i.e. at the base of first story columns and at the top of roof level columns). Figure 4.11, adopted from Priestley M.J.N et al. 2007 [6]), it is equal to unity ($\omega_f = 1.0$) [6, 54].

$$\omega_{f,c} = 1.15 + 0.13(\mu^0 - 1) \tag{4.50}$$

Where:

μ^0 is reduced ductility by using $\emptyset^0$.

For one way and two way frames, μ^0 can be found using set of Equation 4.51.

$$\mu^0 = \frac{\mu}{\emptyset^0} \geq 1.0, \qquad \text{for one way frame} \qquad (4.51a)$$

$$\mu_D^o = \frac{\mu}{\sqrt{2}\emptyset^0} \geq 1.0, \qquad \text{for two way frame} \qquad (4.51b)$$

Where:

μ is the design ductility of the frame at expected strength, obtained through DDBD procedure (Section 4.1.1, Equation 4.9).

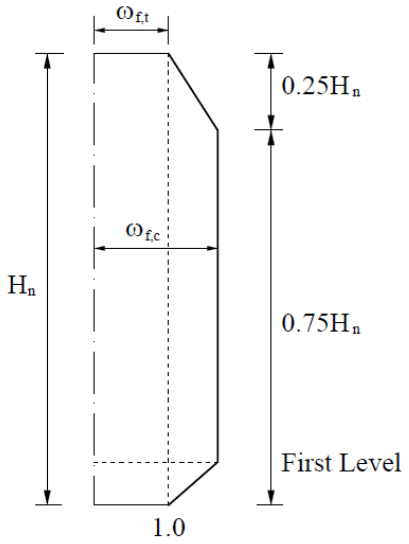

Figure 4.11. Dynamic Amplification Factor for Column Moments of a Frame (Adopted from Priestley et al., 2007 [6])

4.3.1.4 Column Shear Design Forces

In the content of capacity design, shear strength of columns should satisfy following condition, as given for one way and two way frames by Equation 4.52 and Equation 4.53, respectively [6].

$$\emptyset_s V_N \geq \emptyset^0 V_E + 0.1\mu V_{E,base} \leq \frac{M_{top}^0 - M_{bot}^0}{H_C} \qquad (4.52)$$

$$\emptyset_s V_N \geq \sqrt{2}(\emptyset^0 V_E + 0.1\frac{\mu}{\sqrt{2}} V_{E,base}) \leq \frac{M_{top}^0 - M_{bot}^0}{H_C} \qquad (4.53)$$

Where:

V_N is nominal shear strength.

$\emptyset_s$ is strength reduction factor.

V_E is shear forces in columns due to earthquake loads.

$V_{E,base}$ is shear forces at the base of the columns due to earthquake loads.

M_{top}^0 and M_{bot}^0 are the amplified moments (obtained by amplifying the moments due to earthquake loads) at the top and bottom of columns, respectively.

CHAPTER 5

APPLICATION OF DDBD FOR THE CASE STUDY

The aim of this study is the application of DDBD approach in the content of PBSD for the design of irregular reinforced concrete moment resistance frames. For this purpose four office buildings have been selected. They are similar in plans, but different in height, 3, 5, 8 and 12 stories, and irregular reinforced concrete frames are the only earthquake resistance system of these buildings. From each of these buildings, one frame, critical in terms of gravitational loads, is chosen. In Figure 5.1, a typical plan of the building has been shown, the dimensions are all in *cm*, and frame 2-2, surrounded by shaded area is the frame of interest.

In addition, compressive strength of concrete used here is 25MPa, the modulus of elasticity in this case is equal to $31x10^3$ MPa. The yield strength of the steel reinforcement is 420MPa and its modulus of elasticity is equal to $2x10^5$ MPa.

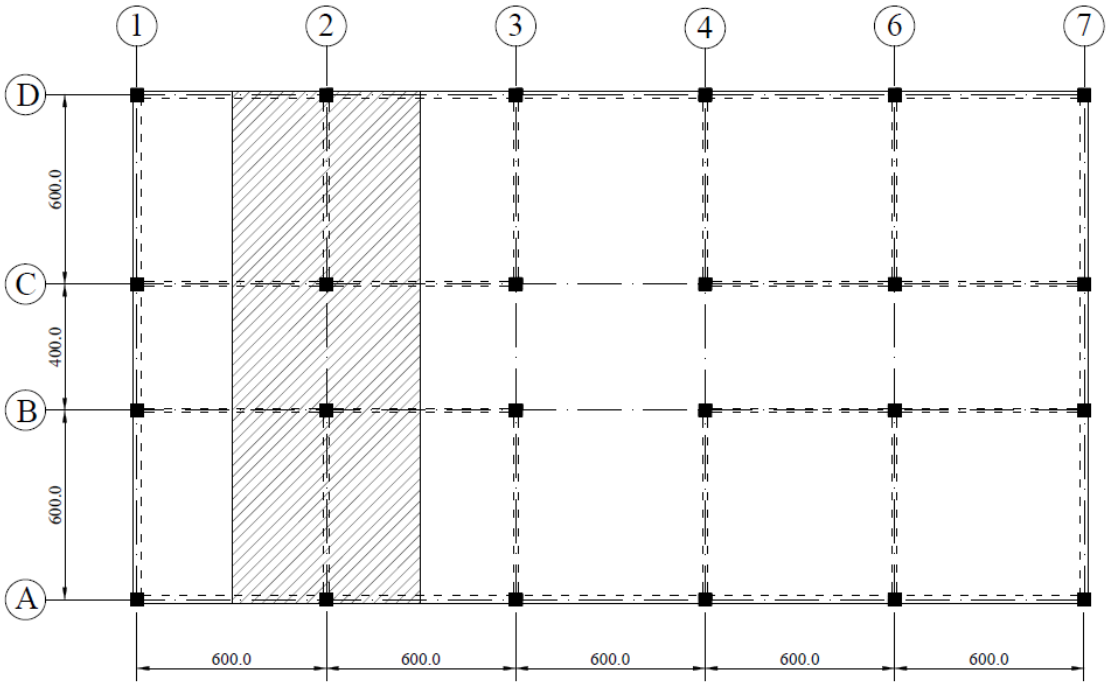

Figure 5.1. Typical Plan of the Office Building

5.1 Frame Description

The reinforced concrete moment resistance frames chosen are having 3 bays, which are irregular in terms of span width and story height i.e. outer bays of the frames are larger than inner bay and the first story height is larger than other stories. In Figure 5.2 the aforementioned 4 irregular reinforced concrete moment resistance frames are shown. It is clear from Figure 5.2 that the span width of outer bays are 6m each and the span width of inner bay is 4m. Furthermore, the first story height is 3.6m and the heights of the remaining stories are 3m each. The dimensions shown in this figure are all in *cm*, and they are chosen from Korkmaz et al. 2006 [63], with some modifications. In addition, since here only one frame from each building has been designed, therefore, it is assumed that frame is one way frame.

For the purpose of implementation of the DDBD procedure, illustrated in chapter 4, only 8 story frame has been covered here, and the results for other frames are given in appendices.

5.2 DDBD Procedure for the Case Study

5.2.1 Representation of MDOF System by an SDOF System

1. Choosing Deformation Level

According to first step of PBSD procedure, Section 2.4.1, two different performance objectives are selected. The selected performance objectives correspond to functional or operational and life safety performance levels for occasional (20% chance of exceedance in 50years with 225 years mean return period), and rare (10% chance of exceedance in 50years with 475 years mean return period) earthquake hazard levels, respectively (refer to Figure 2.2).

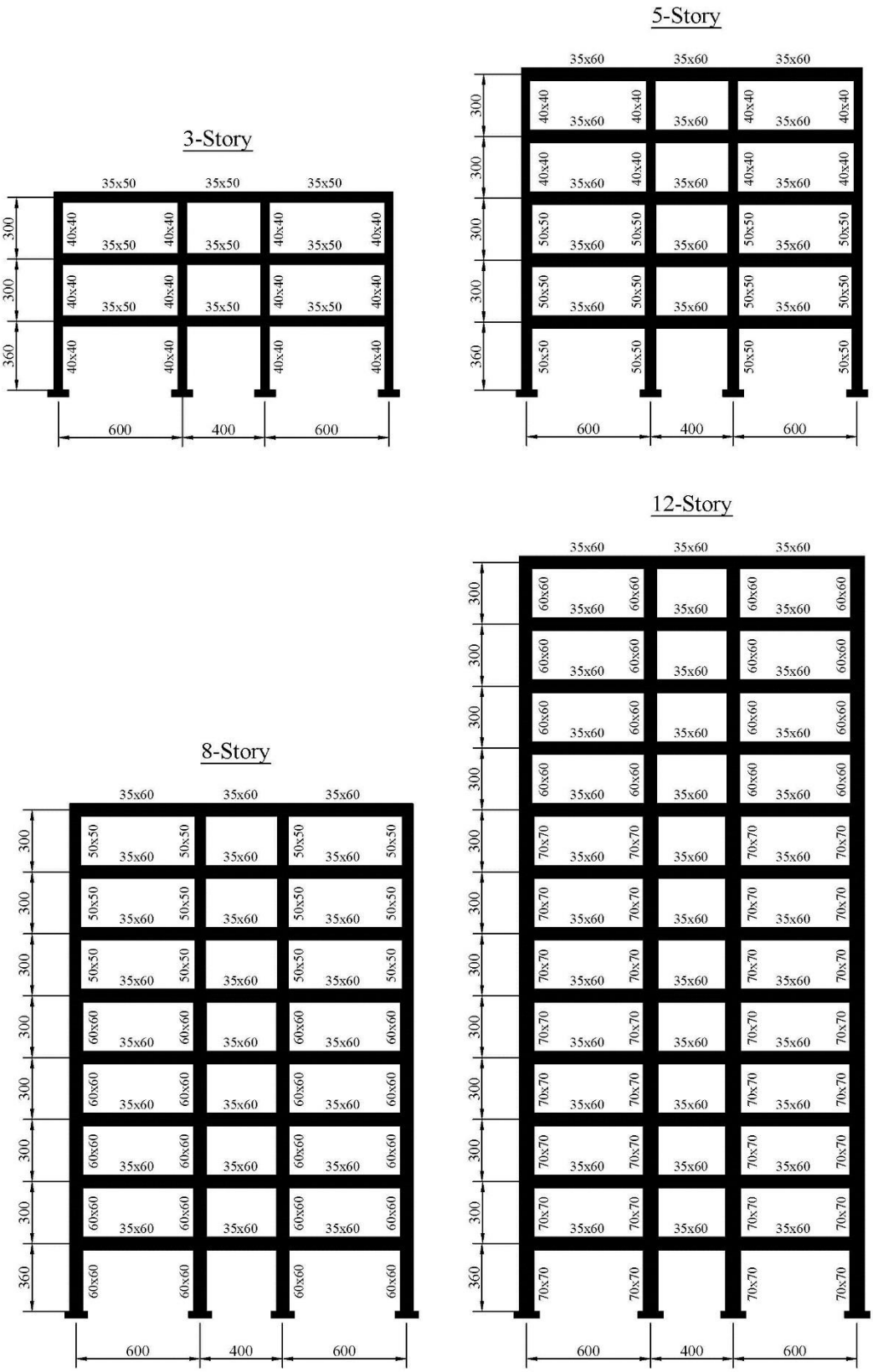

Figure 5.2. Elevation of Frames with Their Vertical and Horizontal Dimensions

As mentioned in Section 2.4.1.1, that performance level describes the damage condition, and the damages are directly related to the deformations. Therefore, here performance levels are selected in terms of deformations (drift ratios). According to ATC-40 (Table 11-2 of ATC-40) [7], drift ratios for operational and life safety performance levels are 1% and 2%, respectively. For these performance levels the earthquake hazard levels are chosen from earthquake hazard maps in Turkey. These earthquake hazard levels corresponds to PGA of 0.2g and 0.4g with mean return period of 72 years and 475 years, respectively.

Note that calculations are done for both drift ratios up to obtaining base shear forces for each frame. Since the base shear forces obtained for 2% drift ratio are significantly larger than the base shear forces obtained for 1% drift ratio, therefore, here calculations for only 2% drift ratio are covered.

2. Design Story Displacement

To find the design story displacements (Δ_i), Equation 4.2 to Equation 4.5 are used and the results for design story displacements and normalized mode shapes (δ_i) are tabulated in Table 5.1 and the results for others are given as follows:

$$\Delta_C = 0.02x3.6 = 0.072\ m$$
$$\omega_\theta = 1.15 - 0.0034x24.6 = 1.066 > 1.0$$

Since $\omega_\theta = 1.066 > 1.0$, therefore, $\omega_\theta = 1.0$ is used for further calculations.

Seismic masses, at the top of each story, are also given in column 2 of Table 5.1. In calculation of these masses, 100% of dead loads and 30% of live loads, recommended in Turkish Seismic Design Code [8], are considered.

Table 5.1. Calculations for Design Displacement, Effective Height and Effective Mass of 8 Story Irregular Frame

Story i	Height H_i (m)	Mass m_i (ton)	δ_i	Δ_i (m)	$m_i\Delta_i$	$m_i\Delta_i^2$	$m_i\Delta_i H_i$
0	1	2	3	4	5	6	7
8	24.60	55.059	1.000	0.383	21.09	8.08	518.77
7	21.60	68.995	0.914	0.350	24.15	8.45	521.56
6	18.60	68.995	0.818	0.313	21.61	6.77	401.85
5	15.60	70.117	0.711	0.273	19.11	5.21	298.07
4	12.60	71.520	0.595	0.228	16.31	3.72	205.53
3	9.60	71.520	0.470	0.180	12.86	2.31	123.48
2	6.60	71.520	0.334	0.128	9.14	1.17	60.34
1	3.60	79.253	0.188	0.072	5.71	0.41	20.54
Total		556.98			129.97	36.11	2150.16

3. Design Displacement of the Equivalent SDOF System

It has been obtained using Equation 4.6.

$$\Delta_d = 0.278m = 278\,mm$$

4. Effective Height of the Equivalent SDOF System

Equation 4.7 is used for determining effective height of the equivalent SDOF system.

$$H_e = 16.54\,m$$

5. Effective Mass of the Equivalent SDOF System

Equation 4.8 is used for obtaining effective mass of the equivalent SDOF system.

$$m_e = 467.76\,ton$$

6. Design Ductility Factor for Equivalent SDOF System

For calculation of design ductility factor for equivalent SDOF system Equation 4.9 to Equation 4.15 are used and the results are tabulated in Table 5.2.

Table 5.2. Calculations for Ductility Factor of 8 Story Irregular Frame

f_y (MPa)	E_s (MPa)	f_{ye} (MPa)	ε_y	h_{bi} (m)	L_{bi} (m)		θ_{yi}		M_1/M_2	Δ_y (m)	μ
					1	2	1	2			
420	2x10^5	462	0.0023	0.60	6.00	4.00	0.0116	0.0077	1.00	0.17	1.64

7. Equivalent Viscous Damping for the Equivalent SDOF System

Using Equation 4.16 equivalent viscous damping for the equivalent SDOF system is equal to:

$$\xi_{eq} = 0.1199 = 11.99\%$$

8. Effective Period at Peak Displacement Response

By using Equation 4.17 to Equation 4.21, the graphs shown in Figure 5.3 are obtained for elastic acceleration and design displacement response spectrums. It is assumed that the structure is located in seismic zone 1 and the site class is assumed to be Z_2, therefore, from Table 4.1 and Table 4.2 the following can be written:

$$A_0 = 0.40$$
$$T_A = 0.15\ sec$$
$$T_B = 0.40\ sec$$

Since the buildings are assumed to be an office building, as a result, the importance factor (I) from Table 2.3 of Turkish Seismic Design Code [8], is equal to:

$$I = 1.0$$

By entering the value for design displacement (Δ_d) in Figure 5.3, the value for effective period (T_{eff}) can be obtained.

$$\Delta_d = 278\,mm \quad \Rightarrow \quad T_{eff} = 2.52\,sec$$

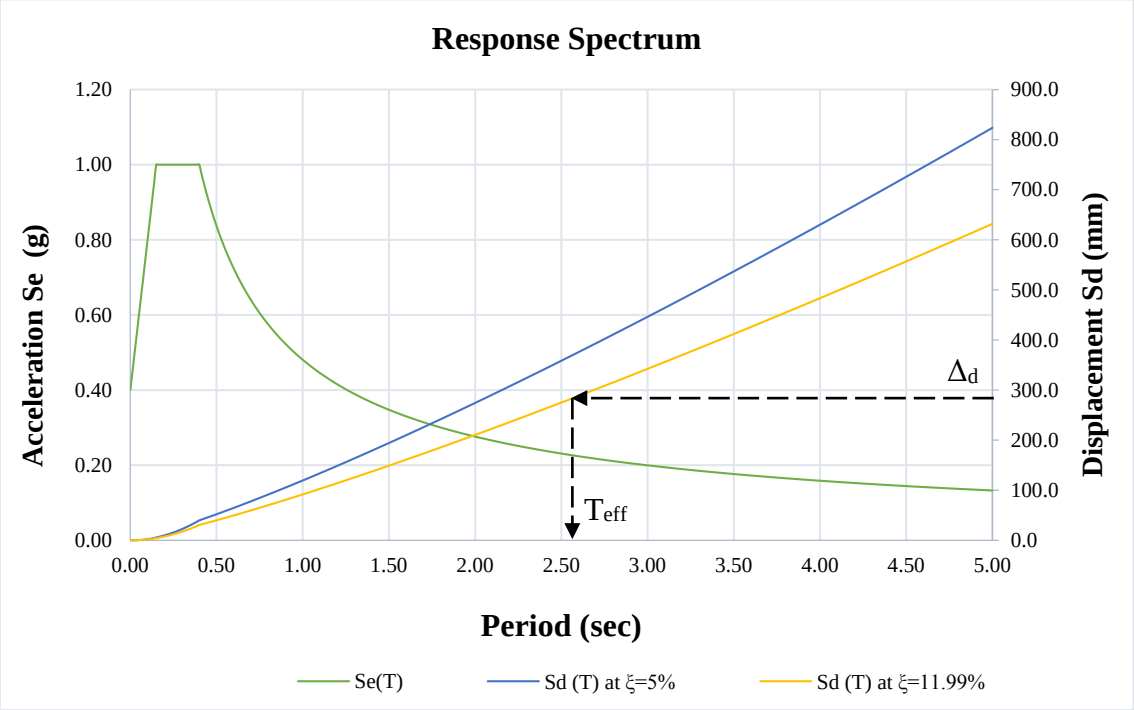

Figure 5.3. Elastic Acceleration (S_e) and Design Displacement (S_d) Response Spectrum for 8 Story Irregular Frame

9. Effective Stiffness of the Equivalent SDOF System

To determine effective stiffness, Equation 4.22 is used.

$$K_{eff} = 2904.77\,kN/m$$

10. Base Shear Force

Base shear force is finally obtained using Equation 4.23.

$$V_{Base} = 807.11\,kN$$

5.2.2 Design Actions for MDOF System from SDOF Base Shear Force

1. Calculation of Lateral Forces at the Top of Each Story

Lateral forces at the top of each story has been calculated by using Equation 4.24 and Equation 4.25. The results are arranged in Table 5.3.

2. Calculation of the Total Overturning Moment (M_{OTM})

Overturning moment at the top of each story and at the base of the frame are calculated to find the total overturning moment (Equation 4.26), and the results are given in Table 5.3.

Table 5.3. Lateral Forces and Overturning Moments at the Top of Each Story of 8 Story Irregular Frame

Story i	Height H_i (m)	Mass m_i (ton)	m_iH_i	F_i (kN)	$M_{OTM,i}$ (kN.m)
0	1	2	3	4	5
8	24.60	55.059	1354.45	184.23	0.00
7	21.60	68.995	1490.29	149.42	552.68
6	18.60	68.995	1283.31	128.67	1553.63
5	15.60	70.117	1093.82	109.67	2940.58
4	12.60	71.520	901.15	90.35	4656.54
3	9.60	71.520	686.59	68.84	6643.56
2	6.60	71.520	472.03	47.33	8837.09
1	3.60	79.253	285.31	28.61	11172.61
0	0.00	0.000	0.00	0.00	14078.20
Total			7566.95	807.11	

3. P-Delta Effects

To find out whether P-Delta effects should be considered or no, stability index has been found, using Equation 4.27.

$$\theta_\Delta = \frac{6158.35x0.278}{14078.20} = 0.122$$

Since $0.1 < \theta_\Delta = 0.122 < 0.33$, thus P-Delta effects should be considered. The base shear force has to be modified, using Equation 4.28. As a result, modified base shear force is equal to:

$$V_{Base} = 2904.77x\ 0.278 + 0.5x\frac{6158.35x0.278}{16.54}$$
$$V_{Base} = 858.83\ kN$$

Using the modified base shear force, the lateral forces and overturning moments at the top of each story are obtained and tabulated in Table 5.4.

4. Story Shear Forces

Story shear forces (at each story level) are obtained through Equation 4.29, and the results are given in Table 5.4.

Table 5.4. Lateral Forces and Overturning Moments at the Top of Each Story, and Story Shear Forces of 8 Story Irregular Frame

Story i	Height H_i (m)	Mass m_i (ton)	m_iH_i	F_i (kN)	$M_{OTM,i}$ (kN.m)	V_{si} (kN)
8	24.60	55.06	1354.45	196.03	0.00	196.03
7	21.60	69.00	1490.29	159.00	588.10	355.03
6	18.60	69.00	1283.31	136.91	1653.18	491.94
5	15.60	70.12	1093.82	116.70	3129.00	608.64
4	12.60	71.52	901.15	96.14	4954.92	704.78
3	9.60	71.52	686.59	73.25	7069.25	778.03
2	6.60	71.52	472.03	50.36	9403.34	828.39
1	3.60	79.25	285.31	30.44	11888.50	858.83
0	0.00	0.000	0.00	0.00	14980.28	858.83
Total			7566.95	858.83		

5.3 Analysis of the Frame Based on Equilibrium Consideration

5.3.1 Beam Internal Forces

Internal forces of the beams (shear forces and moments) are obtained by using Equation 4.31 to Equation 4.36 of Section 4.2.1.1 and 4.2.1.2. The results of the calculations are tabulated in Table 5.5.

Table 5.5. Internal Forces in Beams of 8 Story Irregular Frame

Story i	V_{si} (kN)	Beam Shear Forces (kN)		Beam Moments (kN/m)			
		Outer	Inner	Outer		Inner	
				Left	Right	Left	Right
0	1	2	3	4	5	6	7
8	196.03	29.65	44.47	88.94	-88.94	88.94	-88.94
7	355.03	53.69	80.54	161.07	-161.07	161.07	-161.07
6	491.94	74.40	111.59	223.19	-223.19	223.19	-223.19
5	608.64	92.04	138.07	276.13	-276.13	276.13	-276.13
4	704.78	106.58	159.88	319.75	-319.75	319.75	-319.75
3	778.03	117.66	176.49	352.98	-352.98	352.98	-352.98
2	828.39	125.28	187.92	375.83	-375.83	375.83	-375.83
1	858.83	129.88	194.82	389.64	-389.64	389.64	-389.64
Total	4821.66						

Note that, beam moments given in Table 5.5 are calculated at the center of supports (columns).

5.3.2 Column Internal Forces

Column internal forces are obtained by using Equation 4.38 to 4.43, which are given in Section 4.2.2.1 and 4.2.2.2 and the final results are arranged in Table 5.6. The values of moments for columns in this table are calculated at the center of the beams. As mentioned in Section 4.2.2.1 that the internal columns takes two times larger shear forces with compare to external columns, this can be clearly seen comparing columns 3 and 4 of Table 5.6.

Table 5.6. Internal Forces in Columns of 8 Story Irregular Frame

Story i	Story Height h_i (m)	V_{si} (kN)	Columns Shear Forces (kN)		Columns Moments (kN.m)		Location
			Outer	Inner	Outer	Inner	
0	1	2	3	4	5	6	7
8	3.00	196.03	32.67	65.34	88.94	177.88	Top
					9.08	18.16	Bot
7	3.00	355.03	59.17	118.34	151.99	303.99	Top
					25.52	51.04	Bot
6	3.00	491.94	81.99	163.98	197.67	395.34	Top
					48.30	96.60	Bot
5	3.00	608.64	101.44	202.88	227.83	455.66	Top
					76.49	152.98	Bot
4	3.00	704.78	117.46	234.93	243.26	486.52	Top
					109.13	218.26	Bot
3	3.00	778.03	129.67	259.34	243.86	487.71	Top
					145.16	290.32	Bot
2	3.00	828.39	138.06	276.13	230.67	461.34	Top
					183.52	367.04	Bot
1	3.60	858.83	143.14	286.28	206.12	412.24	Top
					309.18	618.36	Bot

5.4 Capacity Design Principles for DDBD

5.4.1 Capacity Design for Frames

In this study, overstrength factor $\emptyset^0 = 1.25$ is adopted, and the dynamic amplification factore ω is calculated. After capacity design principles are applied for the elements of the 8 story irregular moment resistance frame, the results are presented here. It should be noted that the results for 3, 5, and 12 story irregular reinforces concrete moment resistance frames are given in appendices.

5.4.1.1 Beam Flexural Design Forces

For the flexural design of the beams at plastic hinge locations, the moments due to earthquake loads (E) obtained through DDBD procedure, without amplifying (i.e.

$\emptyset^0 = 1.0$ and $\omega = 1.0$), are considered. The moments due to gravity loads (i.e. factored gravity loads) are obtained using load combination described by Equation 4.45. Further, as mentioned in Section 4.3.1.1 that for flexural design of plastic hinge regions of beams the design moments are the larger of the factored gravity load (F.G) or earthquake load (E), thus, after comparison it has been found that moments due to earthquake loads are significantly higher than moments due to gravity loads. As a result, the design moments for plastic hinge regions are selected from only earthquake loads and they are tabulated in Table 5.7 (columns 1, 3, 4, and 6).

In addition, for flexural design of other regions rather than plastic hinge regions (i.e. beam midspan design), the moments due to earthquake loads (E) are amplified only using overstrength factor $\emptyset^0 = 1.25$, and dynamic amplification factor is assumed to be unity ($\omega = 1.0$). Moments due to reduced gravity loads (G_E) used in Equation 4.45b and Equation 4.45c (Denoted as G and Q) are obtained by assuming that beams are simply supported, as mentioned in Section 4.3.1.1. After using combinations described by set of Equation 4.45, the design moments at midspan of the beams are the maximum obtained from these combinations and tabulated in Table 5.7 (columns 2 and 5).

Table 5.7. Beam Design Moments at the Face of Columns and at Midspan of the Beams of 8 Story Irregular Frame

Story i	Beam Design Moments (kN)					
	Outer			Inner		
	Left	Span	Right	Left	Span	Right
0	1	2	3	4	5	6
8	81.53	96.63	-81.53	77.82	43.83	-77.82
7	147.65	132.18	-147.65	140.94	49.17	-140.94
6	204.59	132.18	-204.59	195.29	49.17	-195.29
5	248.52	132.18	-248.52	234.71	49.17	-234.71
4	287.78	131.78	-287.78	271.79	49.17	-271.79
3	317.68	131.78	-317.68	300.04	49.17	-300.04
2	338.25	131.78	-338.25	319.46	49.17	-319.46
1	350.68	131.78	-350.68	331.19	49.17	-331.19

It should be noted that, for flexural design of plastic hinge regions no strength reduction factors ($\emptyset_s$) are used, while for flexural design of regions rather than plastic hinge regions they are used. However, design moments given in Table 5.7 for mid-span of beams are not reduced using strength reduction factor.

5.4.1.2 Beam Shear Design Force

For the shear design of the beams, the shear forces due to earthquake loads (E) obtained through DDBD process are amplified only using overstrength factor.

Table 5.8. Beams Design Shear Forces of 8 Story Irregular Frame

Story i	Beam Shear Forces due to Earthquake Loads (kN)				From Load Combinations (kN)	
	Non-Amplified		Amplified			
	Outer	Inner	Outer	Inner	Outer	Inner
0	1	2	3	4	5	6
8	29.65	44.47	37.06	55.59	84.00	82.37
7	53.69	80.54	67.11	100.67	128.19	130.73
6	74.40	111.59	93.00	139.49	154.61	169.55
5	92.04	138.07	115.06	172.58	175.31	201.84
4	106.58	159.88	133.23	199.84	193.13	229.10
3	117.66	176.49	147.08	220.61	207.36	249.87
2	125.28	187.92	156.60	234.89	217.25	264.15
1	129.88	194.82	162.35	243.53	223.75	272.79

Beam shear forces due to earthquake loads are constant along the beam. They are given as amplified and non-amplified shear forces in columns 1 to 4 of Table 5.8, respectively. Shear forces given in column 5 and 6 of Table 5.8 are due to load combinations, and these values are at a distance d (effective depth of the beam) from the face of the supports (i.e. from the face of the columns). However, strength reduction factors are not used yet.

5.4.1.3 Column Flexural Design Forces

As mentioned in Section 4.3.1 that columns should be protected against formation of plastic hinges except the base of first story columns and the top of roof level columns. Therefore, columns' moments obtained through DDBD procedure (Table 5.6), are amplified by using overstrength factor ($\emptyset^0 = 1.25$) and dynamic amplification factor (ω), illustrated in Section 4.3.1.3.

Since it is assumed that the frame is a one way frame, therefore, reduced ductility factor is found by using Equation 4.51a, and it is equal to:

$$\mu^0 = \frac{1.64}{1.25} = 1.31$$

Dynamic amplification factor is calculated at the top of each story according to Section 4.3.1.3. The results of calculations are shown in Figure 5.4 and the amplified moments at the top and bottom of columns at each story are given in Table 5.9.

5.4.1.4 Column Shear Design Forces

Amplified shear forces in columns are found using Equation 4.52. The results are tabulated in Table 5.9.

Table 5.9. Amplified Internal Forces in Columns of 8 Story Irregular Frame

Story i	ω_f	Shear Forces V^0 (kN)		Moments M^0 (kN.m)		Location
		Outer	Inner	Outer	Inner	
0	1	2	3	4	5	6
8	1.00	40.84	81.68	-111.17	-222.34	Top
				11.35	22.70	Bot
7	1.10	80.99	161.98	-208.04	-416.08	Top
				25.52	69.86	Bot
6	1.19	115.90	231.80	-294.07	-588.13	Top
				71.86	143.72	Bot
5	1.19	143.39	286.79	-338.94	-677.87	Top
				113.79	227.58	Bot
4	1.19	166.05	332.09	-361.89	-723.79	Top
				162.35	324.69	Bot
3	1.19	183.30	366.61	-362.78	-725.55	Top
				215.95	431.90	Bot
2	1.19	187.12	374.24	-288.34	-576.68	Top
				273.02	546.04	Bot
1	1.00	178.92	357.84	-257.65	-515.30	Top
				386.47	772.94	Bot

It should be noted that, the internal forces of the columns shown in this table are only due to earthquake loads with considering capacity design principles, and no load combinations are applied yet. Therefore, strength reduction factors are not applied for

both shear forces and moments (denoted as $\emptyset_s$ for shear and $\emptyset_f$ for moments. See Equation 4.48 and Equation 4.52), they are applied later. Further, the moments shown in this table for columns are at the center of beams.

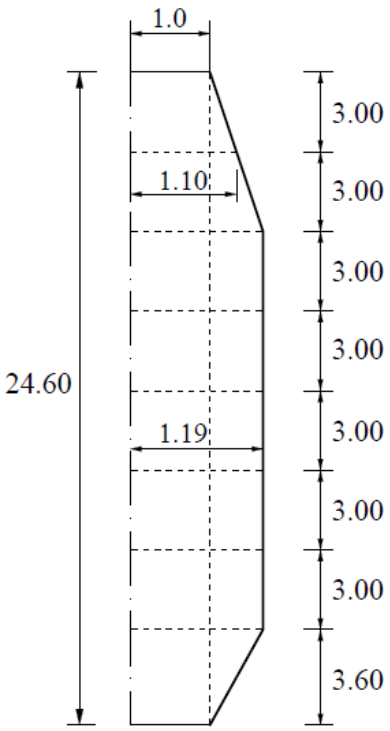

Figure 5.4. Calculated Dynamic Amplification Factor for Column Moments of 8 Story Irregular Frame

5.5 Design of Members

In this section, a brief information has been provided regarding detailed design of sections. For the design of the sections of beams and columns the detailed procedures given in Ersoy et al. 2013 [10] are adopted in compliance with TS500 [9].

5.5.1 Flexural and Shear Design of Beams

For the flexural design of the beams, they are designed as doubly reinforced concrete rectangular beams. For this purpose, a program which has been written in Microsoft ® Excel 2000, by Ersoy et al in 2000, and the information about this program has been provided in Ersoy et al. 2013 [10], is used. The design moments entered in this

program as input data, are the moments at the face of the supports (columns). In this program, the limits for reinforcement ratio are considered (i.e. minimum and maximum reinforcement ratios are taken into account), as recommended in TS500 [9].

The aim for shear design for frame members in seismic region is to avoid shear failure in collapse limit state, instead it should be happen in flexure, in case if a failure occurs (i.e. if a failure occur it should be flexure failure rather than shear failure). For the shear design of beams the procedure given in Ersoy et al. 2013 [10] are adopted, and design were carried out stepwise, manually (without using any software).

The diagonal tension failure, which is due to local compressive forces from supports, cannot occur very close to the face of the supports. Therefore, shear forces for the shear design of the beams are taken at the critical sections, which are at a distance d (effective depth) from the faces of the supports (columns) [10]. The details for reinforcements, estimated for beams are tabulated in Table 5.10, and the arrangement of reinforcements in cross sections are shown in Figure 5.5.

Table 5.10. Reinforcement Details of Beams of 8 Story Irregular Frame

Story	Location	Inner Bay		Outer Bay		Cross Sectional Size
		Support	Span	Support	Span	
Longitudinal Reinforcements						
0	1	2	3	4	5	6
1-4	Top	6Ø18	2Ø18	6Ø18	2Ø18	350x600
	Bot	3Ø18	3Ø16	3Ø18	3Ø16	
5-8	Top	5Ø16	2Ø16	5Ø16	2Ø16	
	Bot	3Ø16	4Ø16	3Ø16	4Ø16	
Transverse Reinforcements						
1-4	2 legs	Ø10/140	Ø10/200	Ø10/140	Ø10/200	
5-8	2 legs	Ø10/140	Ø10/200	Ø10/140	Ø10/200	

The dimensions given in Table 5.10 and shown in Figure 5.5, are all in “mm”. In this table, the transverse reinforcement has 2 legs, and Ø10/140 means diameter is 10mm at a distance of 140mm center to center of hoops. The cross sections shown in Figure 5.5 are same for the beams of outer and inner bays, as can be seen in Table 5.10. It should be noted that in Table 5.10 support refers to the densely confined region of the beams and span refers to less confined regions.

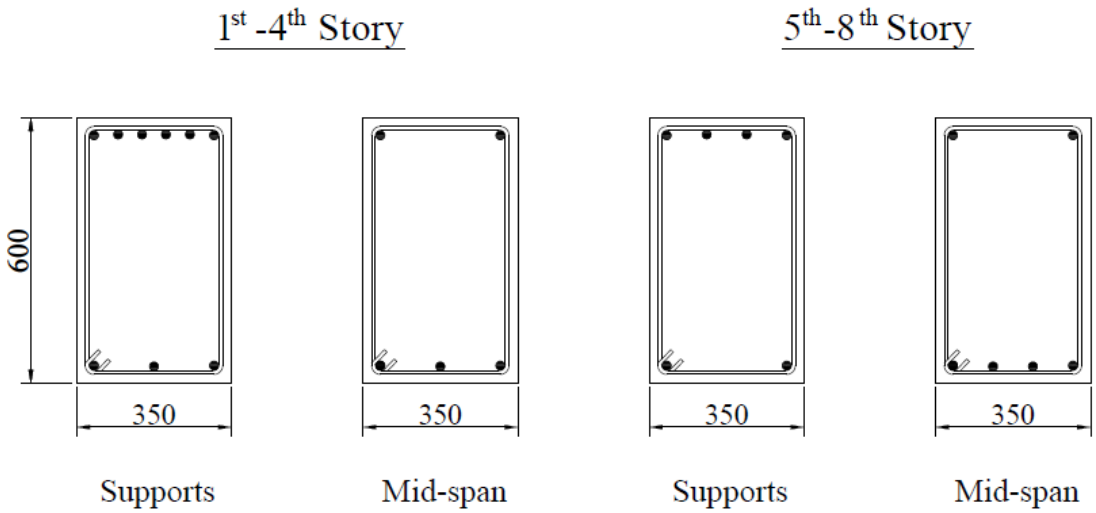

Figure 5.5. Cross Sections for Beams of 8 Story Irregular Frame

5.5.2 Flexural and Shear Design of Columns

For the columns the design forces obtained through DDBD procedure, which are due to earthquake loads, are then combined by using load combinations presented by set of Equation 4.45 with forces obtained from gravitational loads. Then the most critical condition is being considered for the design of the columns.

For flexural design of the columns, second order moments are also taken into account in addition to the forces obtained from load combinations by using recommendations given in TS500 [9]. To calculate second order moments, an approximate method is utilized. This method, which is also known as Moment Magnification Method, is given in TS500, and its detailed procedure is provided in Ersoy et al. 2013 [10]. After obtaining design moments, an excel program which has been written in Microsoft ® Excel 2000, by Ersoy et al in 2000, and the information about this program has been provided in Ersoy et al. 2013 [10], is used.

The assumptions in this program are as follows:

- Tensile strength of the concrete is neglected.
- Strain hardening of reinforcement bars is not considered.
- Stress block which is used for concrete in compression is assumed to be rectangular.

As mentioned earlier, that the basic principle in the shear design is that to resist shear forces by providing adequate reinforcement. The important thing is that adequate shear reinforcement gives capability to the member to reach its ultimate limit state by flexure rather than by shear. In addition, to avoid brittle failure of the member, it is recommended in codes and standards to provide minimum shear reinforcement [10].

For the shear design of columns the procedure described in details for seismic resistance in Ersoy et al. 2013 [10], and the recommendation given in TS500 [9], is utilized. It should be noted that shear design in this study has been carried out without using any program (i.e. by creating excel sheets manually).

The details for reinforcements, estimated for columns are tabulated in Table 5.11, and the arrangement of longitudinal reinforcements and the transverse reinforcements in cross sections are shown in Figure 5.6.

Table 5.11. Reinforcement Details of Columns of 8 Story Irregular Frame

Story	Longitudinal Reinforcement		Transverse Reinforcements				Cross Sectional Size
	Inner	Outer	Inner		Outer		
			Confined Region	Unconfined Region	Confined Region	Unconfined Region	
0	1	2	3	4	5	6	7
1-5	16Ø26	12Ø20	Ø10/100 4 legs	Ø10/115 4 legs	Ø10/100 4 legs	Ø10/115 4 legs	600x600
6	16Ø26	12Ø20	Ø10/100 4 legs	Ø10/115 4 legs	Ø10/100 4 legs	Ø10/115 4 legs	500x500
7	16Ø22	12Ø18	Ø10/100 4 legs	Ø10/115 4 legs	Ø10/100 4 legs	Ø10/115 4 legs	500x500
8	16Ø16	12Ø18	Ø10/100 4 legs	Ø10/115 4 legs	Ø10/100 4 legs	Ø10/115 4 legs	500x500

In this table, inner and outer refers to the inner and outer columns. The dimensions are all in “mm”.

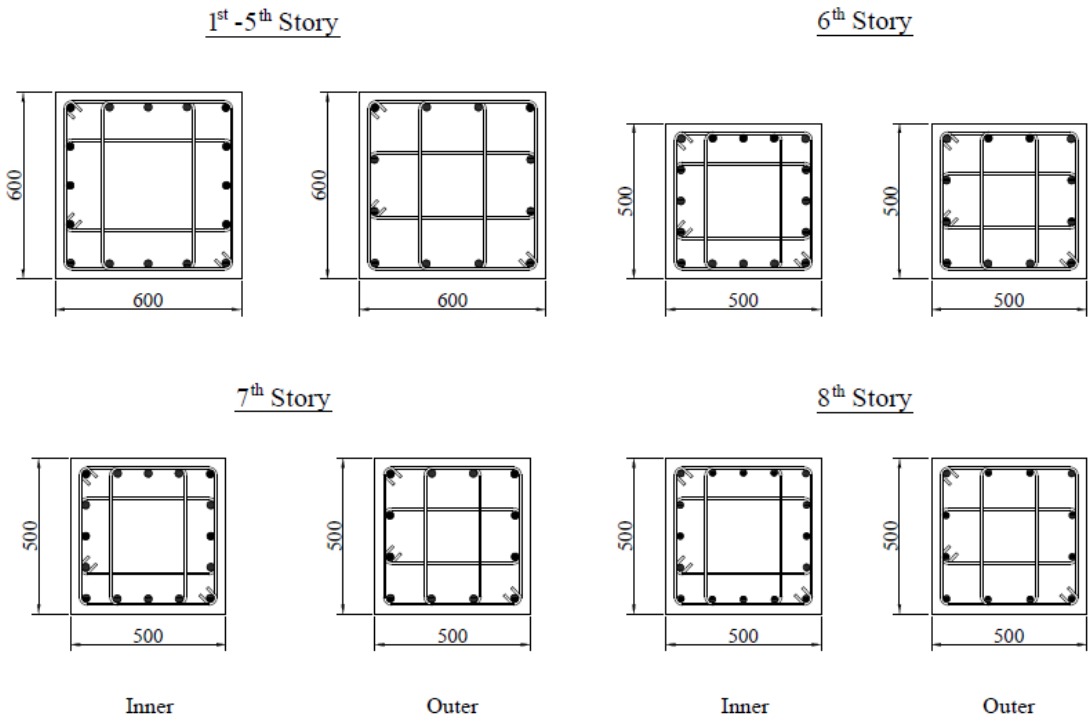

Figure 5.6. Cross Sections for Columns of 8 Story Irregular Frame

Note that, the results for other frames are provided in the relevant appendices.

CHAPTER 6

PERFORMANCE ASSESSMENT

The probable performance of the building is assessed by utilizing a series of simulations, i.e. response analysis of the building due to loadings. The process of the detailed performance assessment of the building is shown in Figure 2.4 which is included in the content of PBSD approach. It starts with the characterization of the ground shaking hazard and ends with the prediction of the losses as a function of the damage. It is important to achieve statistical relationship between, earthquake hazard, building response, damage and then loss to accomplish the performance assessment process.

In this study, performance assessment of the designed frames are carried out without getting into much details and the results are presented. Here just damage states of the members of the frames are checked, and the drift ratios are controlled with the one chosen, and it is assumed that there are no nonstructural members and content system.

For the purpose of evaluation of the performance of the frames, designed by DDBD approach, nonlinear static pushover and nonlinear time history analysis are conducted. Brief information is provide about each of these methodologies. In addition, some information which are necessary for modeling frames for nonlinear static pushover and nonlinear time history analysis, are provided.

For the assessment of the performance of the frames, Turkish Seismic Design Code (2007) [8], has been used. Although recommendations are given for the evaluation of the existing buildings, they can be implemented for assessment of the newly designed buildings.

6.1 Cross-Sectional Member Damage Limits and Damage Regions

In Turkish Seismic Design Code [8], three damage limits for the cross-sections of the members of a frame and shear wall are provided. These damage limits are Minimum Damage limit (MN), Safety Limit (GV), and Collapsing limit (GÇ). In addition, four damage regions for the members are given. They are shown in Figure 6.1.

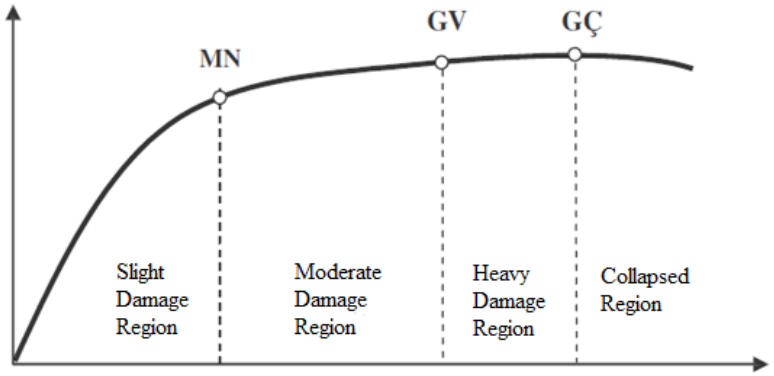

Figure 6.1. Cross-Sectional Member Damage Limits
(Adopted from Turkish Seismic Design Code, 2007 [8])

Minimum damage limit correspond to the behavior of the member when it first yields which is the border between slight and moderate damage regions. Safety limit correspond to the behavior of the member which can ensure safety, and as shown in Figure 6.1, it is border between moderate damage and heavy damage regions. The last limit given is collapsing limit, which is the state of the member just before collapse. This shows a border between heavy damage and collapsed regions [8].

In Turkish Seismic Design Code, the following strain limits are given for different damage limits of the members.

For minimum damage limit, the strain limits are given for concrete as compression strain and for steel bars as tensile strain. These limits are equal to:

$$(\varepsilon_{cu})_{MN} = 0.0035 \tag{6.1a}$$

$$(\varepsilon_{s})_{MN} = 0.010 \tag{6.1b}$$

For safety limit, the strain limits for each concrete and steel bars are given as follows. It should be noted, that strain limit for concrete is given at the outmost fiber of hoop (i.e. at the exterior face of the outer hoop).

$$\left(\varepsilon_{cg}\right)_{GV} = 0.0035 + 0.01\left(\frac{\rho_s}{\rho_{sm}}\right) \leq 0.0135 \tag{6.2a}$$

$$(\varepsilon_{s})_{GV} = 0.040 \tag{6.2b}$$

For the collapse limit these limits are given as follows:

$$\left(\varepsilon_{cg}\right)_{GÇ} = 0.004 + 0.014\left(\frac{\rho_s}{\rho_{sm}}\right) \leq 0.018 \quad (6.3a)$$

$$\left(\varepsilon_s\right)_{GÇ} = 0.060 \quad (6.3b)$$

In aforementioned formulas:

ρ_s is the volumetric ratio of existing transverse reinforcements.

ρ_{sm} is the minimum volumetric ratio of the transverse reinforcements.

In this study, since the members are newly designed and at least they satisfy the minimum requirements. Therefore, the ratio (ρ_s/ρ_{sm}) will be one or greater than one. As a consequence the limits for concrete at later two cases will be constant values, which are equal to:

$$\left(\varepsilon_{cg}\right)_{GV} = 0.0135 \qquad \text{for safety limit}$$

$$\left(\varepsilon_{cg}\right)_{GÇ} = 0.018 \qquad \text{for collapse limit}$$

6.2 Moment-Curvature Diagram

To find these limits for a given cross section, moment-curvature diagram for the cross section is obtained through analysis. For this purpose a program, written in Microsoft ® Excel 2000, by Ersoy et al in 2000, and the information about this program has been provide in Ersoy et al. 2013 [10], is utilized.

In this program strain hardening for steel and tension for concrete are considered. Moreover the following assumptions are made:

- Modified Kent and Park Model is used for confined concrete.
- For steel reinforcement stress-strain curve is assumed to be a tri-linear curve. This is given in following figure.

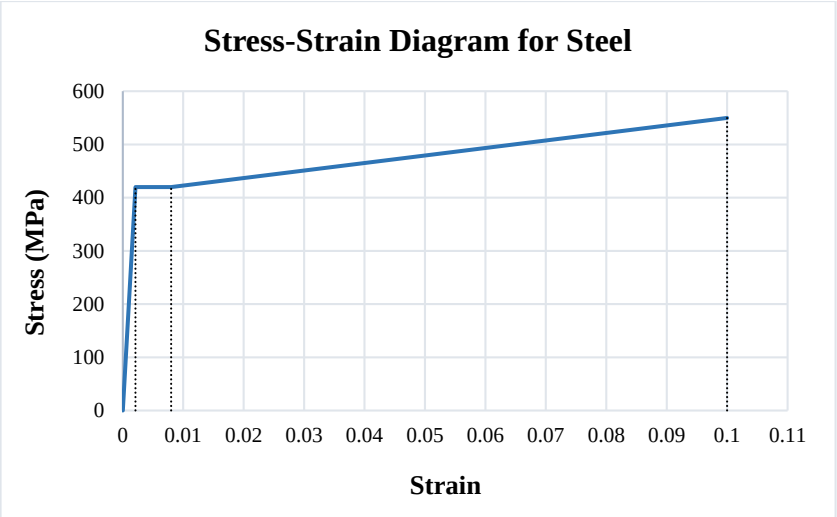

Figure 6.2. Stress-Strain Relation for Steel
(Adopted from Turkish Seismic Design Code, 2007 [8])

The stress strain curve, shown in Figure 6.2, is adopted from Turkish Seismic Design Code. The corresponding values of this figure are given in Table 6.1.

Table 6.1. Stress-Strain Values for S420

Grade	f_{sy} (MPa)	f_{su} (MPa)	ε_{sy}	ε_{sh}	ε_{su}
S420	420	-	0.0021	0.008	-
	-	550	-	-	0.1

In Table 6.1, ε_{sy}, ε_{sh}, and ε_{su} are yield strain, strain till the end of strain hardening and ultimate strain, respectively. Further, f_{sy} and f_{su} are the yield and ultimate strength of the steel reinforcement, respectively. It should be noted that in the program for calculation of moment-curvature relation, these values can be applied as input data.

- Stress-strain curve of the unconfined concrete is divided into two, parts the ascending part is given by following equation:

$$\sigma_c = f_c \left[\frac{2\varepsilon_c}{0.002} - \left(\frac{\varepsilon_c}{0.002} \right)^2 \right] \tag{6.4}$$

The descending portion of the stress-strain curves is assumed to be linear with the slope of (-185f_c), and it is assumed that the strain at the end of the descending portion is equal to $\varepsilon_{cu} = 0.004$.

- A bi-linear curve which is shown in Figure 6.3c, is given for stress-strain relation of concrete in tension. The following values are given in the program for some parameters as shown in Figure 6.3c.

$$c_1 = 0.5, \quad \varepsilon_{ct} = 0.001, \quad \text{and} \quad \varepsilon_{cty} = 0.0002$$

After $\varepsilon_{cty} = 0.0002$ the stress drops to zero.

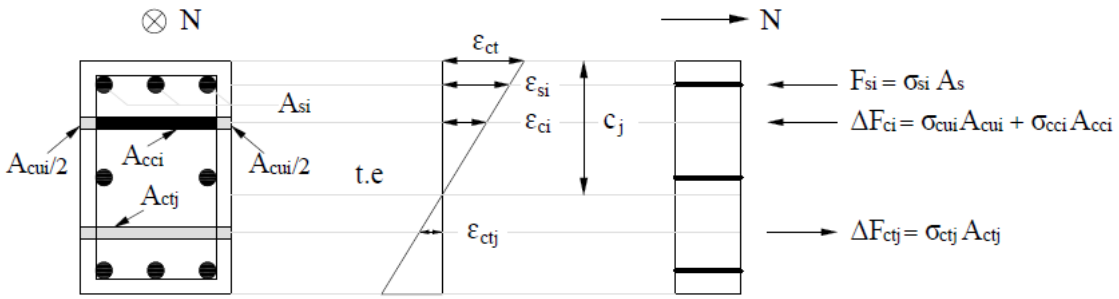

a) Strain Distribution and Internal Forces of a Typical Rectangular Section

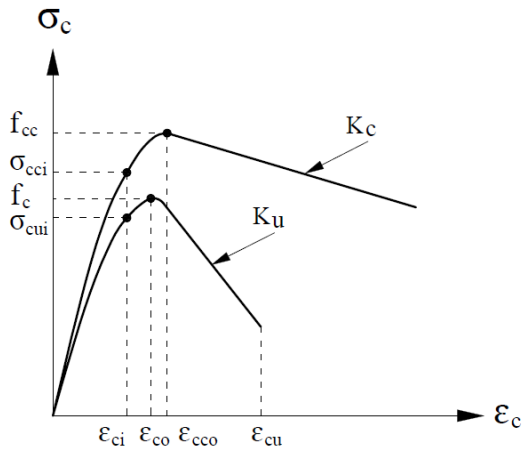

b) Compressive Stress-Strain Curve for Confined and Unconfined Concrete

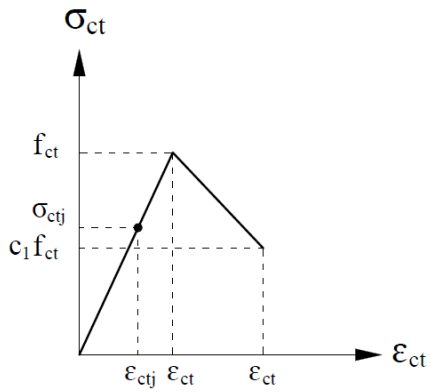

c) Tension Stress-strain Curve for Concrete

Figure 6.3. Strain Distribution of Rectangular Section and Concrete Stress-Strain Curves (Adopted from Ersoy et al., 2013 [10])

In addition, to find out the moment-curvature diagram for sections, an approach which is called layer by layer evaluation of sections forces, is utilized. Since this program

is only written for a rectangular cross section, therefore cross section of a member is divided into "n" number of rectangles as shown in Figure 6.3a. In compression zone of the section, each rectangle is divided into two parts, confined and unconfined concrete, except the area which is out of the core (i.e. which is at the top outside the hoops). Initially, a value is chosen for ε_c (shown in Figure 6.3a), and a value for the depth of the neutral axis is assumed. The strain in each rectangle and steel reinforcements is obtained from the geometry and then using relations between strains and forces, forces are obtained [10]. The summation of these forces with external forces should be equal to zero.

For each value of ε_c a moment and corresponding curvature can be obtained, and for a range of values for ε_c moment curvature diagram can be achieved. The program automatically does these calculations and gives the results in terms of diagram with calculated data.

Since the output data is in terms of moment and curvature for different values of ε_c, therefore the corresponding curvature for strain limits are obtained, which are then entered in SAP2000 v17.1 as input data. The relation between strain and curvature is given by following equation, which is adopted from Ersoy et al. 2013 [10].

$$K = \frac{\varepsilon_c}{c} \tag{6.5}$$

Where:

c is the depth of the neutral axis.

K is curvature.

ε_c is strain at the outmost fiber in compression zone of the concrete.

Once the strain limits are obtained for each member then it is easy to determine the building performance levels.

6.3 Seismic Performance Levels of Buildings

Four seismic performance levels for reinforced concrete buildings are given in Turkish Seismic Design Code (2007) [8]. The performance levels are, immediate occupancy performance level, life safety performance level, collapse prevention performance level and collapse. They are described briefly as follows:

Immediate Occupancy Performance Level (IO):

In this performance level, under given earthquake hazard for a given direction, 10% of beams at a story can be in moderate damage region, the rest of the elements must be in slight damage zone [8].

Life Safety Performance Level (LS)

For the direction of earthquake, for a building to be in this performance level, 30% of the beams in a story is allowed to be in heavy damage region. The shear forces in the columns, which are in heavy damage zone, should not exceed 20% of the total shear force in a story. In addition, shear forces in columns which are in moderate damage zone should be at most 40% of total shear forces at the top floor, while for other stories, this percentage must be at most 30%. It should be noted that this percentage corresponds to the both upper and lower sections of the columns in that floor. The remaining elements should be in minimum damage zone [8].

Collapse Prevention Performance Level (CP)

In this performance level, only 20% of the beams can be in collapsed region, the rest of the elements can be minimum or slight damage, moderate damage and heavy damage regions. Columns which are in a damage state beyond the minimum damage region (i.e. with moderate or higher damage level), should not contribute to the total shear force of that level more than 30%, both from upper and lower sections [8].

6.4 Nonlinear Static Pushover Analysis

Pushover analysis is a useful and practical tool for the performance evaluation of existing structures and newly designed structures [64]. It is one of the simplest analysis methods and it is used for inelastic analysis of the structure, under a vector of forces or a vector of displacements. The vector of forces presents the expected inertial forces in structures, due to earthquake loads while displacement vector presents the expected displacement response in the structures [6]. In pushover analysis the vector of forces or

displacements is increasing monotonically on the structure (i.e. the vector of forces or displacements are incrementally applied) [65].

The main outcome of pushover analysis is a capacity curve (Base shear force vs top displacement), from which target displacement, a displacement induced by design earthquake, can be determined. The capacity curve shows nonlinear behavior of the structure under increasing base shear force. Furthermore, at each step of pushover analysis structural elements will start yielding continuously one after other which will cause different damage states to develop in these elements (i.e. plastic hinges will occur in elements), and after the structure reaches to its yield capacity, the structure as a whole will start losing its lateral stiffness [65]. The slope of the capacity curve will change, which shows a nonlinear behavior of the structure.

There are some limitations about implementation of pushover analysis. First, in pushover analysis only single mode can be considered, mostly first mode is adopted. Second, since pushover analysis include only one direction analysis, therefore, it is not possible to consider hysteretic characteristic of the structure in the analysis [6].

Since pushover analysis itself is an equivalent lateral load method, therefore, according to Turkish Seismic Design Code (2007) [8], it cannot be applied to the building structures with having more than 8 story or total height of 25m. This is because, as mentioned earlier, that in pushover analysis only a single mode of vibration can be considered and higher mode effects cannot be included.

Two types of analytical models can be prepared for frames structures to implement pushover analysis. One of them is distributed plasticity (plastic zone) and the other is concentrated plasticity (plastic hinges) [65]. In addition, in pushover analysis, two possibilities exist for controlling, while performing analysis. The first one is to choose applied lateral loads as control parameter and the second one is to control the analysis by choosing top displacement of the structure [66].

For implementation of nonlinear static pushover analysis of the designed frames, as mentioned earlier, SAP2000 v17.1 is utilized. For modelling frames in SAP2000 v17.1 the following steps with corresponding assumptions are made.

- All frames are modeled as 2D frames.
- Material properties for members (beams and columns) are taken homogenous.
- Material properties for concrete and steel reinforcements are defined, with considering their nonlinear properties. For steel reinforcement strain hardening effects are

considered, as given in Turkish Seismic Design Code [8], (refer to Figure 6.2). For concrete, stress-strain model developed by Mander et al. (1988) [67] (refer to Figure 6.4), used as default model by SAP2000 v17.1, is conducted. It should be noted that tension strength of concrete is also considered in this model.

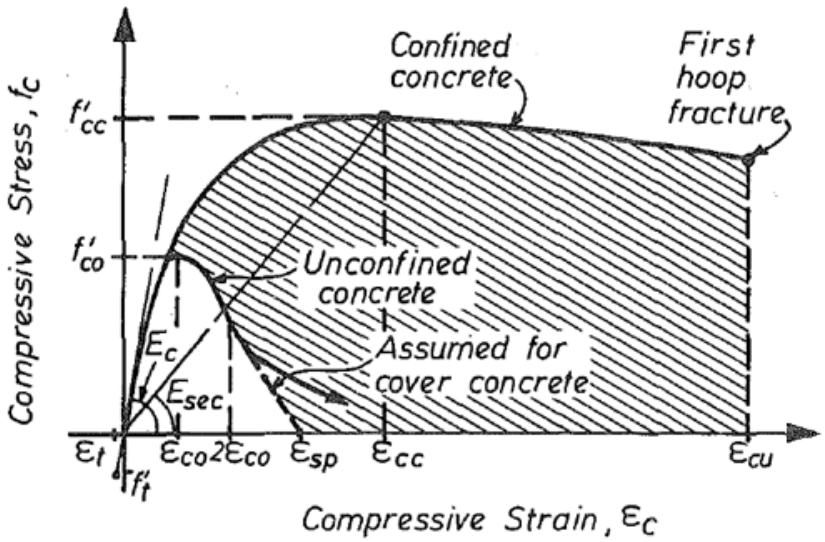

Figure 6.4. Stress-Strain Model for Confined and Unconfined Concrete (Adopted from Mander et al., 1988 [67])

In Figure 6.4:

f'_{co} is compressive strength of unconfined concrete.

f'_{cc} is compressive strength of confined concrete.

f'_t is the tensile strength of concrete.

ε_{cc} is compressive strain at f'_{cc}.

ε_{cu} is ultimate concrete compressive strain.

ε_{co} is compressive strain at f'_{co}.

ε_{sp} strain at which cover concrete is considered to have completely spalled and ceases to carry any stress.

E_c Modulus of elasticity of concrete.

E_{sec} secant modulus of elasticity of confined concrete at peak strength.

For more details about stress-strain model for concrete the reader is referred to Mander et al. 1988 [67].

- In the next step, cross sectional properties are defined. To consider cracked section stiffness, the gross stiffness of the section is reduced as recommended in Turkish Seismic Design Code (see Section 3.1.5).
- Later, hinge properties are defined. Since the frames are modeled in Y axis (i.e. the direction of seismic loading is in Y axis), for beams "Moment-M3" type of hinges are considered, while for columns, "P-M2" type of hinges are used. Moment-curvature type of diagram is chosen, and the limits for different damage states, which are obtained from moment-curvature diagram for each element of the frame, with respect to Turkish Seismic Design Code are assigned.
- For columns, hinge interaction surface is chosen as default, given in SAP2000 v17.1 as "Concrete, ACI 318-02 with $\emptyset = 1$" ($\emptyset$ is strength reduction factor). In addition, elastic- perfectly plastic relation is used for axial load-displacement relationship. Further, a single curvature angle for moment curvature curves of columns, is assumed, and it is also assumed that the moment curvature curves are symmetric for both columns and beams. The number of axial loads on each column for moment curvature curve is taken as 2. These axial loads are the maximum and minimum axial loads on columns which are obtained through analysis with considering load combinations.
- Columns and beams are assumed to be line elements, and it is assumed that the boundary condition of columns at the base of the first story are fully fixed.
- Load patterns are then defined, for different types of loadings. Loads are applied on the frames as distributed loads and concentrated loads on the beams and on joints respectively.
- A nonlinear static case, considering only gravity loads is defined to be an initial case for implementing other nonlinear cases. Here, in content of gravity loads 100% of dead loads are considered, and as recommended in Turkish Seismic Design Code, 30% of live load is used.
- Nonlinear static pushover analysis case has been defined. Here, a set of equivalent lateral forces obtained through DDBD approach (using Equation 4.24) has been used. The equivalent lateral forces are applied at the top of each story at the beam-column joints. P-Delta effects are also considered, as have been considered in DDBD approach. In addition, the displacement is chosen as the controlling parameter for load, and for this purpose, monitored displacements at the top of the frames are chosen.

- Plastic hinges are assigned at the end of each member (columns and beams), with considering end-offsets. The length of plastic hinge regions according to Turkish Seismic Design Code, is equal to the half of the depth of the cross section of the member in the direction of earthquake.

$$L_P = \frac{h}{2} \tag{6.6}$$

Where:

L_P is the length of the plastic hinge.

h is the cross sectional depth of the member at the direction of the earthquake.

6.5 Nonlinear Time History Analysis

Time history analysis is one of the most powerful and reliable analysis methods for achieving performance of a structure under design seismic intensity. Two types of time history analysis are common in literature, linear and nonlinear time history analysis. The analysis is done stepwise, the outcome is dynamic response of the structure under time dependent loadings (e.g. earthquake loading).

In this study, nonlinear time history analysis is conducted. Therefore, seven synthetic accelerograms are created artificially by using SeismoArtif, V2.1.2 [68]. For this purpose, elastic acceleration response spectrum utilized in DDBD approach is used as target response spectrum. The following assumptions are made while creating these accelerograms.

- Far field, inter-plate regime is assumed.
- The distance between main event and construction site is assumed to be 11.7Km as recommended by program, automatically.
- Moment-magnitude is assumed to be 7.5.
- The soil type is assumed to be generic rock with linear sites effects. This is close to the soil group B of site class Z_2, given in Turkish Seismic Design Code.
- PGA is given as 0.4g and 5% elastic damping is used.

The results are tabulated in the following table.

Table 6.2. Overall Statistics for Target Spectrum

No	Mean Error	Coefficient of Variation	PGA (g)	PGV (cm/sec)	PGD (cm/sec)	Significant Duration (sec)
1	6.900	4.500	0.399	47.969	76.502	17.340
2	6.740	4.090	0.400	46.696	35.106	19.000
3	6.490	3.850	0.400	55.476	38.705	15.890
4	6.470	3.980	0.400	93.254	169.789	15.075
5	6.970	4.480	0.400	57.422	41.450	14.510
6	6.550	4.150	0.400	167.097	1248.774	16.810
7	6.870	4.270	0.400	70.358	101.030	17.370
Average	**6.710**	**4.190**	**0.400**	**76.896**	**244.480**	**16.571**

The total duration for each of these accelerograms is just above 29 sec. The accelerograms are shown in Figure 6.5a, while their average with target Acceleration Response Spectrum (ARS), i.e. elastic acceleration response spectrum for 5% damping, is shown in Figure 6.5b. As can be seen from Figure 6.5b that the average of these accelerograms are matching the acceleration response spectrum in excellent manner.

In addition, these accelerograms are changed to displacement and the graphs for their displacements are shown in Figure 6.6a, and in similar way with the accelerograms, their average is shown with target Displacement Response Spectrum (DRS), i.e. displacement response spectrum obtained for 5% damping, in Figure 6.6b. The agreement between average of generated displacements and the target DRS is very well.

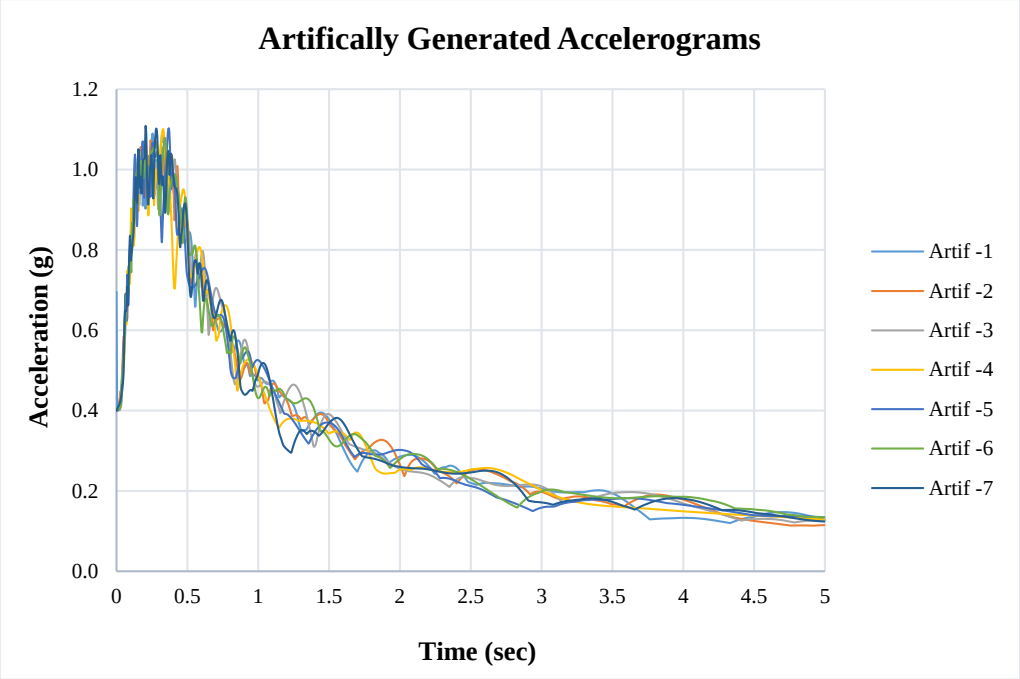

a) Artificially Generated Accelerograms

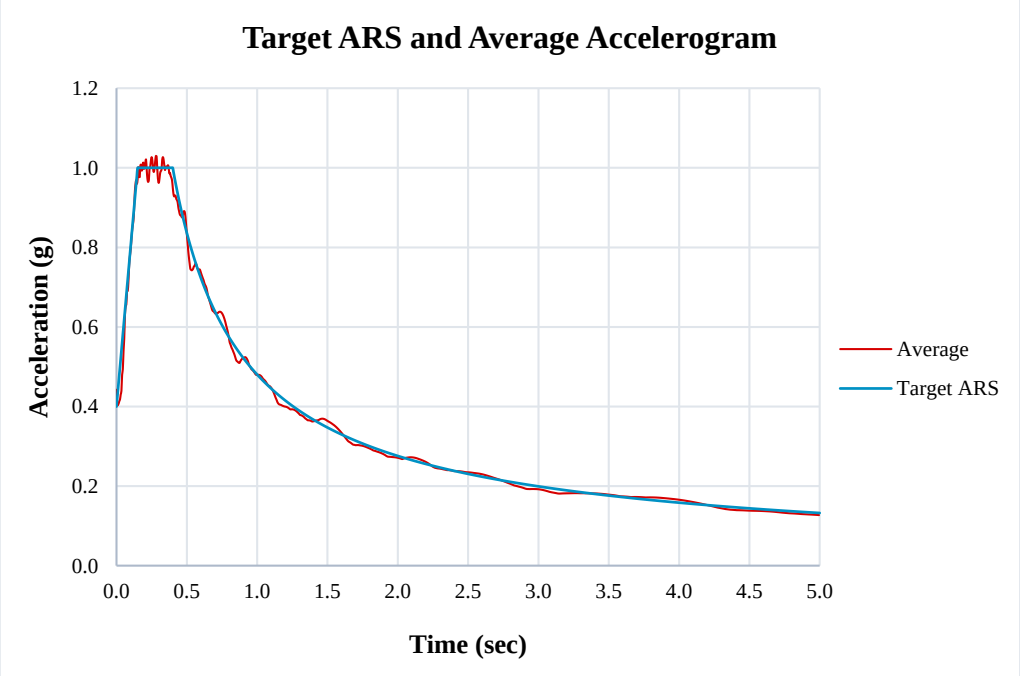

b) Target ARS with the Average of Artificially Generated Accelerograms

Figure 6.5. Target ARS and Artificially Generated Accelerograms

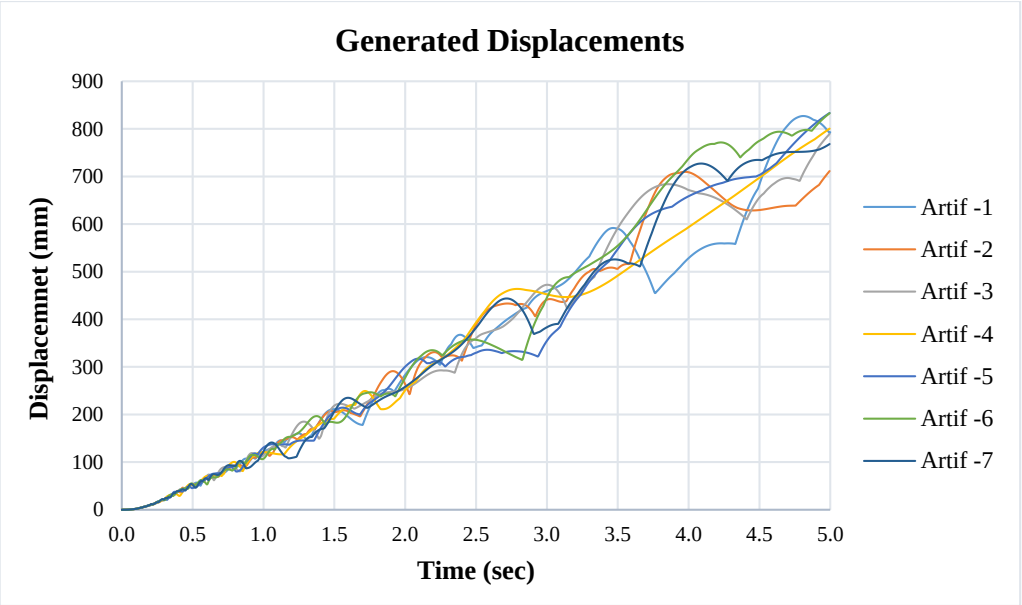

a) Displacements for Artificially Generated Accelerograms

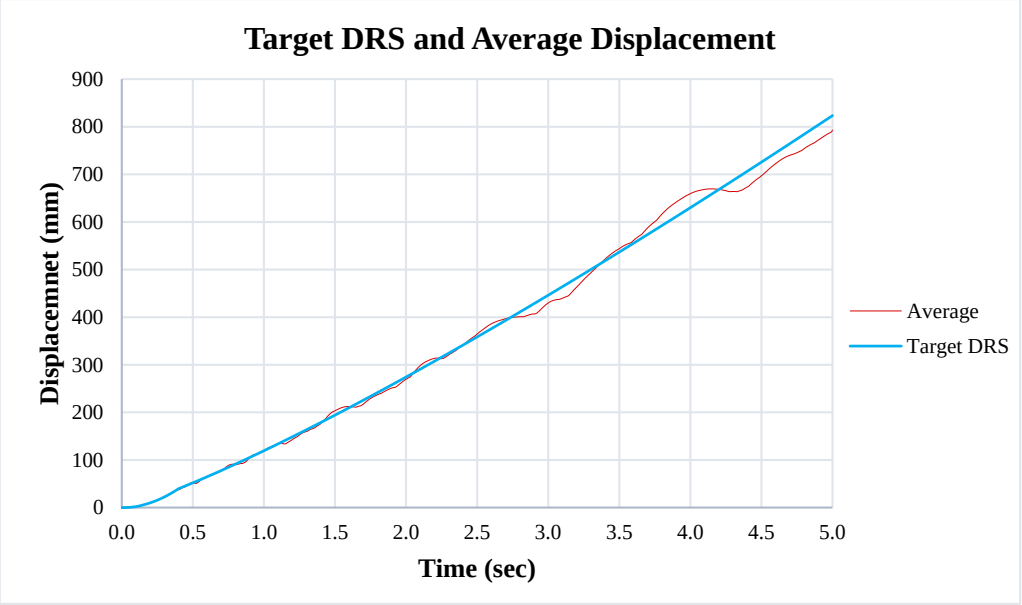

b) Target DRS and the Average Generated Displacement

Figure 6.6. Target DRS and Artificially Generated Displacements

For modelling frames for nonlinear time history analysis in SAP2000 V17.1 in addition to the steps and assumptions made for nonlinear static pushover analysis, the following steps with corresponding assumptions are included.

- Time history functions are defined using artificially created accelerograms.
- Two types of solutions are available for nonlinear time history analysis in SAP2000 v17.1, modal and direct integration. In modal type of solution, mode superposition is

used, while in direct integration type of solution, the equations of motions are being solved for the structure at each time step [69]. In this study, direct integration type of solution is assumed for nonlinear time history cases.

- For direct integration nonlinear time history analyses, viscous proportional damping is used. For an element, damping matrix is calculated by using following equation [66].

$$C = c_M M + c_K K^0 \tag{6.7}$$

Where:

c_M is mass coefficient.

c_K is stiffness coefficient.

M is the mass matrix of the element.

K^0 is the stiffness matrix of the element.

It should be noted that K^0 is the initial stiffness of a nonlinear element, at zero initial condition, without considering the current nonlinear state of the element [66].

Viscous proportional damping for the direct integration nonlinear time history analysis can be defined in three different ways. First, damping can be specified directly by using mass and stiffness proportional coefficients. Second, it can be specified by using two different modal damping with their corresponding periods. Finally it can be specified, by using frequencies of two different modes [66].

For implementation of direct integration nonlinear time history analysis in SAP2000 v17.1 "Hilber-Hughes-Taylor alpha" method is chosen in this study. In this method only one single parameter "$\propto$" is used. This parameter can take value between 0 and -1/3, and it is recommended to take it zero or close to zero for more accurate results [66]. Thus, in this study, this parameter is taken zero ($\propto = 0$).

- For members to show nonlinear behavior in nonlinear time history analysis, it is necessary to define hysteretic properties for both members and for the type of materials used in these members. Nonlinear response of members can be determined by force-deformation relation which is the result of loading, unloading and reloading of the members [6]. In this study, Modified Takeda model is used for representing hysteresis type for members and materials. In SAP2000 v17.1, takeda model is only available for beams, while for materials, it is available for both concrete and reinforcement. It should

be noted that in SAP2000 v17.1 parameters related to modified takeda model is taken automatically, and no modifications are possible.

6.6 Results of Nonlinear Analysis

6.6.1 Results of Nonlinear Static Pushover Analysis

The results from nonlinear static pushover analysis are presented in terms of capacity curves, sway mechanism for life safety performance level, and interstory drift ratios. In these curves limits for different performance levels are also shown.

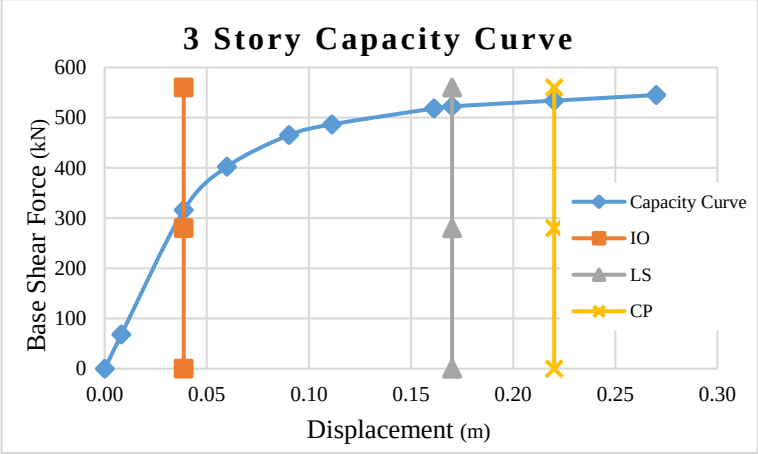

a) 3 Story Capacity Curve

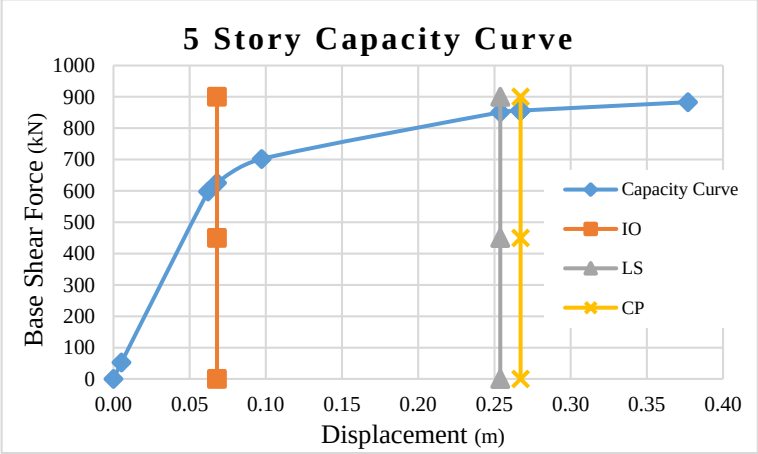

b) 5 Story Capacity Curve

Figure 6.7. Capacity Curves for 3 and 5 Story Irregular RC Frames Obtained Through Nonlinear Static Pushover Analysis

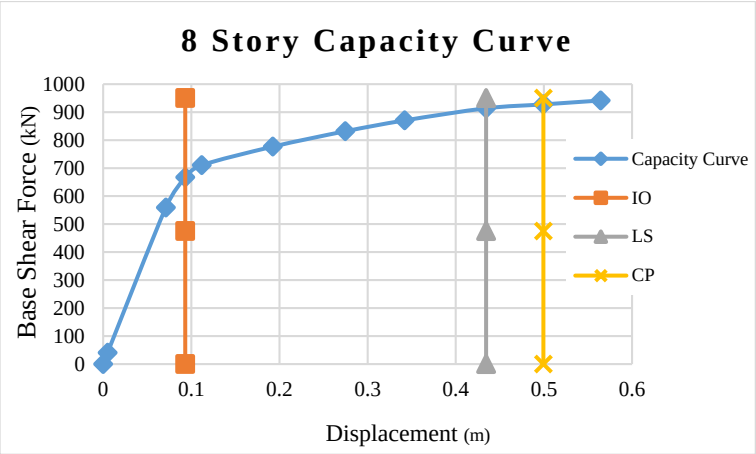

a) 8 Story Capacity Curve

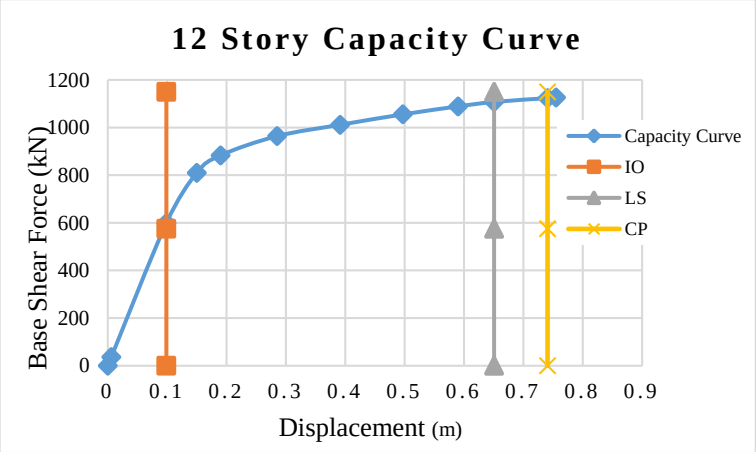

b) 12 Story Capacity Curve

Figure 6.8. Capacity Curves for 8 and 12 Story Irregular RC Frames Obtained Through Nonlinear Static Pushover Analysis

In Figure 6.7 and Figure 6.8 capacity curves for the designed frames are obtained by using nonlinear static pushover analysis. In these figures, for each structure the approximate limits for three performance levels, immediate occupancy, life safety and collapse prevention performance levels are shown. It should be noted that, it is not recommended in Turkish Seismic Design Code, to perform equivalent lateral load analysis, i.e. to perform pushover analysis for buildings with more than 25m height. However, in this study for 12 story irregular frame with 36.6m height larger than 25m, nonlinear static pushover analysis is performed just to show the performance levels, and to check the sway mechanism.

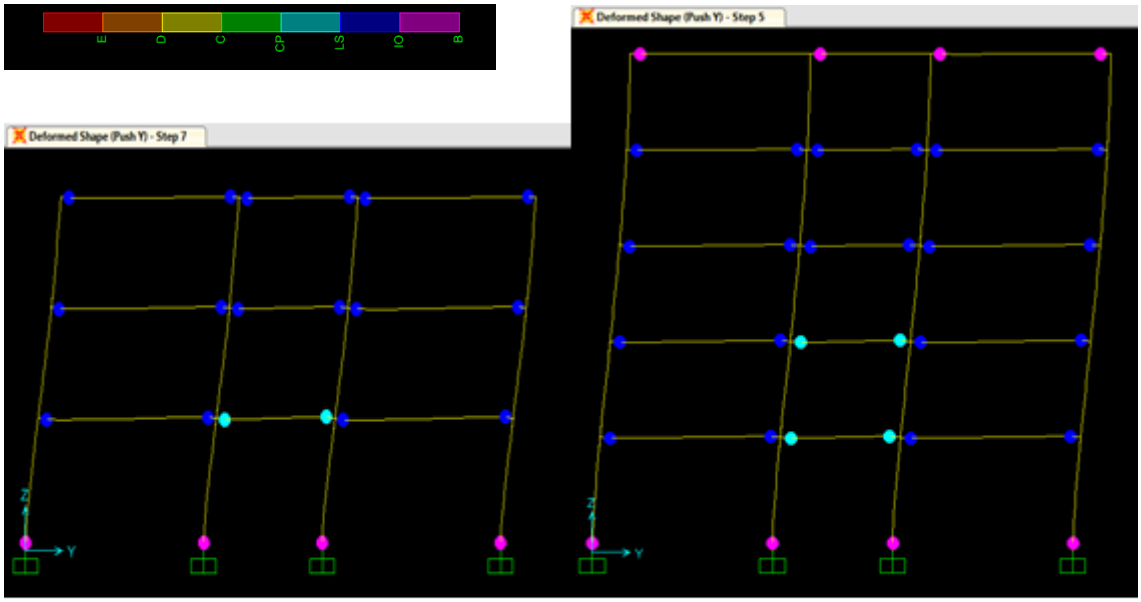

a) 3 Story Sway Mechanism b) 5 Story Sway Mechanism

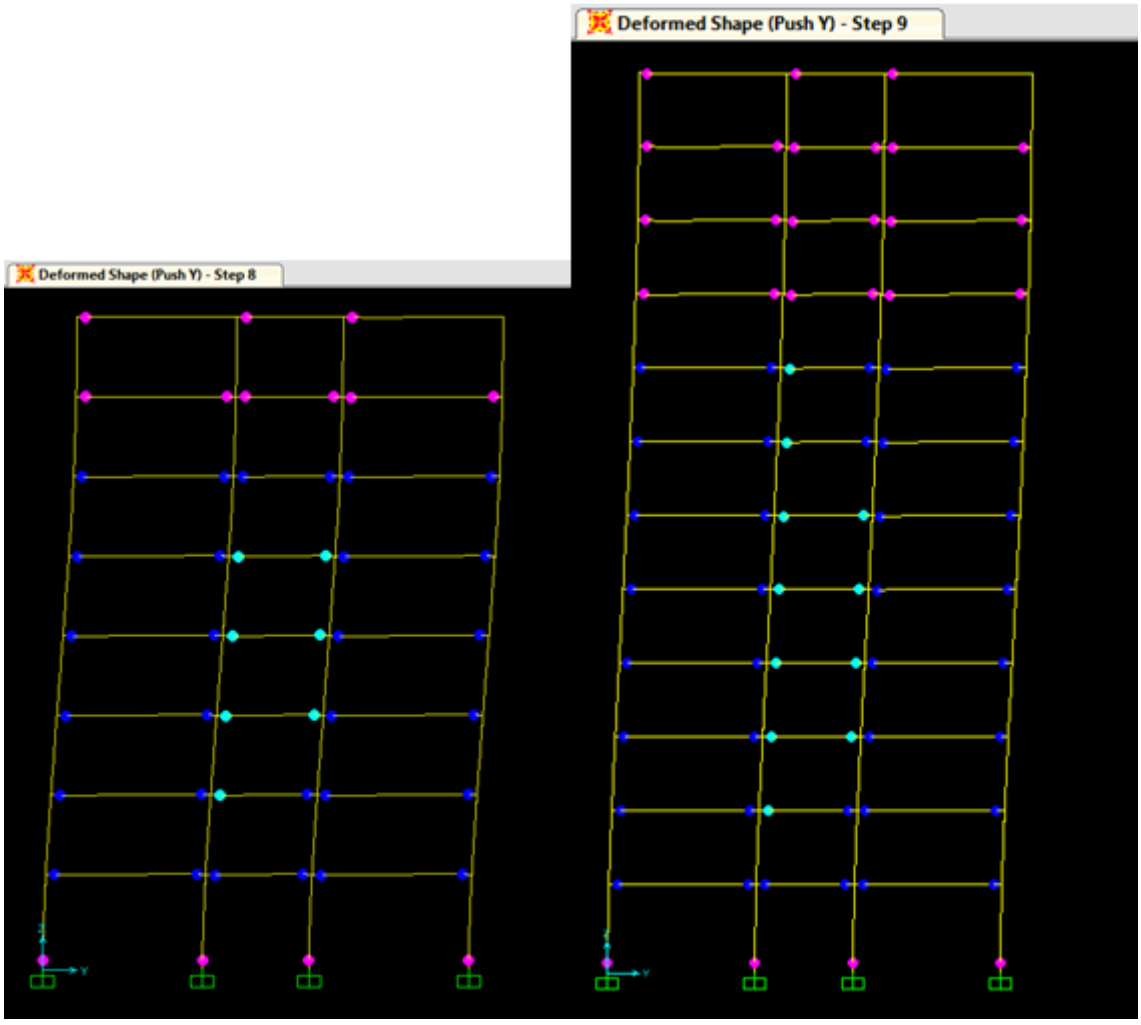

c) 8 Story Sway Mechanism d) 12 Story Sway Mechanism

Figure 6.9. Sway Mechanisms of Irregular RC Frames Obtained Through Nonlinear Static Pushover Analysis

It should be reminded that according to Turkish Seismic Design Code for a frame building to be in life safety performance level, no more than 30% of the beams in a story can be in heavy damage zone. In addition, the columns which are in moderate damage zone, shall not take more than 30% of the total shear force at a story, except for roof level in which up to 40% is allowed. However, since in this study only one frame of a building structure is considered, hence the percentage for beams has been accepted to be almost 33.33% (which represents one beam out of 3 beams).

From the capacity curves of the frames, shown in Figure 6.7 and Figure 6.8, it can be seen that the limits for life safety performance levels in terms of top displacements are approximately 17cm, 25.4cm, 43.4cm, and 65.1cm which correspond to 523kN, 851kN, 914kN and 1108kN base shear forces, for 3, 5, 8 and 12 story frames, respectively.

The design displacements for the roof level of 3 story frame, obtained through DDBD approach, which is 19.2cm and the corresponding base shear force is almost 441kN, is not satisfied. For 5 story frame the top displacement achieved through nonlinear static pushover analysis is just a little bit larger than the one obtained by DDBD procedure which is 24.8cm, but the corresponding base shear force gained by nonlinear static pushover analysis is significantly larger than the one obtained through DDBD procedure (851kN>>656kN). The result for top displacement of 8 story frame is 43.4cm and 38.3cm, obtained through nonlinear static pushover and DDBD procedures, with corresponding base shear forces of 914kN and 859kN, respectively.

To conclude, the frames are much stiffer than expected, and the stiffest frame amongst these three frames is the 5 story frame, while the 8 story structure is least stiff. It should be noted that the result for the 12 story is not compared, since the result of nonlinear static pushover analysis for this frame is not reliable according to Turkish Seismic Design Code, 2007. On the other, all frames, beam sway mechanism, discussed in capacity design principles (Section 4.3), are well satisfied for all frames (refer to Figure 6.9) at the target performance level (i.e. life safety performance level).

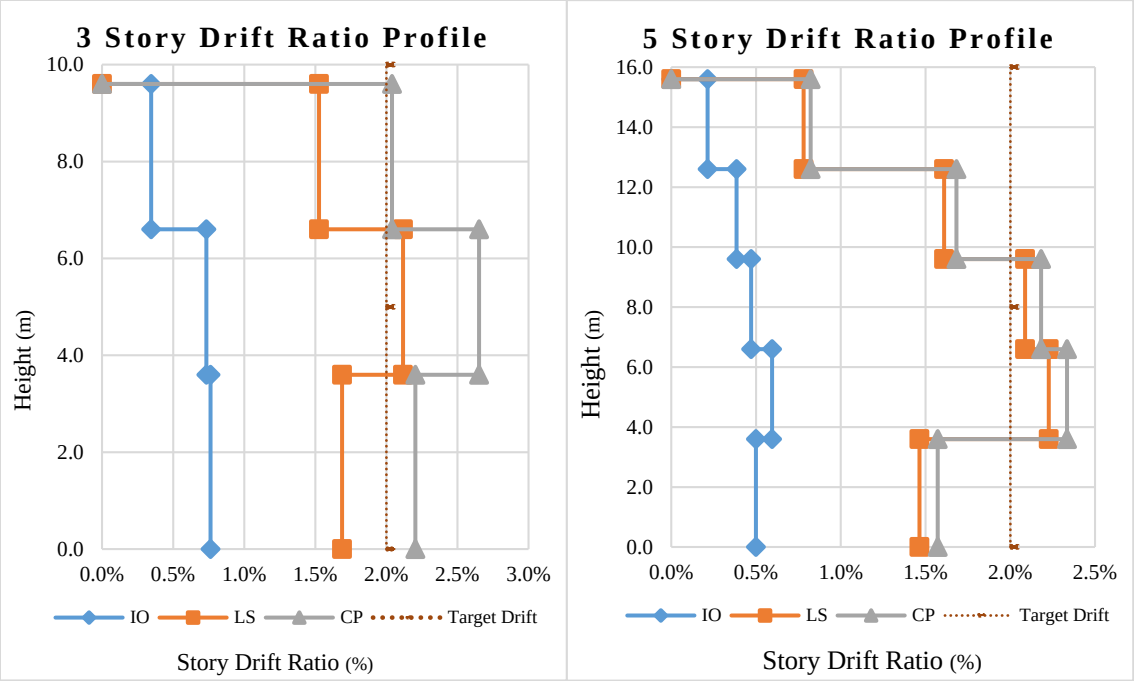

a) 3 Story Interstory Drift Ratio

b) 5 Story Interstory Drift Ratio

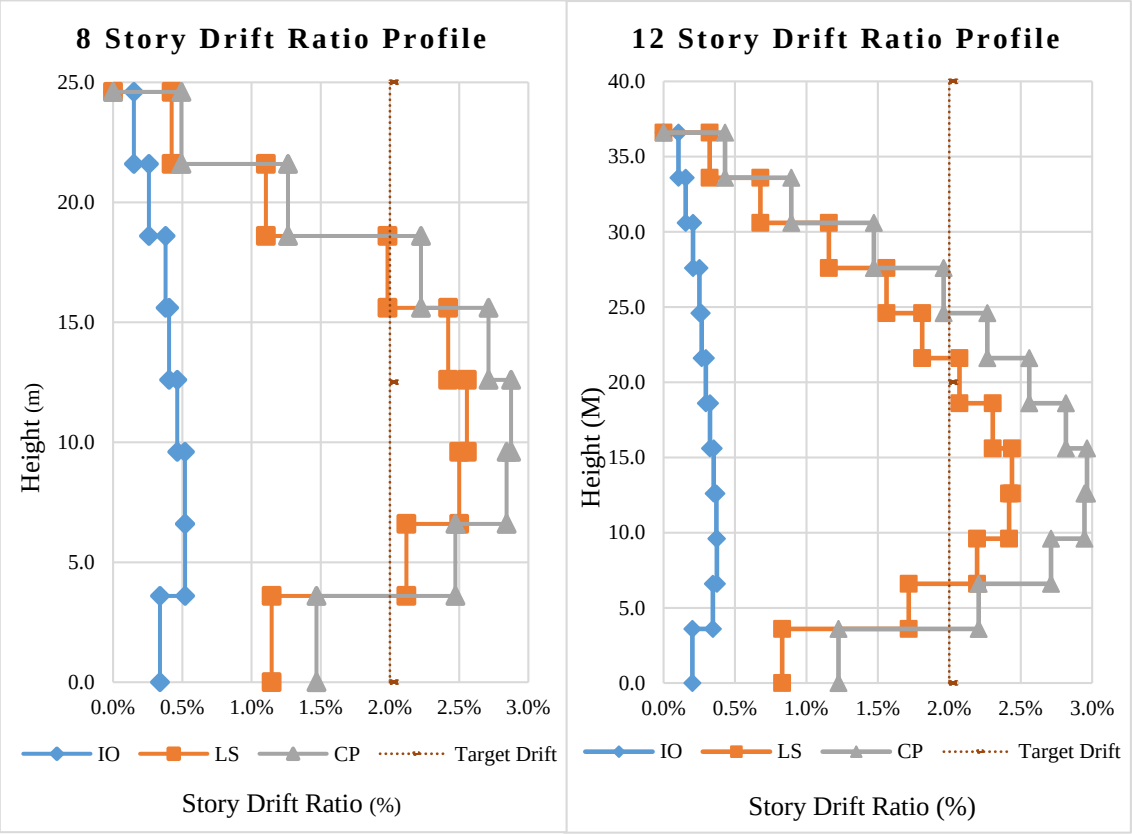

c) 8 Story Interstory Drift Ratio

d) 12 Story Interstory Drift Ratio

Figure 6.10. Interstory Drift Ratios of Irregular RC Frames Obtained Through Nonlinear Static Pushover Analysis

The interstory drift ratios, shown in Figure 6.10, are for three different steps of the nonlinear static pushover analysis, which correspond to the immediate occupancy, life safety, and collapse prevention performance levels. The story drift ratios for life safety performance level in this figure for frames are just to check if they meet the one chosen for the corresponding life safety performance level.

The story drift ratios for all frames are larger than target drift ratio in life safety performance level. To compare, the 3, 5, and 8 story frame, the maximum interstory drift ratio occurs in 8 story frame. This is due to larger displacement obtained using nonlinear static pushover analysis than the design target displacement obtained through DDBD approach.

The larger drift ratios occurred at those levels of the frames, at which beams entered the heavy damage zone (refer to Figure 6.9). These drift ratios occurred mostly at the lower levels as can be expected from a frame structure. For example, for 3 story frame the maximum interstory drift occurred at the second story, if Figure 6.9a is checked the midspan beam at the top of first floor has reached to heavy damage region. For 8 story frame, the maximum drift occurred at the 4^{th} story, which corresponds to the level where the upper and lower beams of this level reached to heavy damaged region.

6.6.2 Results of Nonlinear Time History Analysis

The results of the nonlinear time history analysis are just shown in terms of intersory drift ratios. The maximum interstory drift ratios, similar to the results of nonlinear static pushover analysis occurred at the lower stories (refer to Figure 6.11 and Figure 6.12). The average interstory drift ratios for all frames are close to each other, they are 1.23%, 1.12%, 1.13% and 1.31% for 3, 5, 8, and 12 story frames, respectively. The lowest drift ratios belongs to the 5 story frame, which implies that it is the stiffest frame amongst them.

For 3, 5, and 8 story frames, the maximum interstory drift ratios occurred at the 2^{nd} story, which are approximately 1.48%, 1.23%, and 1.28%, respectively. These maximum interstory drift ratios are due to different artificially created accelerograms for different frames. For 3, 5, and 8 story frames, the maximum drifts are due to Artif-2, Artif-5, and Artif-1, respectively.

For 12 story frame, the maximum interstory drift ratio is almost 1.76% caused by Artif-7 accelerogram, which occurred at the 3^{rd} story.

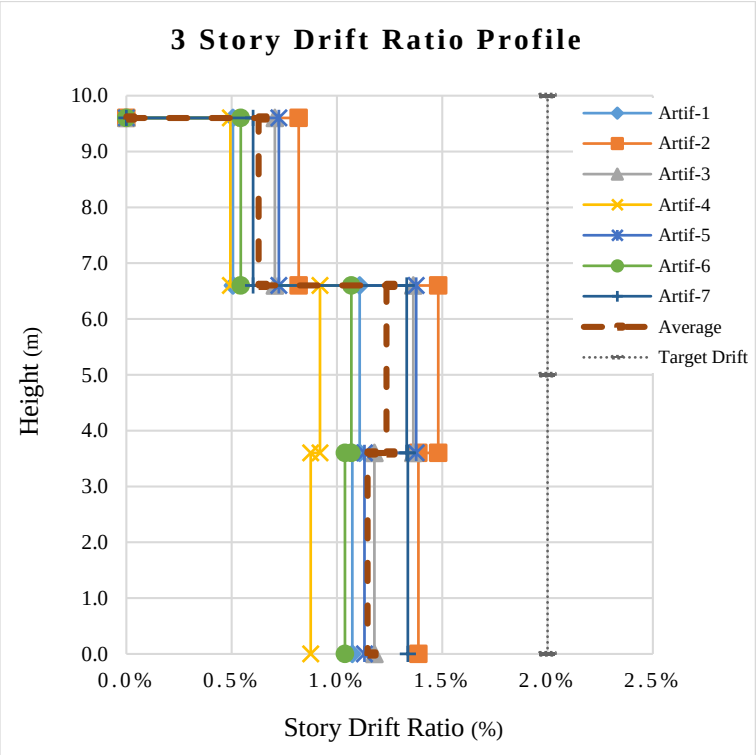

a) 3 Story Interstory Drift Ratio

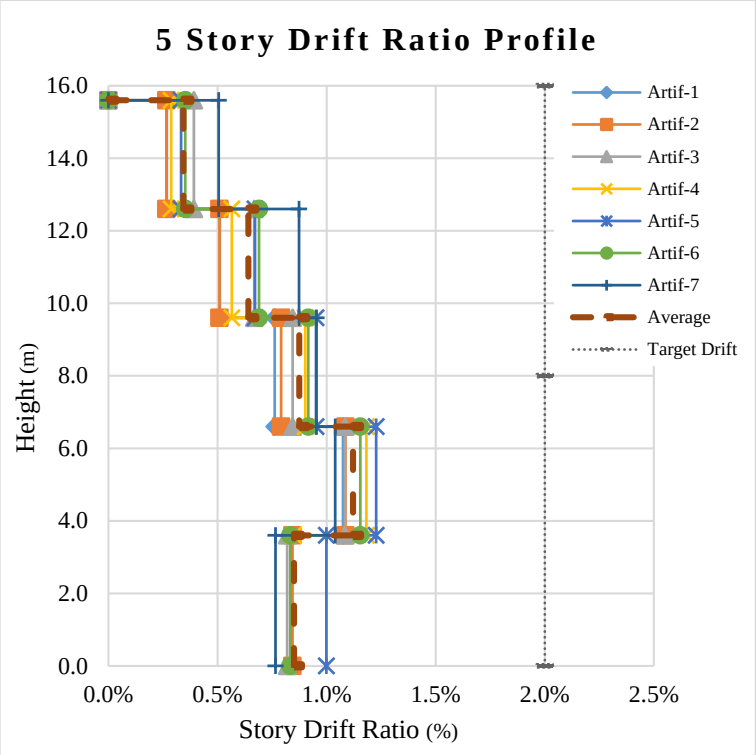

b) 5 Story Interstory Drift Ratio

Figure 6.11. Interstory Drift Ratios of 3 and 5 Story Irregular RC Frames Obtained Through Nonlinear Time History Analysis

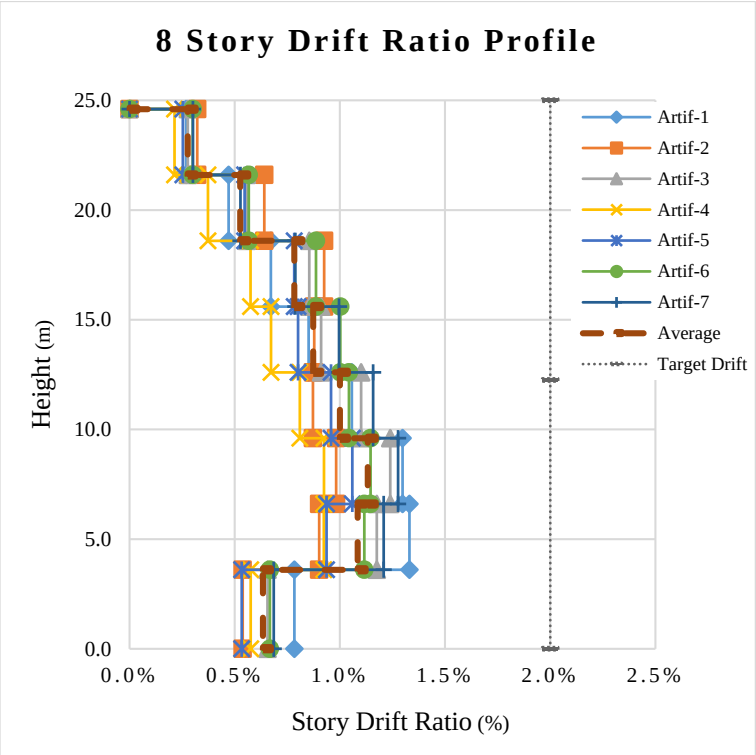

a) 8 Story Interstory Drift Ratio

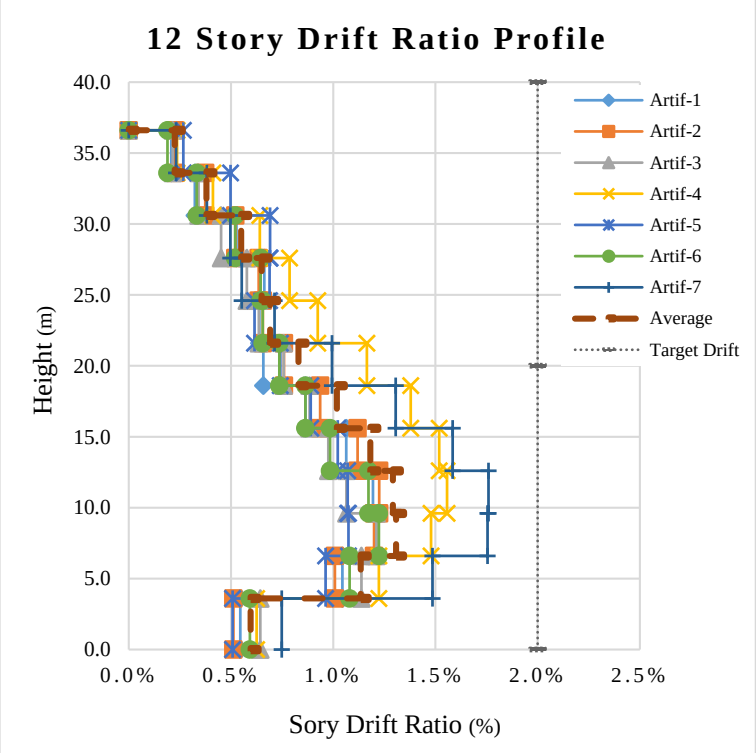

b) 12 Story Interstory Drift Ratio

Figure 6.12. Interstory Drift Ratios of 8 and 12 Story Irregular RC Frames Obtained Through Nonlinear Time History Analysis

The maximum tope displacement for 3, 5, 8 and 12 story frames are 11.25cm, 12.2cm, 19.8cm, and 35.0cm, respectively, for the accelerograms that provides maximum interstory drift ratios. The related base shear force at maximum top displacement for aforementioned frames are 399kN, 688kN, 853kN, and 1097kN, respectively. The top displacements are very small with compare to the ones obtained through DDBD approach.

If the base shear forces are compared which correspond to the maximum top displacements, for 3 story frame the base shear force obtained through nonlinear time history analysis is much smaller with compare to the one obtained by using DDBD approach. On the other hand, for 5 and 12 story frames the base shear forces are larger than the ones achieved through DDBD approach. Furthermore, the base shear force for 8 story is close to the one resulted from DDBD approach.

The results of nonlinear time history analysis is the confirmation for nonlinear static pushover analysis to some extent. Both the results from nonlinear static pushover analysis and nonlinear time history analysis have shown that the lateral stiffness of the frames are larger than expectations.

It should be noted that the two different performance levels, immediate occupancy and life safety performance levels were selected. The design interstory drift ratios for these two performance levels are 1% and 2%, respectively. The results of nonlinear time history analysis shown that the interstory drift ratios for both immediate occupancy and life safety performance levels are lower than the design values, which satisfies the code limits.

CHAPTER 7

CONCLUSIONS

Performance-Based Seismic Design (PBSD), which is a new concept in seismic design of structures, is a reliable approach for seismic design of structures. PBSD approach is currently under the research of professionals, and it is being developed progressively.

In this study, Direct Displacement-Based Design (DDBD) approach, which is a PBSD procedure, is utilized. This approach has been implemented on four irregular reinforced concrete frames which are different in terms of number of stories. In the content of DDBD approach Turkish Seismic Design Code, 2007 [8], is used. Story drift ratios were chosen as deformation limits to define the performance levels for specific intensity of ground motions (i.e. specific earthquake hazard levels). The results of the DDBD approach is summarized in the following table.

Table 7.1. Initial Design Values of Frames Obtained Through DDBD Approach

	3-Story	5-Story	8-Story	12-Story
Drift Limit, θ_d (%)	2.0	2.0	2.0	2.0
Design Displacement, Δ_d (mm)	144.25	184.79	277.86	403.14
Effective height, H_e (m)	7.21	10.83	16.54	24.22
Effective Mass, m_e (ton)	164.36	292.01	467.76	719.02
Yield Displacement, Δ_y (mm)	88.86	111.15	169.85	248.67
Design Displacement Ductility, μ	1.62	1.66	1.64	1.62
Equivalent Damping, ξ_{eff} (%)	11.91	12.17	11.99	11.89
Effective Period, T_{eff} (sec)	1.46	1.80	2.52	3.43
Effective Stiffness, K_{eff} (kN/m)	3055.62	3547.29	2904.77	2413.09
Base Shear Force, V_{Base} (kN)	440.77	655.52	807.11	972.82
Stability Index, θ_Δ	0.09	0.09	0.12	0.15
Final Base Shear Forces, V_{Base} (kN)	440.77	655.52	858.83	1053.00

Furthermore, once the forces are obtained through DDBD approach for each element of the frames, capacity design principles were adopted to make sure that plastic

hinges occur in beams rather than occurring of such hinges in columns. After obtaining design internal forces (design moments, shear forces and axial forces), TS500 2003, is utilized to design members. Damage states for each member was determined, and non-linear static pushover and time history analysis were implemented by using SAP 2000 v17.10, the results, in terms of interstory drift ratios, top displacements and base shear forces, were controlled with the ones obtained through DDBD approach.

The results given in Table 7.1, conclude that for studied frames with increase in height of the frames, having same cross sectional size for beams (depth of the beams has significant effects on the ductility ratio), the ductility ratios and subsequently effective damping are slightly different for different cases (i.e. they are almost constant). The effective stiffness of the frames, having same cross sectional size for beams, are decreasing with increase in the height of the frames. For 3 story frame since the depth of the beams are smaller with compare to the remaining frames, hence the effective stiffness of 3 story frame is smaller than the effective stiffness of the 5 story frame.

Furthermore, the effective periods for studied frames are increasing with increase in the height of the structure, as expected. The base shear forces are not significantly increasing with significant changes in the height of the frames. To clarify, the difference between shear forces of 3, and 5, 5 and 8, 8 and 12 story frames are almost constant, which is around 200kN. While the difference between numbers of stories are not constant, because the differences are from 3 to 5, 5 to 8, and 8 to 12 stories are 2, 3, and 4 stories, respectively.

The results obtained through DDBD approach and using capacity design principles does follow similar path with the results provided in some literature, which implies that the DDBD approach has been applied accurately.

Table 7.2. Base Shear Forces and Top Displacement of the Irregular Reinforced Concrete Frames from Different Methods of Analysis

Frames	DDBD		NSPA		NTHA	
	Base Shear (kN)	Top Disp (m)	Base Shear (kN)	Top Disp (m)	Base Shear (kN)	Top Disp (m)
3-Story	440.77	19.20	522.45	17.01	443.21	9.44
5-Story	655.52	24.83	850.51	25.38	725.01	11.50
8-Story	858.83	38.30	913.82	43.44	538.71	17.08
12-Story	1023.00	56.28	1107.49	65.09	904.03	27.40

In Table 7.2 top displacements of the frames with corresponding base shear forces are shown which are obtained through DDBD, Nonlinear Static Pushover Analysis (NSPA), and Nonlinear Time History Analysis (NTHA). The results for base shear forces and corresponding top displacements from nonlinear static pushover analysis, given in this table correspond to limits of life safety performance levels for the studied frames. In addition, the results shown in Table 7.2 for nonlinear time history analysis are the average values from the analysis of the frames for 7 synthetic accelerograms.

As can be seen from Table 7.2, only for 3 story frame the top displacement obtained from nonlinear static pushover analysis is lower than the top displacement obtained through DDBD approach, and for the rest of the frames the top displacements obtained through nonlinear static pushover analysis are larger than the ones obtained through DDBD approach. The corresponding base shear forces from nonlinear static pushover analysis are larger with compare to the base shear forces obtained through DDBD approach. This conclude that the performance of the designed frames for life safety performance levels are within limits.

Furthermore, the results for top displacements from nonlinear time history analysis are significantly lower than the results of DDBD approach. The corresponding base shear forces for 3 story frame are very close for both nonlinear time history analysis and DDBD approach, however for 5 story base shear force obtained from nonlinear time history analysis is significantly larger than the one obtained from DDBD approach. In contrary, the base shear forces for 8 and 12 story frames obtained through nonlinear time history analysis are significantly lower than the o for the mentioned frames obtained from DDBD approach. This and the results shown for interstory drift ratios which are obtained through nonlinear time history analysis (refer to Figure 6.11 and Figure 6.12), conclude that performance of the frames are within the limits.

The results obtained from both nonlinear static pushover and nonlinear time history analysis showed, that the structures are stiffer than being expected. As mentioned in chapter two that the procedure of PBSD is an iterative procedure, and since DDBD approach itself is a PBSD procedure, thus iteration can be carried out to redesign frames to show better results.

As mentioned in previous paragraph that structures are designed stiffer than being expected, this can be due to the following reasons:

- Second order moments are considered, in addition to the P-Delta effects which were considered in DDBD approach. While calculating second order moments, the design moments which were obtained through DDBD approach and the application of capacity design rules, in some cases were significantly increased.
- Second, while detailed cross sectional design was carried out, strain hardening for reinforcements and tensile strength of concrete were ignored. However, these properties were considered while obtaining moment curvature diagram, due to limitation of the program used for this purpose.
- While modelling the frames in SAP2000 v17.10, the aforementioned properties were considered too.
- Using smaller strength reduction factor, recommended in TS500 for flexural design of columns.

For future studies, application of DDBD approach for following different types of 2D and 3D buildings in compliance with Turkish Seismic Design Code 2007 is recommended.

- Reinforced concrete dual wall-frame buildings.
- Reinforced concrete wall-steel frame buildings.
- Steel braced-RC frame buildings.
- Steel braced-steel frame buildings.

It should be noted, that for the types of the buildings listed above, DDBD approach should be implemented on different height of the buildings, to see the effectiveness of the method.

In addition, a risk analysis would provide insight if the PBSD would really provide a uniform risk level for different type of structures.

REFERENCES

1. FEMA-445, (2006). *Next-Generation Performance-Based Seismic Design Guidelines*: Prepared for Federal Emergency Management Agency: Washington, DC, USA by Applied Technology Council, August 2006.

2. Xue, Q., Wu, C.W., Chen, C.C., and Chen, K.C., (2008). *The draft code for performance-based seismic design of buildings in Taiwan.* Engineering Structures. 30(6): p. 1535-1547. DOI 10.1016/j.engstruct.2007.10.002.

3. FEMA-349, (2000). *Action Plan for Performance Based Seismic Design* Prepared for Federal Emergency Management Agency: Washington, DC, USA by Earthquake Engineering Research Institute, April 2000.

4. Priestley, M.J.N. and Kowalsky, M.J., (2000). *Direct Displacement-Based Seismic Design of Conrete Building.* Bulletin of The New Zealand Society For Earthquake Engineering. 33 (4), 421-444.

5. Malekpour, S. and Dashti, F., (2013). *Application of the Direct Displacement Based Design Methodology for Different Types of RC Structural Systems.* International Journal of Concrete Structures and Materials. 7(2): p. 135-153.

6. Priestley, M.J.N., Calvi, G.M., and Kowaisky, M.J., (2007). *Displacement-Based Seismic Design of Structures*. Pavia, ITALY: IUSS PRESS. ISBN: 978-88-6198-000-6.

7. ATC-40, (1996). *Seismic Evaluation and Retrofit of Concrete Buildings*: Vol. 1. Applied Technology Council, Redwood City, California. Report No. SSC 96-01. November 1996.

8. Turkish Seismic Design Code, (2007). *Specification for Structures to be Built in Disaster Areas*, Ministry of Public Works and Settlement Government of Republic of Turkey.

9. TS500, (2003). *Requirements for Design and Construction of Reinforced Concrete Structures*. English version, publication NO.2003/1. Turkish Standards Institute, Ankara Turkey.

10. Ersoy, U., Özcebe, G., and Tankut, T., (2013). *Reinforce Concrete*. Middle East Technical University (METU), Ankara Turkey: METU Press. ISBN:978-605-4362-17-2.

11. Ellingwood, B.R., (2008). *Structural Reliability and Performance-Based Engineering.* Proceedings of the Institution of Civil Engineers-Structures and Buildings. 161(4): p. 199-207. DOI 10.1680/stbu.2008.161.4.199.

12. Haugbølle, K., (2005). *Performance-Based Procurement in Denmark*: CIB 2005. Combining Forces-Advancing Facilities Management and Construction Through Innovation, pp 125-136.

13. Sood, S., (2010). *Performance Based Seismic Design of Buildings*, Master's Thesis. Thesis of structural engineering. Department of Civil Engineering.Thapar University: Patiala, Punjab, India. July 2010. p. 140.

14. NEHRP, (2009). *Research Required to Support Full Implementation of Performance-Based Seismic Design*: Prepared for The National Institute of Standards and Technology Building and Fire Research Laboratory Gaithersburg, Maryland 20899-8600 by The Building Seismic Safety Council of The National Institute of Building Sciences Washington, DC 20005. NIST GCR 09-917-2. April 2009.

15. Ronald HAMBURGER, J.M., Robert BACHMAN, Craig COMARTIN, Andrew WHITTAKER, and Chris ROJAHN, (2004). *The ATC-58 Project : Development of Next-Generation Performance-Based Earthquake Engineering Design Criteria for Buildings.*: 13th World Conference on Earthquake Engineering .Vancouver, B.C., Canada. August 1-6, 2004.

16. FEMA-389, (2004). *Primer for Design Professionals: Communicating with Owners and Managers of New Buildings on Earthquake Risk*. Federal Emergency Management Agency: Washington, DC, USA. January 2004.

17. NRC, (2003). *Living on an Active Earth: Perspectives on Earthquake Science*. National Research Council of the National Academies. Publisher, The National Academies Press. Washington, DC, USA. ISBN 0-309-06562-3 (Book) and ISBN 0309-50631-X (PDF).

18. SEAOC, (1995). *A Framework for Performance-Based Design*. Structural Engineers Association of California, Vision 2000 Committee. Sacramento, California, USA. Vol. I, II, III, 1995.

19. FEMA-356, (2000). *Prestandard and Commentary for the Seismic Rehabilitation of Buildings.*, Prepared for Federal Emergency Management Agency: Washington, DC, USA by American Society of Civil Engineers, Reston, Virginia. November 2000.

20. FEMA-273, (1997). *NEHRP Guidelines for the Seismic Rehabilitation of Buildings*. Prepared for the Building Seismic Safety Council Washington, DC, USA by Applied Technology Council (ATC-33 project), Redwood City, California, with funding by Federal Emergency Management Agency: Washington, DC October 1997.

21. Bertero, R.D. and Bertero, V.V., (2002). *Performance-Based Seismic Engineering: the Need for a Reliable Conceptual Comprehensive Approach.* Earthquake Engineering & Structural Dynamics. 31(3): p. 627-652. Doi 10.1002/Eqe.146.

22. Eurocode8, (2004). *Design of Structures for Earthquake Resistance-Part 1: General rules, seismic actions and rules for buildings*.

23. Li, W. and Li, Q.N., (2012). *Performance-Based Seismic Design of Complicated Tall Building Structures Beyond the Code Specification.* Structural Design of Tall and Special Buildings. 21(8): p. 578-591. Doi 10.1002/Tal.637.

24. Krawinkler, H., (1999). *Challenges And Progress in Performance-Based Earthquake Engineering*: International Seminar on Seismic Engineering for Tomorrow-In Honor of Professor Hiroshi Akiya, Tokyo, Japan, Novemnber 26, 1999.

25. Hamburger, R.O., (2004). *Development of Next-Generation Performance-Based Seismic Design Guidelines*, P. Fajfar and H. Krawinkler, Editors: Proceeding of the International Workshop, Bled, Slovenia, 28 June to 1 July 2004. Berkeley, CA: Pacific Earthquake Engineering Research Center (PEER).

26. Deierlein, G.G., (2004). *Overview of a Comprehensive Framework for Earthquake Performance Assessment*, P. Fajfar and H. Krawinkler, Editors: Proceeding of the International Workshop, Bled, Slovenia, 28 June to 1 July 2004. Berkeley, CA: Pacific Earthquake Engineering Research Center (PEER).

27. Zareian, F. and Krawinkler, H., (2012). *Conceptual Performance-Based Seismic Design Using Building-Level and Story-Level Decision Support System.* Earthquake Engineering & Structural Dynamics. 41(11): p. 1439-1453, Doi 10.1002/Eqe.2218.

28. Zareian, F. and Krawinkler, H., (2009). *Simplified Performance Based Earthquake Engineering*: Report No. 169. The John A. Blume Earthquake Engineering Center. April 2009.

29. Mayengbam, S.S. and Choudhury.S, (2011). *An economic comparison of Direct Displacement Based Design with IS-1893 Response Spectrum Method for R.C. Frame Buildings.* International Journal of Civil and Structural Engineering. 2(1): p. 338-350.

30. Benedetti, A., Landi, L., and Malavolta, D., (2008). *On the Design and Evaluation of Seismic Response of RC Buildings According To Direct Displacement-Based Design Approach.*

31. Pettinga, J.D., (2005). *Dynamic Behaviour of Reinforced Concrete Frames Designed with Direct Displacement-Based Design*: Master's Thesis. European School for Advance Studies in Reduction of Seismic Risk (ROSE School). Research Report No. ROSE-2005/02. University of Pavia, Via Ferrata, 27100 Pavia, Italy. May 2005.

32. Elattar, A., Zaghw, A., and Elansary, A., (2014). *Comparison between the Direct Displacement Based Design and the Force Based Design Methods in Reinforced Concrete Framed Structures*: The paper is presented in the Second European Conference on Earthquake Engineering and Seismology. 2014, Istanbul, Turkey.

33. Priestley, N., (2007). *The Need for Displacement-Based Design and Analysis*. p. 121-133.

34. Priestley, M.J.N., (1998). *Brief Comments on Elastic Flexibility of Reinforced Concrete Frames and Significance to Seismic Design.* Bulletin of The New Zealand Society For Earthquake Engineering. 31 (4), 246-259.

35. Priestley, M.J.N. and Kowalsky, M.J., (1998). *Aspects of Drift and Ductility Capacity of Rectangular Contilivar Structural Walls.* Bulletin of The New Zealand Society For Earthquake Engineering. 31 (2), 73-85.

36. Priestley, M.J.N., (2000). *Performance Based Seismic Design.* Bulletin of the New Zealand Society for Earthquake Engineering. 33(3): p. 325-346.

37. Fajfar, P., (2000). *A Nonlinear Analysis Method for Performance-Based Seismic Design.* Earthquake spectra. 16(3): p. 573-592.

38. Kreslin, M. and Fajfar, P., (2011). *The extended N2 method taking into account higher mode effects in elevation.* Earthquake Engineering & Structural Dynamics. 40(14): p. 1571-1589.

39. FAJFAR, P., (1999). *Capacity Spectrum Method Based on Inelastic Demand Spectrum.* Earthquake Engineering and Structural Dynamics. 28(9): p. 979-993.

40. Džakić, D., Kraus, I., and Dragan Morić, (2012). *Direct Displacement Based Design of Regular Concrete Frames in Compliance with Eurocode 8.* Tehnički vjesnik. 19(4): p. 973-982.

41. GULKAN, P. and SOZEN, M.A., (1974). *Inelastic Responses of Reinforced Concrete Structures to Earthquake Motions.* ACI Journal. 71(12): p. 604-610.

42. Shibata, A. and Sozen, M.A., (1976). *Substitute-Structure Method for Seismic Design in R/C.* Journal of the Structural Division. 102(1): p. 1-18.

43. Moehle, J.P., (1992). *Displacement-Based Design of Building Structures Subjected to Earthquakes.* Earthquake Spectra. 8(3): p. 403-428.

44. Kowalsky, M.J., Priestley, M.J.N., and MacRae, G.A., (1995). *Displacement-Based Design of RC Bridge Columns in Seismic Regions.* Earthquake Engineering and Structural Dynamics. 24(12): p. 1623-1643.

45. Calvi, G.M. and Kingsley, G.R., (1995). *Displacement-Based Seismic Design of Multi-Degree-of-Freedom Bridge Structures.* Earthquake Engineering and Structural Dynamics. 24(9): p. 1247-1266.

46. Calvi, G.M. and Pavese, A., (Year). *Displacement-Based Design of Building Structures*. 1995. European seismic design practice: research and application. Proceedings of the fifth SECED Conference, Elnashai AS (ed.) A. A. Balkema. Rotterdam: Chester, United Kingdom, 127-132, October 26-27 1995.

47. Chopra, A.K. and Goel, R.K., (2001). *Direct Displacement-Based Design: Use of Inelastic Design Spectra Versus Elastic Design Spectra.* Earthquake Spectra. EERI 17(1): p. 47-64.

48. Sullivan, T.J., Priestley, M.J.N., and Calvi, G.M., (2006). *Direct Displacement-Based Design of Frame-Wall Structures.* Journal of Earthquake Engineering. 10(sup001): p. 91-124.

49. Belleri, A., (2009). *Displacement-Based Design for Precast Concrete Structures*, PhD Dissertation, University of Trento.

50. Sullivan, T., Priestley, N., and Calvi, G.M., (2010). *Introduction to a Model Code for Displacement-Based Seismic Design.* Advances in Performance-Based Earthquake Engineering. 13: p. 137-148. Springer Netherlands.

51. Pennucci, D., Calvi, G.M., and Sullivan, T.J., (2009). *Displacement-Based Design of Precast Walls with Additional Dampers.* Journal of Earthquake Engineering. 13(sup1): p. 40-65.

52. Garcia, R., Sullivan, T.J., and Corte, G.D., (2010). *Development of a Displacement-Based Design Method for Steel Frame-RC Wall Buildings.* Journal of Earthquake Engineering. 14(2): p. 252-277.

53. Sullivan, T.J. and Lago, A., (2012). *Towards a simplified Direct DBD procedure for the seismic design of moment resisting frames with viscous dampers.* Engineering Structures. 35: p. 140-148.

54. DBD12, (2012). *A Model Code for the Displacement Based Seismic Design of Structures*, ed. M.J.N.P. T.J. Sullivan, G.M. Calvi. Via Ferrata 1, Pavia, 27100, Italy: IUSS Press. ISBN: 978-88-6198-072-3.

55. Malekpour, S., Ghaffarzadeh, H., and Dashti, F., (2013). *Direct displacement-based design of steel-braced reinforced concrete frames.* Structural Design of Tall and Special Buildings. 22(18): p. 1422-1438.

56. Pettinga, J.D. and Priestley, M.J.N., (2005). *Dynamic behaviour of reinforced concrete frames designed with direct displacement-based design.* Journal of Earthquake Engineering. 9: p. 309-330.

57. Sullivan, T.J., Priestley, M.J.N., and Calvi, G.M., (2005). *Development of an innovative seismic design procedure for frame-wall structures.* Journal of Earthquake Engineering. 9(Sup2): p. 279-307.

58. Massena, B., Bento, R., and Degée, H., (2010). *Direct Displacement Based Design of a RC Frame – Case of Study*. ISSN: 0871-7869.

59. Vidot-Vega, A.L., (2008). *The Impact of Load History on Deformation Limit States for the Displacement-Based Seismic Design of RC Moment Frame Buildings*, in *Civil Engineering*North Carolina State University: Raleigh, North Carolina, USA.

60. Chopra, A.K., (2012). *Dynamics of Structres, Theory and Applications to Earthquake Engineering*. 4th edition. USA, Pearson Education, Inc., publishing as Prentice Hall: ISBN 13: 978-0-13-285803-8. 944 pages.

61. Faccioli, E., Paolucci, R., and Rey, J., (2004). *Displacement Spectra for Long Periods.* Earthquake Spectra. 20(2): p. 347-376.

62. T.Paulay and Priestley, M.J., (1992). *Seismic Design of Reinforced Concrete and Masonry Building*. United States of America John Wiley & Sons, INC.

63. KORKMAZ, A. and AKTAŞ, E., (2006). *Probability Based Seismic Analysis for R/C Frame Structures.* Civil Engineering, Structural Mechanics. Gazi University 21(1): p. 55-64.

64. MAGENES, G., (2000). *A Method for Pushover Analysis in Seismic Assessment of Masonry Buildings*, in *Proceedings of the12th world conference on earthquake engineering*.

65. Kadid, A. and Boumrkik, A., (2008). *Pushover Analysis of Reinforced Concrete Frame Structures.* Asian Journal of Civil Engineering (Building and Housing). 9(1): p. 75-83.

66. SAP2000, (2014). *CSI Analysis Reference Manual For SAP2000®, ETABS®, SAFE® and CSiBridge*. CSI Computers & Structures, Inc. Berkeley, California, USA. ISO# GEN062708M1 Rev.11.

67. Mander, J.B., Priestley, M.J.N., and Park, R., (1988). *Theoretical Stress-Strain Model for Confined Concrete.* Journal of Structural Engineering. 114(8): p. 1804-1826.

68. Seismosoft, (2013). *SeismoArtif v2.1 – A Computer Program for Generating Artificial Earthquake Accelerograms Matched to a Specific target Response Spectrum.* Available from http://www.seismosoft.com.

69. ALTUNTOP, M.A., (2007). *Analysis of Building Structures with Soft Stories*: Master's Thesis. Atilim University.

APPENDIX A

CALCULATED RESULTS FOR 3 STORY IRREGULAR REINFORCED CONCRETE FRAME

Here, most of the results are tabulated in tables, which are related to each story. While the single values for whole frame are given separately.

$$\Delta_C = 0.02x3.6 = 0.072\ m$$

$$\omega_\theta = 1.15 - 0.0034x9.60 = 1.117 > 1.0$$

Since $\omega_\theta = 1.117 > 1.0$, therefore, $\omega_\theta = 1.0$ is used for further calculations.

Table A.1. Calculations for Design Displacement, Effective Height and Effective Mass of 3 Story Irregular Frame

Story i	Height H_i (m)	Mass m_i (ton)	δ_i	Δ_i (m)	$m_i\Delta_i$	$m_i\Delta_i^2$	$m_i\Delta_i H_i$
0	1	2	3	4	5	6	7
3	9.60	51.96	1.00	0.19	9.98	1.92	95.77
2	6.60	65.12	0.69	0.13	8.60	1.13	56.73
1	3.60	71.33	0.38	0.07	5.14	0.37	18.49
Total		188.42			23.71	3.42	171.00

$$\Delta_d = 0.144m = 144\ mm$$

$$H_e = 7.21\ m$$

$$m_e = 164.36\ ton$$

Table A.2. Calculations for Ductility Factor of 3 Story Irregular Frame

f_y (MPa)	E_s (MPa)	f_{ye} (MPa)	ε_y	h_{bi} (m)	L_{bi} (m)		θ_{yi}		M_1/M_2	Δ_y (m)	μ
					1	2	1	2			
420	2x10^5	462	0.0023	0.50	6.00	4.00	0.0139	0.0092	1.00	0.09	1.62

$$\xi_{eq} = 0.1191 = 11.91\%$$

$$A_0 = 0.40$$

$$T_A = 0.15\ sec$$

$$T_B = 0.40\ sec$$

$$I = 1.0$$

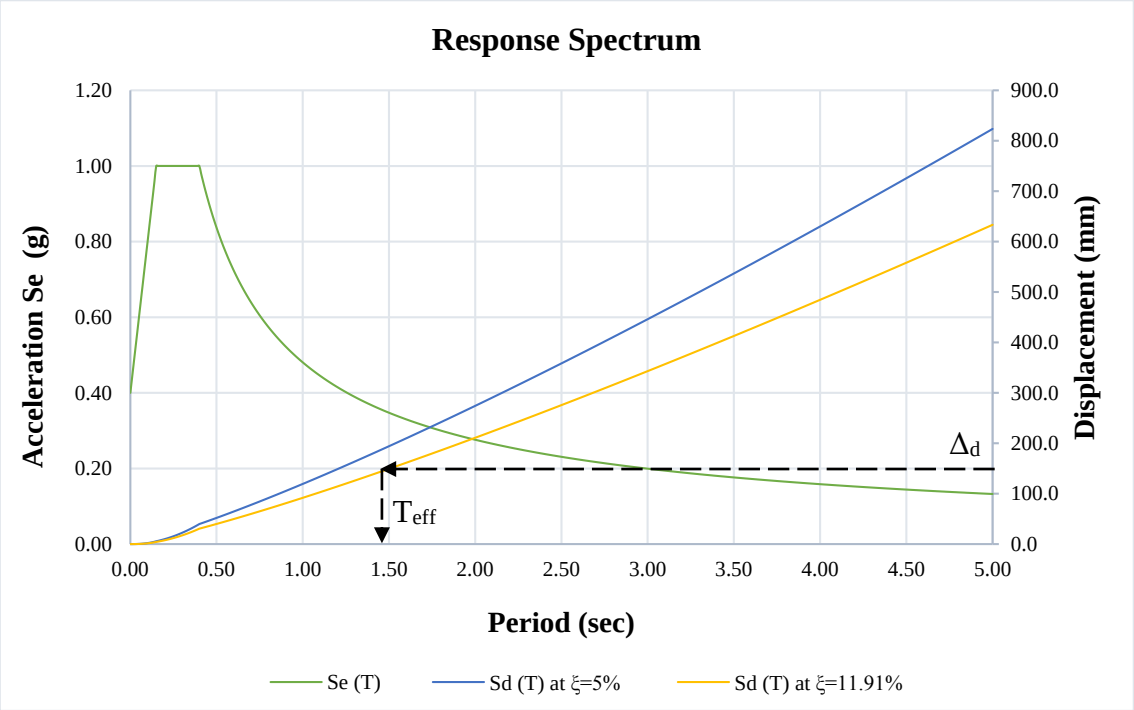

Figure A.1. Elastic Acceleration (S_e) and Design Displacement (S_d) Response Spectrum for 3 Story Irregular Frame

$$\Delta_d = 144\ mm \quad \Rightarrow \quad T_{eff} = 1.46\ sec$$

$$K_{eff} = 3055.62\ kN/m$$

$$V_{Base} = 440.77\ kN$$

Table A.3. Lateral Forces and Overturning Moments at the Top of Each Story of 3 Story Irregular Frame

Story i	Height H_i (m)	Mass m_i (ton)	$m_i H_i$	F_i (kN)	$M_{OTM,i}$ (kN.m)
0	1	2	3	4	5
3	9.60	51.96	498.82	191.22	0.00
2	6.60	65.12	429.80	156.22	573.66
1	3.60	71.33	256.80	93.34	1615.96
0	0.00	0.00	0.00	0.00	3202.74
Total			1185.42	440.77	

$$\theta_\Delta = \frac{2094.76x0.144}{3202.74} = 0.094$$

Since $\theta_\Delta = 0.094 < 0.1$, thus P-Delta effects is ignored. For further calculations Table A.3 is used. The story shear forces are shown in the following table.

Table A.4. Internal Forces in Beams of 3 Story Irregular Frame

Story i	V_{si} (kN)	Beam Shear Forces (kN)		Beam Moments (kN/m)			
		Outer	Inner	Outer		Inner	
				Left	Right	Light	Right
0	1	2	3	4	5	6	7
3	191.22	24.41	36.62	73.24	-73.24	73.24	-73.24
2	347.43	44.35	66.53	133.06	-133.06	133.06	-133.06
1	440.77	56.27	84.41	168.81	-168.81	168.81	-168.81
Total	980.43						

Note that, beam moments given in Table A.4 are calculated at the center of supports (columns).

Table A.5. Internal Forces in Columns of 3 Story Irregular Frame

Story i	Story Height h_i (m)	V_{si} (kN)	Columns Shear Forces (kN)		Columns Moments (kN.m)		Location
			Outer	Inner	Outer	Inner	
0	1	2	3	4	5	6	7
3	3.00	191.22	31.87	63.74	73.24	146.47	Top
					22.37	44.75	Bot
2	3.00	347.43	57.91	115.81	110.69	221.38	Top
					63.03	126.05	Bot
1	3.60	440.77	73.46	146.92	105.79	211.57	Top
					158.68	317.36	Bot

Table A.6. Beam Design Moments at the Face of Columns and at Midspan of the Beams of 3 Story Irregular Frame

Story i	Beam Design Moments (kN.m)					
	Outer			Inner		
	Left	Span	Right	Left	Span	Right
0	1	2	3	4	5	6
3	68.35	93.84	-68.35	65.91	42.08	-65.91
2	124.19	128.44	-124.19	119.76	47.42	-119.76
1	157.56	128.44	-157.56	151.93	47.42	-151.93

Table A.7 Beams Design Shear Forces of 3 Story Irregular Frame

Story i	Beam Shear Forces due to Earthquake Loads (kN)				From Load Combinations (kN)	
	Non-Amplified		Amplified			
	Outer	Inner	Outer	Inner	Outer	Inner
0	1	2	3	4	5	6
3	24.41	36.62	30.51	45.77	79.03	73.57
2	44.35	66.53	55.44	83.17	120.99	114.48
1	56.27	84.41	70.34	105.51	136.94	136.82

$$\mu^0 = \frac{1.62}{1.25} = 1.30$$

Table A.8. Amplified Internal Forces in Columns of 3 Story Irregular Frame

Story i	ω_f	Shear Forces V^0 (kN)		Moments M^0 (kN.m)		Location
		Outer	Inner	Outer	Inner	
0	1	2	3	4	5	6
3	1.00	39.84	79.67	-91.54	-183.09	Top
				27.97	55.94	Bot
2	1.19	81.78	172.10	-164.49	-328.98	Top
				93.66	187.32	Bot
1	1.00	91.83	183.66	-123.05	-246.10	Top
				184.57	369.15	Bot

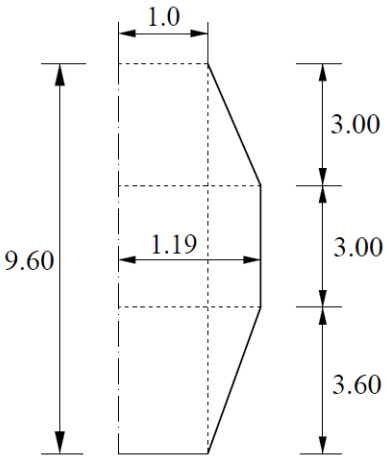

Figure A.2. Calculated Dynamic Amplification Factor for Column Moments of 3 Story Irregular Frame

Table A.9. Reinforcement Details of Beams of 3 Story Irregular Frame

Story	Location	Inner Bay		Outer Bay		Cross Sectional Size
		Support	Span	Support	Span	
Longitudinal Reinforcements						
0	1	2	3	4	5	6
1-2	Top	5Ø16	3Ø16	5Ø16	3Ø16	350x500
	Bot	3Ø16	5Ø16	3Ø16	5Ø16	
3	Top	3Ø16	2Ø16	3Ø16	2Ø16	
	Bot	2Ø16	4Ø16	2Ø16	4Ø16	
Transverse Reinforcements						
1-2	2 legs	Ø8/115	Ø8/200	Ø8/115	Ø8/200	
3	2 legs	Ø8/115	Ø8/200	Ø8/115	Ø8/200	

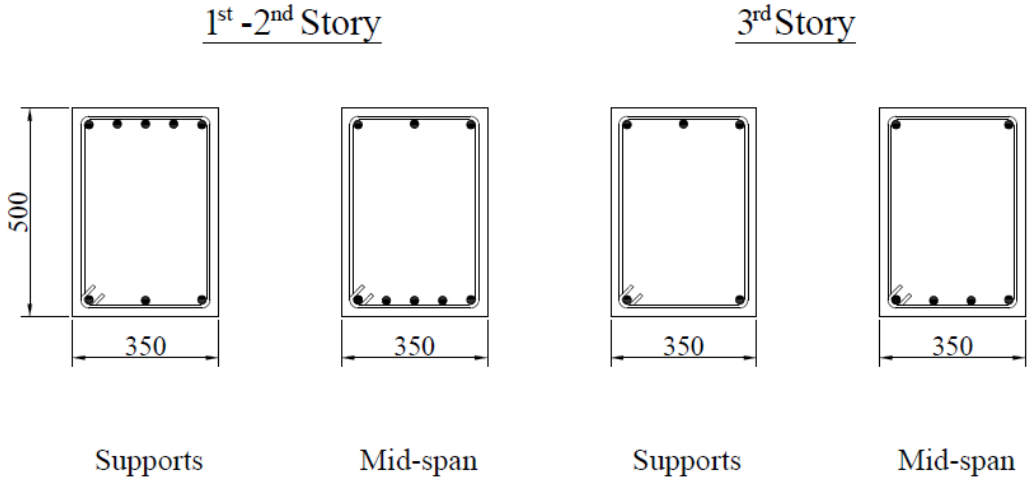

Figure A.3. Cross Sections for Beams of 3 Story Irregular Frame

Table A.10. Reinforcement Details of Columns of 3 Story Irregular Frame

Story	Longitudinal Reinforcements		Transverse Reinforcements				Cross Sectional Size
	Inner	Outer	Inner		Outer		
			Confined Region	Unconfined Region	Confined Region	Unconfined Region	
0	1	2	3	4	5	6	7
1-2	12Ø25	8Ø22	Ø8/100 4 legs	Ø8/160 4 legs	Ø8/100 4 legs	Ø8/160 4 legs	400x400
3	12Ø16	8Ø16	Ø8/100 4 legs	Ø8/160 4 legs	Ø8/100 4 legs	Ø8/160 4 legs	400x400

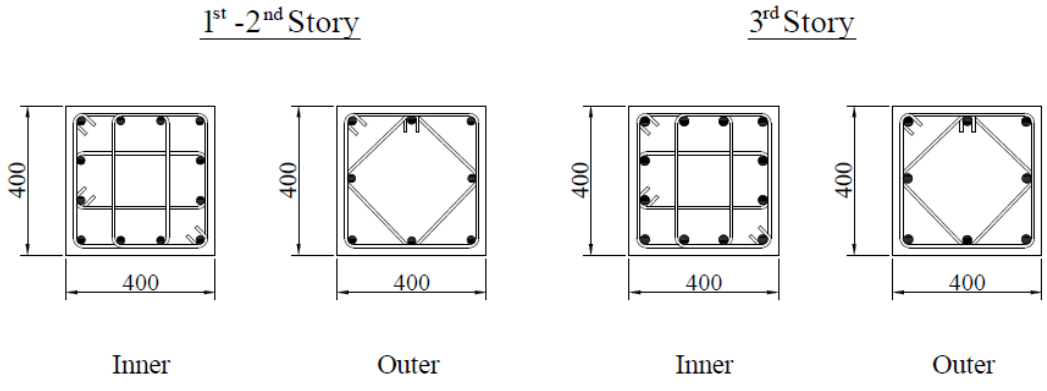

Figure A.4. Cross Sections for Columns of 3 Story Irregular Frame

APPENDIX B

CALCULATED RESULTS FOR 5 STORY IRREGULAR REINFORCED CONCRETE FRAME

Here, most of the results are tabulated in tables, which are related to each story. While the single values for whole frame are given separately.

$$\Delta_C = 0.02x3.6 = 0.072\ m$$

$$\omega_\theta = 1.15 - 0.0034x15.60 = 1.079 > 1.0$$

Since $\omega_\theta = 1.079 > 1.0$, therefore, $\omega_\theta = 1.0$ is used for further calculations.

Table B.1. Calculations for Design Displacement, Effective Height and Effective Mass of 5 Story Irregular Frame

Story i	Height H_i (m)	Mass m_i (ton)	δ_i	Δ_i (m)	$m_i\Delta_i$	$m_i\Delta_i^2$	$m_i\Delta_i H_i$
0	1	2	3	4	5	6	7
5	15.60	54.61	1.000	0.248	13.56	3.37	211.54
4	12.60	67.95	0.859	0.213	14.50	3.10	182.73
3	9.60	68.40	0.694	0.172	11.79	2.03	113.21
2	6.60	69.00	0.504	0.125	8.64	1.08	57.04
1	3.60	75.88	0.290	0.072	5.46	0.39	19.67
Total		335.83			53.96	9.97	584.20

$$\Delta_d = 0.185m = 185\ mm$$

$$H_e = 10.83\ m$$

$$m_e = 292.01\ ton$$

Table B.2. Calculations for Ductility Factor of 5 Story Irregular Frame

f_y (MPa)	E_s (MPa)	f_{ye} (MPa)	ε_y	h_{bi} (m)	L_{bi} (m)		θ_{yi}		M_1/M_2	Δ_y (m)	μ
					1	2	1	2			
420	$2x10^5$	462	0.0023	0.60	6.00	4.00	0.0116	0.0077	1.00	0.11	1.66

$$\xi_{eq} = 0.1191 = 11.91\%$$

$$A_0 = 0.40$$
$$T_A = 0.15\ sec$$
$$T_B = 0.40\ sec$$
$$I = 1.0$$

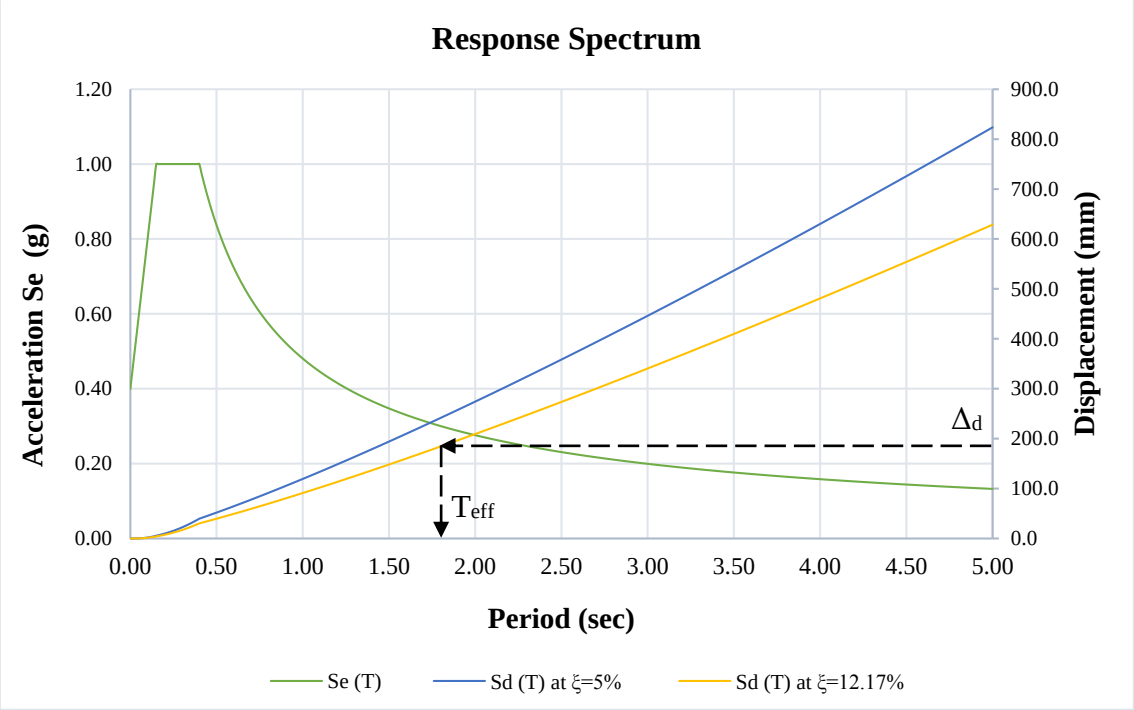

Figure B.1. Elastic Acceleration (S_e) and Design Displacement (S_d) Response Spectrum for 5 Story Irregular Frame

$$\Delta_d = 185\ mm \quad \Rightarrow \quad T_{eff} = 1.81\ sec$$

$$K_{eff} = 3547.29\ kN/m$$

$$V_{Base} = 655.52\ kN$$

Table B.3. Lateral Forces and Overturning Moments at the Top of Each Story of 5 Story Irregular Frame

Story i	Height H_i (m)	Mass m_i (ton)	m_iH_i	F_i (kN)	$M_{OTM,i}$ (kN.m)
0	1	2	3	4	5
5	15.60	54.61	851.87	198.34	0.00
4	12.60	67.95	856.18	174.64	595.02
3	9.60	68.40	656.66	133.94	1713.96
2	6.60	69.00	455.37	92.88	3234.72
1	3.60	75.88	273.16	55.72	5034.13
0	0.00	0.00	0.00	0.00	7394.01
Total			3093.24	655.52	

$$\theta_\Delta = \frac{3720.12x0.185}{7394.01} = 0.093$$

Since $\theta_\Delta = 0.093 < 0.1$, thus P-Delta effects is ignored. For further calculations Table B.3 is used. The story shear forces are shown in the following table.

Table B.4. Internal Forces in Beams of 5 Story Irregular Frame

Story i	V_{si} (kN)	Beam Shear Forces (kN)		Beam Moments (kN.m)			
		Outer	Inner	Outer		Inner	
				Left	Right	Light	Right
0	1	2	3	4	5	6	7
5	198.34	28.23	42.34	84.68	-84.68	84.68	-84.68
4	372.98	53.08	79.62	159.25	-159.25	159.25	-159.25
3	506.92	72.15	108.22	216.44	-216.44	216.44	-216.44
2	599.80	85.36	128.05	256.09	-256.09	256.09	-256.09
1	655.52	93.29	139.94	279.88	-279.88	279.88	-279.88
Total	2333.56						

Note that, beam moments given in Table B.4 are calculated at the center of supports (columns).

Table B.5. Internal Forces in Columns of 5 Story Irregular Frame

Story i	Story Height h_i (m)	V_{si} (kN)	Columns Shear Forces (kN)		Columns Moments (kN.m)		Location
			Outer	Inner	Outer	Inner	
0	1	2	3	4	5	6	7
5	3.00	198.34	33.06	66.11	84.68	169.37	Top
					14.49	28.97	Bot
4	3.00	372.98	62.16	124.33	144.76	289.52	Top
					41.73	83.45	Bot
3	3.00	506.92	84.49	168.97	174.71	349.42	Top
					78.75	157.50	Bot
2	3.00	599.80	99.97	199.93	177.34	354.69	Top
					122.56	245.12	Bot
1	3.60	655.52	109.25	218.51	157.32	314.65	Top
					235.99	471.97	Bot

Table B.6. Beam Design Moments at the Face of Columns and at Midspan of the Beams of 5 Story Irregular Frame

Story i	Beam Design Moments (kN.m)					
	Outer			Inner		
	Left	Span	Right	Left	Span	Right
0	1	2	3	4	5	6
5	78.33	98.63	-78.33	75.16	43.83	-75.16
4	147.30	132.54	-147.30	141.33	49.17	-141.33
3	198.40	132.54	-198.40	189.38	49.17	-189.38
2	234.75	132.18	-234.75	224.08	49.17	-224.08
1	256.56	132.18	-256.56	244.90	49.17	-244.90

Table B.7 Beams Design Shear Forces of 5 Story Irregular Frame

Story i	Beam Shear Forces due to Earthquake Loads (kN)				From Load Combinations (kN)	
	Non-Amplified		Amplified			
	Outer	Inner	Outer	Inner	Outer	Inner
0	1	2	3	4	5	6
5	28.23	42.34	35.29	52.93	84.10	80.07
4	53.08	79.62	66.35	99.53	129.85	130.00
3	72.15	108.22	90.18	135.27	153.14	165.33
2	85.36	128.05	106.71	160.06	169.25	190.12
1	93.29	139.94	116.62	174.93	180.15	204.99

$$\mu^0 = \frac{1.62}{1.25} = 1.30$$

Table B.8. Amplified Internal Forces in Columns of 5 Story Irregular Frame

Story i	ω_f	Shear Forces V^0 (kN)		Moments M^0 (kN.m)		Location
		Outer	Inner	Outer	Inner	
0	1	2	3	4	5	6
5	1.00	41.32	82.64	-105.86	-211.71	Top
				18.11	36.22	Bot
4	1.19	88.04	176.08	-215.86	-431.72	Top
				62.22	124.44	Bot
3	1.19	119.66	239.31	-363.09	-726.18	Top
				163.66	327.33	Bot
2	1.19	141.58	283.16	-264.44	-528.89	Top
				182.75	365.50	Bot
1	1.00	136.57	273.13	-196.66	-393.31	Top
				294.98	589.97	Bot

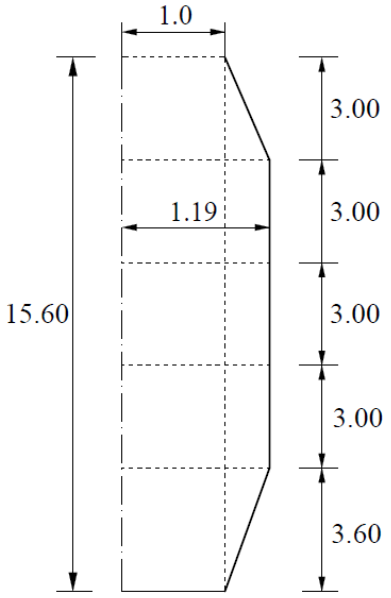

Figure B.2. Calculated Dynamic Amplification Factor for Column Moments of 5 Story Irregular Frame

Table B.9. Reinforcement Details of Beams of 5 Story Irregular Frame

Story	Location	Inner Bay		Outer Bay		Cross Sectional Size
		Support	Span	Support	Span	
Longitudinal Reinforcements						
0	1	2	3	4	5	6
1-3	Top	5Ø18	2Ø18	6Ø18	2Ø18	350x600
	Bot	3Ø18	3Ø16	3Ø18	3Ø16	
4-5	Top	4Ø16	2Ø16	4Ø16	2Ø16	
	Bot	2Ø16	4Ø16	2Ø16	4Ø16	
Transverse Reinforcements						
1-3	2 legs	Ø10/140	Ø10/200	Ø10/140	Ø10/200	
4-5	2 legs	Ø10/125	Ø10/200	Ø10/125	Ø10/200	

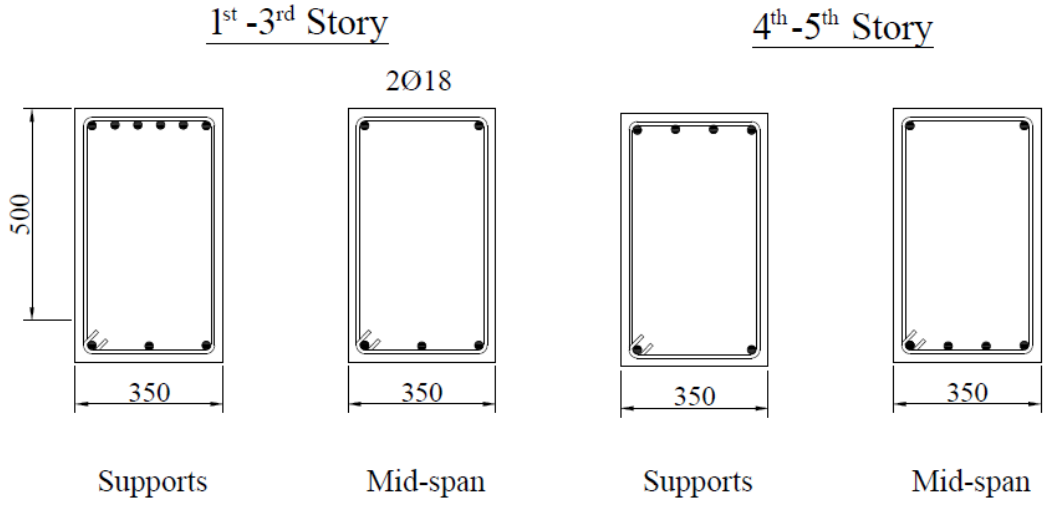

Figure B.3. Cross Sections for Beams of 5 Story Irregular Frame

Table B.10. Reinforcement Details of Columns of 5 Story Irregular Frame

Story	Longitudinal Reinforcements		Transverse Reinforcements				Cross Sectional Size
	Inner	Outer	Inner		Outer		
			Confined Region	Unconfined Region	Confined Region	Unconfined Region	
0	1	2	3	4	5	6	7
1-3	16Ø26	12Ø20	Ø10/100 4 legs	Ø10/120 4 legs	Ø8/100 4 legs	Ø8/115 4 legs	500x500
4	16Ø24	12Ø18	Ø8/100 4 legs	Ø8/115 4 legs	Ø8/100 4 legs	Ø8/115 4 legs	450x450
5	12Ø18	12Ø16	Ø8/100 4 legs	Ø8/115 4 legs	Ø8/100 4 legs	Ø8/115 4 legs	450x450

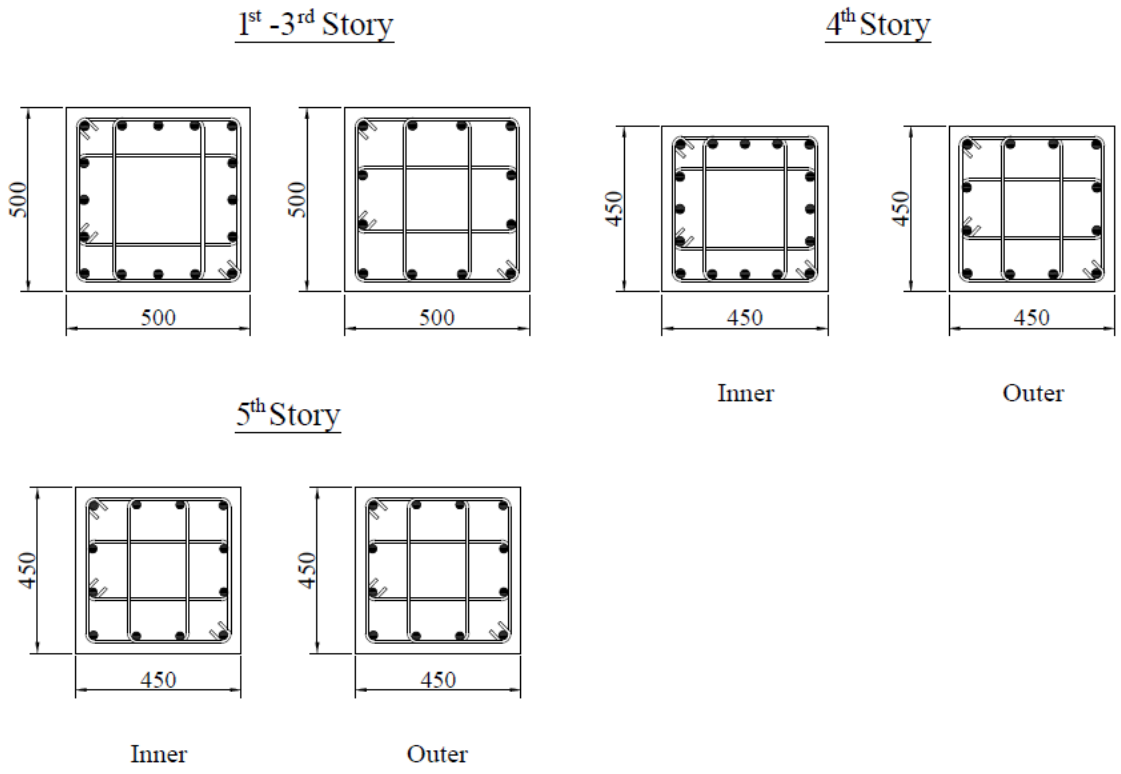

Figure B.4. Cross Sections for Columns of 5 Story Irregular Frame

APPENDIX C

CALCULATED RESULTS FOR 12 STORY IRREGULAR REINFORCED CONCRETE FRAME

Here, most of the results are tabulated in tables, which are related to each story. While the single values for whole frame are given separately.

$$\Delta_C = 0.02x3.6 = 0.072\ m$$

$$\omega_\theta = 1.15 - 0.0034x36.6 = 1.026 > 1.0$$

Since $\omega_\theta = 1.026 > 1.0$, therefore, $\omega_\theta = 1.0$ is used for further calculations.

Table C.1. Calculations for Design Displacement, Effective Height and Effective Mass of 12 Story Irregular Frame

Story i	Height H_i (m)	Mass m_i (ton)	δ_i	Δ_i (m)	$m_i\Delta_i$	$m_i\Delta_i^2$	$m_i\Delta_i H_i$
0	1	2	3	4	5	6	7
12	36.60	56.18	1.000	0.563	0.56	17.80	1157.32
11	33.60	71.52	0.943	0.531	0.53	20.15	1275.60
10	30.60	71.52	0.882	0.496	0.50	17.62	1086.12
9	27.60	71.52	0.816	0.459	0.46	15.08	906.49
8	24.60	72.93	0.746	0.420	0.42	12.84	752.90
7	21.60	74.63	0.671	0.378	0.38	10.64	608.57
6	18.60	74.63	0.592	0.333	0.33	8.27	462.11
5	15.60	74.63	0.508	0.286	0.29	6.09	332.69
4	12.60	74.63	0.420	0.236	0.24	4.16	222.02
3	9.60	74.63	0.327	0.184	0.18	2.52	131.77
2	6.60	74.63	0.230	0.129	0.13	1.25	63.65
1	3.60	83.39	0.128	0.072	0.07	0.43	21.61
Total		874.81			4.09	116.86	7020.85

$$\Delta_d = 0.403m = 403\ mm$$

$$H_e = 24.22\ m$$

$$m_e = 719.02\ ton$$

Table C.2. Calculations for Ductility Factor of 12 Story Irregular Frame

f_y (MPa)	E_s (MPa)	f_{ye} (MPa)	ε_y	h_{bi} (m)	L_{bi} (m)		θ_{yi}		M_1/M_2	Δ_y (m)	μ
					1	2	1	2			
420	2x10^5	462	0.0023	0.60	6.00	4.00	0.0116	0.0077	1.00	0.25	1.62

$$\xi_{eq} = 0.1134 = 11.34\%$$

$$A_0 = 0.40$$
$$T_A = 0.15\ sec$$
$$T_B = 0.40\ sec$$
$$I = 1.0$$

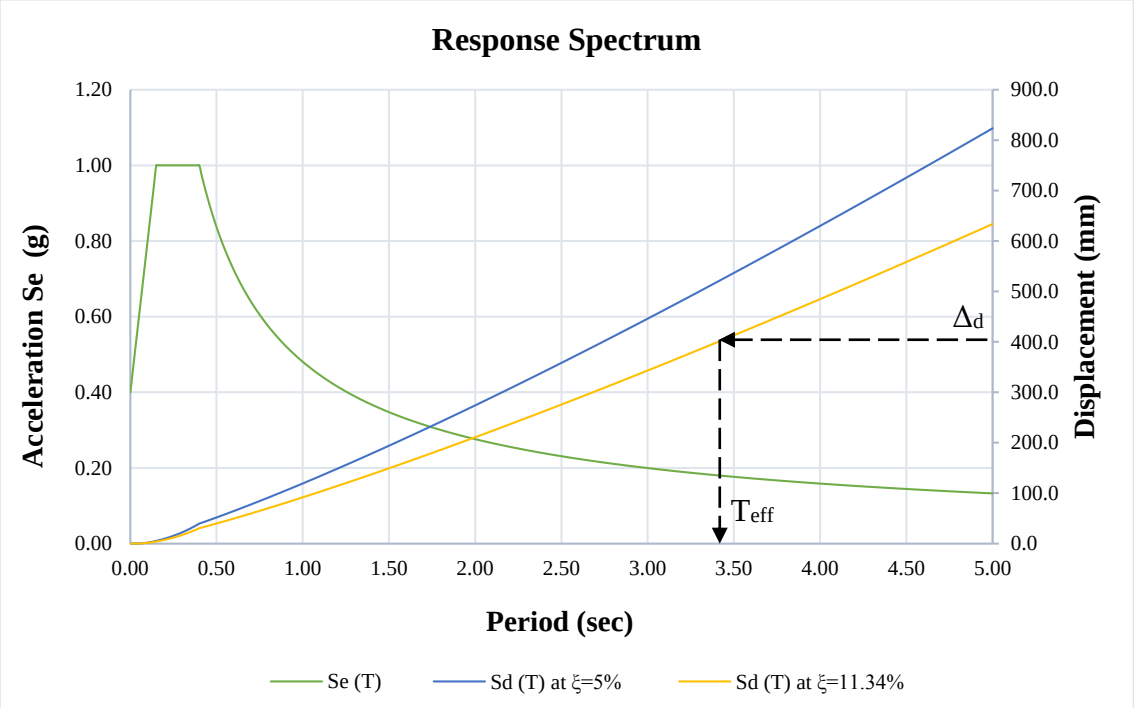

Figure C.1. Elastic Acceleration (S_e) and Design Displacement (S_d) Response Spectrum for 12 Story Irregular Frame

$$\Delta_d = 403\ mm \quad \Rightarrow \quad T_{eff} = 3.43\ sec$$

$$K_{eff} = 2413.09\ kN/m$$

$$V_{Base} = 972.82\ kN$$

Table C.3. Lateral Forces and Overturning Moments at the Top of Each Story of 12 Story Irregular Frame

Story i	Height H_i (m)	Mass m_i (ton)	m_iH_i	F_i (kN)	$M_{OTM,i}$ (kN.m)
0	1	2	3	4	5
12	36.60	56.18	2056.22	194.45	0.00
11	33.60	71.52	2403.06	124.92	583.34
10	30.60	71.52	2188.50	113.77	1541.44
9	27.60	71.52	1973.94	102.61	2840.85
8	24.60	72.93	1794.12	93.27	4448.11
7	21.60	74.63	1611.90	83.79	6335.17
6	18.60	74.63	1388.03	72.16	8473.61
5	15.60	74.63	1164.15	60.52	10828.52
4	12.60	74.63	940.28	48.88	13364.98
3	9.60	74.63	716.40	37.24	16048.09
2	6.60	74.63	492.53	25.60	18842.92
1	3.60	83.39	300.20	15.61	21714.56
0	0.00	0.00	0.00	0.00	25216.71
Total			17029.33	972.82	

$$\theta_\Delta = \frac{9634.69x0.403}{25216.71} = 0.154$$

Since $0.1 < \theta_\Delta = 0.154 < 0.33$, thus P-Delta effects should be considered. The base shear force has to be modified, using Equation 4.28. As a result, modified base shear forces is equal to:

$$V_{Base} = 2413.09x\ 0.403 + 0.5x\frac{9634.69x0.403}{24.22}$$
$$V_{Base} = 1053\ kN$$

Table C.4. Lateral Forces and Overturning Moments at the Top of Each Story and Story Shear Forces of 12 Story Irregular Frame

Story i	Height H_i (m)	Mass m_i (ton)	m_iH_i	F_i (kN)	$M_{OTM,i}$ (kN.m)	V_{si} (kN)
0	1	2	3	4	5	6
12	36.60	56.18	2056.22	210.47	0.00	210.47
11	33.60	71.52	2403.06	135.22	631.42	345.69
10	30.60	71.52	2188.50	123.15	1668.49	468.84
9	27.60	71.52	1973.94	111.07	3075.00	579.91
8	24.60	72.93	1794.12	100.95	4814.73	680.86
7	21.60	74.63	1611.90	90.70	6857.33	771.57
6	18.60	74.63	1388.03	78.10	9172.02	849.67
5	15.60	74.63	1164.15	65.51	11721.03	915.18
4	12.60	74.63	940.28	52.91	14466.56	968.08
3	9.60	74.63	716.40	40.31	17370.81	1008.40
2	6.60	74.63	492.53	27.71	20396.00	1036.11
1	3.60	83.39	300.20	16.89	23504.32	1053.00
0	0.00	0.00	0.00	0.00	27295.13	0.00
Total			17029.33	1053.00		

Table C.5. Internal Forces in Beams of 12 Story Irregular Frame

Story i	V_{si} (kN)	Beam Shear Forces (kN)		Beam Moments (kN.m)			
		Outer	Inner	Outer		Inner	
				Left	Right	Light	Right
0	1	2	3	4	5	6	7
12	210.47	32.92	49.38	98.75	-98.75	98.75	-98.75
11	345.69	54.07	81.10	162.20	-162.20	162.20	-162.20
10	468.84	73.33	109.99	219.98	-219.98	219.98	-219.98
9	579.91	90.70	136.05	272.09	-272.09	272.09	-272.09
8	680.86	106.49	159.73	319.46	-319.46	319.46	-319.46
7	771.57	120.67	181.01	362.02	-362.02	362.02	-362.02
6	849.67	132.89	199.33	398.66	-398.66	398.66	-398.66
5	915.18	143.13	214.70	429.40	-429.40	429.40	-429.40
4	968.08	151.41	227.11	454.22	-454.22	454.22	-454.22
3	1008.40	157.71	236.57	473.14	-473.14	473.14	-473.14
2	1036.11	162.05	243.07	486.14	-486.14	486.14	-486.14
1	1053.00	164.69	247.03	494.06	-494.06	494.06	-494.06
Total	8887.78						

Note that, beam moments given in Table C.5 are calculated at the center of supports (columns).

Table C.6. Internal Forces in Columns of 12 Story Irregular Frame

Story i	Story Height h_i (m)	V_{si} (kN)	Columns Shear Forces (kN)		Columns Moments (kN.m)		Location
			Outer	Inner	Outer	Inner	
0	1	2	3	4	5	6	7
12	3	210.47	35.08	70.16	98.75	197.51	Top
					6.48	12.97	Bot
11	3	345.69	57.62	115.23	155.71	311.43	Top
					17.13	34.26	Bot
10	3	468.84	78.14	156.28	202.84	405.69	Top
					31.57	63.15	Bot
9	3	579.91	96.65	193.30	240.52	481.03	Top
					49.44	98.88	Bot
8	3	680.86	113.48	226.95	270.02	540.04	Top
					70.41	140.82	Bot
7	3	771.57	128.59	257.19	291.60	583.21	Top
					94.18	188.36	Bot
6	3	849.67	141.61	283.22	304.48	608.96	Top
					120.35	240.70	Bot
5	3	915.18	152.53	305.06	309.04	618.09	Top
					148.54	297.09	Bot
4	3	968.08	161.35	322.69	305.68	611.36	Top
					178.36	356.73	Bot
3	3	1008.40	168.07	336.13	294.77	589.54	Top
					209.43	418.85	Bot
2	3	1036.11	172.68	345.37	276.71	553.42	Top
					241.34	482.69	Bot
1	3.6	1053.00	175.50	351.00	252.72	505.44	Top
					379.08	758.16	Bot

Table C.7. Beam Design Moments at the Face of Columns and at Midspan of the Beams of 12 Story Irregular Frame

Story i	Beam Design Moments (kN.m)					
	Outer			Inner		
	Left	Span	Right	Left	Span	Right
0	1	2	3	4	5	6
12	88.88	98.63	-88.88	83.94	43.83	-83.94
11	145.98	131.78	-145.98	137.87	49.17	-137.87
10	197.98	131.78	-197.98	186.98	49.17	-186.98
9	244.88	131.78	-244.88	231.28	49.17	-231.28
8	282.19	131.78	-282.19	263.55	49.17	-263.55
7	319.78	131.37	-319.78	298.66	49.17	-298.66
6	352.15	131.37	-352.15	328.90	49.17	-328.90
5	379.30	131.37	-379.30	354.25	49.17	-354.25
4	401.23	131.37	-401.23	374.73	49.17	-374.73
3	417.94	131.37	-417.94	390.34	49.17	-390.34
2	429.42	131.37	-429.42	401.06	49.17	-401.06
1	436.42	131.37	-436.42	407.60	49.17	-407.60

Table C.8 Beams Design Shear Forces of 12 Story Irregular Frame

Story i	Beam Shear Forces due to Earthquake Loads (kN)				From Load Combinations (kN)	
	Non-Amplified		Amplified			
	Outer	Inner	Outer	Inner	Outer	Inner
0	1	2	3	4	5	6
12	32.92	49.38	41.15	61.72	85.12	87.77
11	54.07	81.10	67.58	101.37	125.43	130.63
10	73.33	109.99	91.66	137.49	149.82	166.75
9	90.70	136.05	113.37	170.06	171.75	199.32
8	106.49	159.73	133.11	199.66	190.50	228.11
7	120.67	181.01	150.84	226.26	208.05	254.71
6	132.89	199.33	166.11	249.16	223.62	277.61
5	143.13	214.70	178.92	268.37	236.76	296.82
4	151.41	227.11	189.26	283.89	247.48	312.34
3	157.71	236.57	197.14	295.71	255.78	324.16
2	162.05	243.07	202.56	303.84	261.70	332.29
1	164.69	247.03	205.86	308.79	265.68	337.24

$$\mu^0 = \frac{1.62}{1.25} = 1.30$$

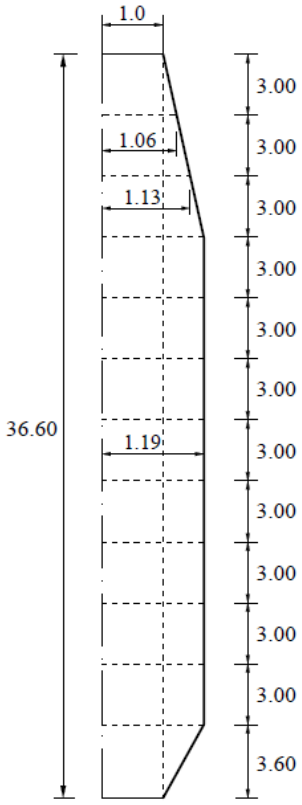

Figure C.2. Calculated Dynamic Amplification Factor for Column Moments of 12 Story Irregular Frame

Table C.9. Amplified Internal Forces in Columns of 12 Story Irregular Frame

Story i	ω_f	Shear Forces V^0 (kN)		Moments M^0 (kN.m)		Location
		Outer	Inner	Outer	Inner	
0	1	2	3	4	5	6
12	1.00	43.85	87.70	-123.44	-246.88	Top
				8.10	16.21	Bot
11	1.06	76.55	153.09	-206.88	-413.76	Top
				22.76	45.52	Bot
10	1.13	109.96	219.91	-285.44	-570.87	Top
				44.43	88.86	Bot
9	1.19	136.48	272.97	-357.35	-714.70	Top
				73.45	146.91	Bot
8	1.19	160.24	320.49	-401.19	-802.37	Top
				104.61	209.23	Bot
7	1.19	181.59	363.18	-433.25	-866.51	Top
				139.93	279.85	Bot
6	1.19	199.97	399.95	-452.39	-904.77	Top
				178.81	357.63	Bot
5	1.19	215.39	430.78	-459.16	-918.33	Top
				220.70	441.40	Bot
4	1.19	227.84	455.68	-454.16	-908.33	Top
				265.01	530.01	Bot
3	1.19	237.33	474.66	-437.96	-875.92	Top
				311.16	622.32	Bot
2	1.19	243.85	487.70	-411.13	-822.25	Top
				358.58	717.16	Bot
1	1.00	219.38	438.75	-315.90	-631.80	Top
				473.85	947.70	Bot

Table C.10. Reinforcement Details of Columns of 12 Story Irregular Frame

Story	Location	Inner Bay		Outer Bay		Cross Sectional Size
		Support	Span	Support	Span	
Longitudinal Reinforcements						
0	1	2	3	4	5	6
1-8	Top	6Ø20	2Ø20	6Ø20	2Ø20	350x600
	Bot	3Ø20	3Ø20	3Ø20	3Ø20	
9-12	Top	5Ø16	2Ø16	5Ø16	2Ø16	
	Bot	3Ø16	4Ø16	3Ø16	4Ø16	
Transverse Reinforcements						
1-8	2 legs	Ø10/140	Ø10/200	Ø10/140	Ø10/200	
9-12	2 legs	Ø10/140	Ø10/200	Ø10/140	Ø10/200	

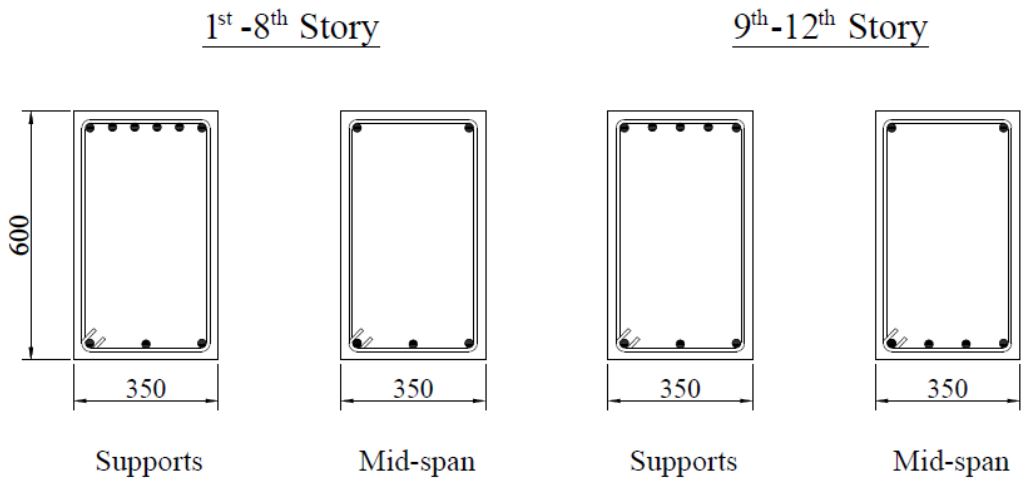

Figure C.3. Cross Sections for Beams of 12 Story Irregular Frame

Table C.11. Reinforcement Details of Columns of 12 Story Irregular Frame

Story	Longitudinal Reinforcement		Transverse Reinforcements				Cross Sectional Size
	Inner	Outer	Inner		Outer		
			Confined Region	Unconfined Region	Confined Region	Unconfined Region	
0	1	2	3	4	5	6	7
1-8	20Ø24	16Ø20	Ø12/100 4 legs	Ø12/140 4 legs	Ø12/100 4 legs	Ø12/140 4 legs	700x700
9	20Ø24	16Ø18	Ø12/100 4 legs	Ø12/140 4 legs	Ø12/100 4 legs	Ø12/140 4 legs	600x600
10-12	20Ø18	16Ø18	Ø12/100 4 legs	Ø12/140 4 legs	Ø12/100 4 legs	Ø12/140 4 legs	600x600

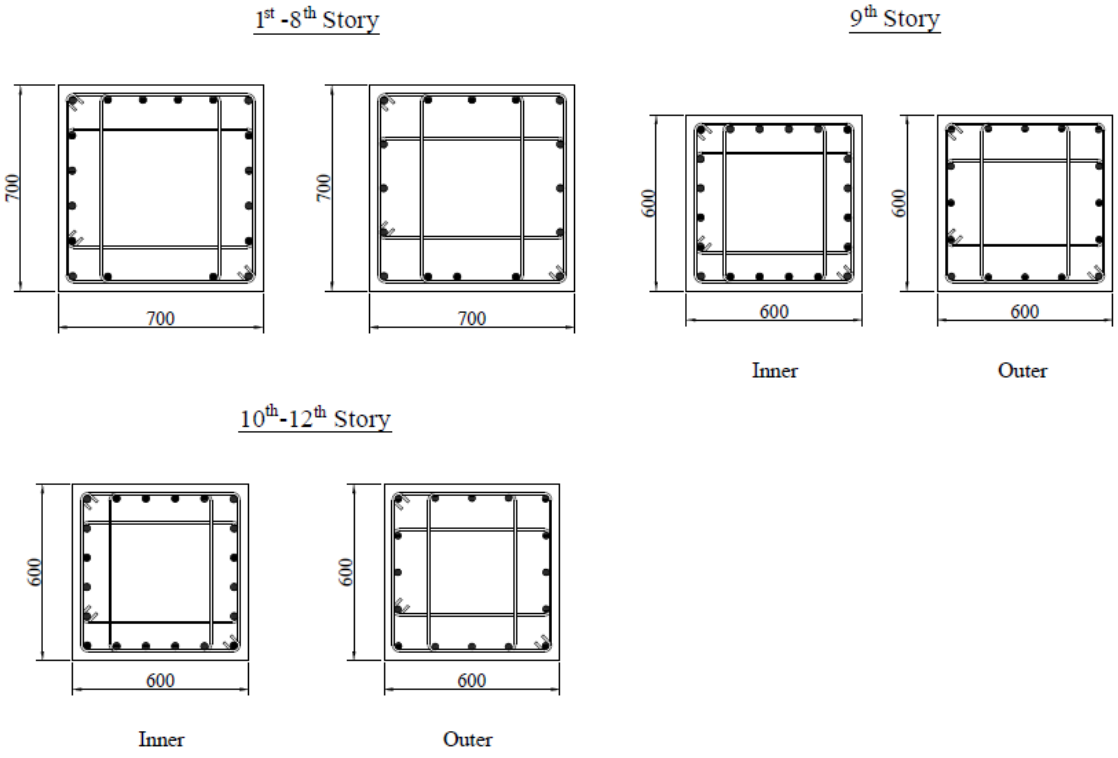

Figure C.4. Cross Sections for Columns of 12 Story Irregular Frame